

# **Midwest Solid-State Chemistry Conference 2005**

**University of Notre Dame**

Thursday, May 26 — Saturday, May 28, 2005  
Notre Dame, Indiana

**Conference Program**

**List of Posters**

**Abstracts**

# Conference Program

## Wednesday, May 25

arrival at Notre Dame and checking in O'Neil residence hall and hotels

## Thursday, May 26

8:00 – 9:00

registration and pickup of conference materials

9:00 – 9:10

opening remarks

### Morning: Slavi Sevov, presiding

9:10 – 9:40

**Prof. John Greedan**, McMaster University

*Structural and Magnetic Phase Transitions in  $BaV_{10}O_{15}$ . Co-existence of Long Range and Glassy Spin Ordering*

9:40 – 10:00

**Prof. Paul Maggard**, North Carolina State University

*Layered Hybrid Solids - Disassembly Not Included*

10:00 – 10:15

**Eric Quarez**, Michigan State University

*Nano-structuring, Compositional Fluctuations and Atomic Ordering in the Thermoelectric Materials  $AgPb_mSbTe_{2+m}$ . The myth of Solid Solutions.*

10:15 – 11:00

poster set-up

11:00 – 11:30

**Prof. Jim Ibers**, Northwestern University

*Adventures in Metal Chalcogenide Chemistry*

11:30 – 11:45

**Indika U. Arachchige**, Wayne State University

*Highly Luminescent Mesoporous CdSe Aerogels*

11:45 – 12:00

**William C. Sheets**, Northwestern University

*Hydrothermal Synthesis of Delafossite-type Oxides*

12:00 – 1:30

lunch

### Afternoon: John Greedan, presiding

1:30 – 2:00

**Prof. Holger Kleinke**, University of Waterloo

*Narrow gap heavy main group semiconductors*

2:00 – 2:15

**Athena Sefat**, McMaster University

*The Magnetic & Electronic Interactions at the Mott Transition in  $Nd_{1-x}TiO_3$*

2:15 – 2:30

**Christos Malliakas**, Michigan State University

*Resolving the distortion in the square nets of tellurium of the modulated  $RETe_3$  ( $RE=Ce, Pr$  and  $Nd$ ) materials*

2:30 – 2:45	<b>Young-II Kim</b> , Ohio State University <i>Dielectric Property of Perovskite Oxynitrides</i>
2:45 – 3:00	<b>Paul A. Giesting</b> , University of Notre Dame <i>Crystal structure of uranyl oxalates</i>
2:55 – 4:00	posters
4:00 – 4:20	<b>Prof. Mario Bieringer</b> , University of Manitoba <i>Exploring Anion Ordered Transition Metal Oxychloride Phases</i>
4:20 – 4:35	<b>Jonathan W. Lekse</b> , Duquesne University <i>Development of a Solid-State Microwave Synthetic Method for Preparation of Diamond-Like Semiconductors</i>
4:35 – 5:05	<b>Prof. Paul McGinn</b> , University of Notre Dame <i>Combinatorial Processing and Characterization of Inorganic Materials</i>
<u>Friday, May 27</u>	<u>Morning: Mario Bieringer, presiding</u>
9:00 – 9:30	<b>Prof. Mercuri Kanatzidis</b> , Michigan State University <i>The Metal Flux – A Preparative Tool for the Exploration of Intermetallic Compounds</i>
9:30 – 9:45	<b>Shahab Derakhshan</b> , University of Waterloo <i>Square Net Distortion Engineering in the Titanium Antimonide <math>Ti_2Sb</math></i>
9:45 – 10:00	<b>Craig Bridges</b> , University of Liverpool <i>Electronic structure and formation pathway of the transition metal oxide hydride <math>LaSrCoO_3H_{0.7}</math></i>
10:00 – 10:20	<b>Yurij Mozharivskij</b> , Iowa State University <i>Chemistry of the Giant Magnetocaloric Effect Material <math>Gd_5Si_2Ge_2</math> and Related Phases</i>
10:20 – 11:00	break (photo)
11:00 – 11:30	<b>Prof. Peter Burns</b> , University of Notre Dame <i>The Crystal Chemistry of Actinyl Peroxides</i>
11:30 – 11:45	<b>Fudong Wang</b> , Washington University <i>Synthesis, photoluminescence, and quantum-confinement effects of colloidal InP quantum wires and quantum rods</i>
11:45 – 12:00	<b>Cheol-Hee Park</b> , Oregon State University <i>Wide band-gap p-type semiconductor <math>BaCuSF</math> and related materials: powder and thin films</i>
12:00 – 1:30	lunch

- Afternoon: Jim Ibers, presiding
- 1:30 – 2:00 **Prof. Arnold Guloy**, University of Houston  
*The Chemical Nature of Polar Intermetallics: New Insights into the Chemical Bonding and Reactivity of Zintl Phases*
- 2:00 – 2:15 **P. Subramanya Herle**, University of Waterloo  
*Redox-Driven Phase Transitions*
- 2:15 – 2:30 **Joseph Wachter**, Michigan State University  
*New Phase-Change Materials For Optical Data Storage Applications*
- 2:30 – 3:00 **Prof. Kenneth Henderson**, University of Notre Dame  
*Use of s-Block Metal Aggregates in Controlling Network Assembly*
- 3:00 – 4:00 posters
- 4:00 – 4:15 **Shawn Resler**, Washington University  
*Evidence for Electrostatic Stabilization in Thermally-Induced Growth of Alkanethiol-Gold Clusters Determined by a Unified Cluster Aggregation and Ripening Model*
- 4:15 – 4:30 **Jose Goicoechea**, University of Notre Dame  
*Transition Metal-Centered Zintl Anions in Solution*
- 4:30 – 5:00 **Dr. Lynda Soderholm**, Argonne National Laboratory  
*Actinide Solution Speciation Using High-Energy X-Ray Scattering*
- Saturday, May 28
- Morning: Svilen Bobev, presiding
- 9:00 – 9:30 **Prof. William Buhro**, Washington University  
*Colloidal Semiconductor Quantum Wires: Synthesis, Spectroscopy, and Confinement Effects*
- 9:30 – 9:45 **Qisheng Lin**, Iowa State University  
*Quasicrystals and Approximants in the Sc-Mg-Zn system: Prediction and Realization*
- 9:45 – 10:00 **Palaniappan Arumugam**, Wayne State University  
*Synthesis and Characterization of Layered Transition Metal Pnictate Nanoparticles – Precursor Materials to Pnictide Nanoparticle Arrays*
- 10:00 – 10:15 **Prof. Patrick Woodward**, Ohio State University  
*Conducting Main Group Metal Oxides*
- 10:15 – 10:30 break
- 10:30 – 10:45 **Paul Kögerler**, Iowa State University  
*Networking Polyoxomolybdate-Based Clusters*
- 10:45 – 11:00 **Pierre Poudeu**, Michigan State University  
*Design in solid state chemistry based on phase homologies.  $Sb_4Te_3$  and  $Sb_8Te_9$  as new members of the series  $(Sb_2Te_3)_m \cdot (Sb_2)_n$*
- 11:00 – 11:30 **Prof. Timothy Hughbanks**, Texas A&M University  
*The Magnetic Properties of Compounds with Clusters and low-D structures*

# Abstracts

## Oral Presentations

**Thursday, May 26**

### **Structural and Magnetic Phase Transitions in $\text{BaV}_{10}\text{O}_{15}$ . Co-existence of Long Range and Glassy Spin Ordering.**

Craig A. Bridges<sup>1</sup>, John E. Greedan<sup>2</sup>, Thomas Hansen<sup>3</sup> and Andrew S. Wills<sup>4</sup>

<sup>1</sup> *Department of Chemistry, University of Liverpool, Liverpool, U.K.*

<sup>2</sup> *Department of Chemistry and the Brockhouse Institute for Materials Research, McMaster University, Hamilton, Canada*

<sup>3</sup> *Institute Laue Langevin, Grenoble, France*

<sup>4</sup> *Department of Chemistry, University College London, London, U.K.*

The structure of the mixed valent oxide,  $\text{BaV}_{10}\text{O}_{15}$ , can be described in terms of a close packed lattice consisting of alternating  $\text{O}_8$  and  $\text{BaO}_7$  layers in which  $8\text{V}^{3+}$  and  $2\text{V}^{2+}$  ions randomly occupy 5/8 of the octahedral sites and is thus a close analog of the well-studied  $\text{V}_2\text{O}_3$ .  $\text{BaV}_{10}\text{O}_{15}$  shows a rich array of properties, including a structural phase transition below 135K, driven by V – V bond formation, which results in an unusual semiconductor to semiconductor transition. Two further phase transitions occur at lower temperatures, 40K and 25K, which are magnetic in origin. The V- sublattice consists of interconnected  $\text{V}_{10}$  clusters involving four tetrahedra which share edges and corners. Such a topology presents the condition for geometric magnetic frustration. Detailed studies of the magnetic phase transitions were carried out using d.c. and a.c. magnetic susceptibility, heat capacity, muon spin relaxation and neutron diffraction. The results are consistent with the presence of geometric magnetic frustration and indicate a very complex state at low temperatures in which long range spin ordering (wave vector  $\mathbf{k} = \_00$ ) co-exists with a spin frozen state which does not appear to be a canonical spin glass.

### **Layered Hybrid Solids - Disassembly Not Included**

Paul Maggard

*North Carolina State University*

A growing interest in hybrid solids is to achieve catalytic and/or gas absorption selectivity via the synthesis of robust open-frameworks that contain highly functionalized and size selective pores. The resultant chemistry is envisioned as an extension of that well-known for zeolites and coordination compounds and major synthetic efforts have been described for many chemical systems. By contrast, our research strategy is directed at the synthesis of layered hybrid solids that contain neutral ligands (e.g.  $\text{H}_2\text{O}$ , pyrazine, etc.) that are easily removed without causing collapse or condensation of the original structure, in order to access pore spaces. This presentation will include the newly-discovered series of perrhenate-containing pillared structures,  $\text{M}(\text{pzc})_2(\text{H}_2\text{O})_2\text{AgReO}_4$  ( $\text{M} = \text{Co}, \text{Ni}, \text{Cu}$ ) and  $\text{Cu}(\text{pzc})_2(\text{H}_2\text{O})_2\text{CuReO}_4$ , that can be reversibly

dehydrated to produce coordinatively-unsaturated metal sites. In addition, the presentation will describe the targeted synthesis and properties of the new layered  $\text{Co}(\text{pyz})\text{V}_4\text{O}_{10}$  and  $\text{Cu}(\text{pyz})_2\text{V}_6\text{O}_{16}\cdot(\text{H}_2\text{O})_{0.22}$ , and the subsequent removal of pyrazine in order to access porous inorganic structures.

## **Nano-structuring, Compositional Fluctuations and Atomic Ordering in the Thermoelectric Materials $\text{AgPb}_m\text{SbTe}_{2+m}$ : The Myth of Solid Solutions**

Eric Quarez,<sup>†</sup> Kuei-Fang Hsu,<sup>†</sup> Robert Pcionek,<sup>†</sup> N. Frangis,<sup>‡</sup> E. K. Polychroniadis,<sup>‡</sup> and Mercuri G. Kanatzidis<sup>†</sup>

<sup>†</sup> *Department of Chemistry, Michigan State University, East Lansing, MI 48824, USA*

<sup>‡</sup> *Solid State Physics Section, Department of Physics, Aristotle University of Thessaloniki, GR-54124 Thessaloniki, Greece*

Recently, we described the family of chalcogenide lead-based compounds,  $\text{AgPb}_m\text{SbTe}_{m+2}$ , or LAST- $m$  materials (LAST for Lead Antimony Silver Tellurium), several members of which exhibit large  $ZT$  values from  $\sim 1.2$  (LAST-10) to  $\sim 2.2$  (LAST-18) at 800 K.<sup>1</sup> Preliminary electron microscopic examination of these samples revealed endotaxially dispersed quantum nanodots (i.e. regions 2 to 4 nm in size that are rich in Ag-Sb and are surrounded by a PbTe matrix). This is a significant observation and raises important new questions as to the possible impact of these nanostructural features on the thermoelectric properties.

We present here extensive TEM studies to fully characterize the LAST materials on the atomic scale and probe the extent and nature of nano structuring.  $\text{Ag}_{1-x}\text{Pb}_m\text{SbTe}_{m+2}$  with different  $m$  value were prepared and characterized by powder/single crystal X-ray diffraction, electron diffraction and high resolution transmission electron microscopy. Powder diffraction patterns of different members ( $m = 0, 6, 12, 18, 4$ ) are consistent with pure phases crystallizing in the NaCl-structure type ( $\text{Fm}\bar{3}m$ ) and the proposition that the LAST family behaved as solid solutions between the PbTe and  $\text{AgSbTe}_2$  compounds. However, electron diffraction and high resolution transmission electron microscopy studies suggest the LAST phases are inhomogeneous at the nano scale with at least two co-existing sets of well defined phases. Moreover, within each nano-domain we observe extensive long range ordering of Ag, Pb and Sb atoms. The long range ordering can be confirmed by single crystal X-ray diffraction studies. Indeed, data collections of five different single crystals were successfully refined in space groups of lower symmetry than  $\text{Fm}\bar{3}m$  including  $\text{P4}/\text{mmm}$  and  $\text{R}\bar{3}m$ . The results reported here dispel the decades long belief that the systems  $(\text{AgSbTe}_2)_{1-x}(\text{PbTe})_x$  are solid solutions.

(1) Hsu, K. F.; Loo, S.; Guo, F.; Chen, W.; Dyck, J. S.; Uher, C.; Hogan, T.; Polychroniadis, E. K.; Kanatzidis, M. G. *Science* **2004**, 303, 818.

## Adventures in Metal Chalcogenide Chemistry

James A. Ibers  
*Northwestern University*

The syntheses and structures of a potpourri of metal chalcogenides will be discussed. These will probably include the following compounds (co-authors in parentheses):

$Ln_4Yb_{11}Q_{22}$  ( $Ln = \text{rare-earth metal}$ ;  $Q = \text{chalcogen}$ ) (*Danielle Gray*):

What is wrong with the structures? Formal oxidation states?

$Er_3SmS_6$  and  $Er_{2,x}Sm_xSe_3$  (*Danielle Gray*)

Subtleties in reaction conditions; ICP versus X-ray “determination” of composition.

$Ln_4MnOQ_6$  (*Bin Deng*):

Unusual  $Ln$  coordination geometry.

$RbVSe_2$  (*Bin Deng, Fu Qiang Huang, Donald E. Ellis*):

V–V bonding? Too little material for a magnetic measurement? Try theory.

*Some Cu/Sb/S systems* (*Bin Deng, George H. Chan, Richard P. Van Duyne, Donald E. Ellis*):

Cu–Sb bonds?

## Highly Luminescent Mesoporous CdSe Aerogels

Indika U. Arachchige and Stephanie L. Brock  
*Department of Chemistry, Wayne State University, Detroit, Michigan 48202*

Aerogels are a unique class of inorganic polymers that have low densities, large open pores and high inner surface area. This results in interesting physical properties as well as a wide variety of potential applications as catalysts/catalyst supports, sensors and novel electrochemical device components. So far, a great deal of research has been conducted on aerogels based on single and mixed metal oxides. However, non-oxide aerogels, with the exception of carbon aerogels, are virtually nonexistent. Properties of aerogels can be effectively modified by substitution of the primary gel component to make a chemically unique framework. Also an extensive range of aerogel chemical and physical properties may be achieved if the framework can be assembled from semiconducting materials. We have recently synthesized a highly luminescent pure chalcogenide based semiconductor aerogel of CdSe from controlled aggregation of primary particles followed by super-critical fluid extraction. Herein we describe the structural, optical and electronic properties of the resultant material along with the surface area and porosity. The effect of synthetic parameters on the primary particle size, morphology, surface area, and optical properties of CdSe aerogel will be discussed.

## Hydrothermal Synthesis of Delafossite-type Oxides

William C. Sheets, Tobin J. Marks & Kenneth R. Poeppelmeier  
*Department of Chemistry, Northwestern University*

Owing to their application as catalysts, luminescent materials, batteries and transparent p-type conducting oxides, delafossite-type oxides ( $ABO_2$ ) have been intensely studied. Delafossite-type oxides that incorporate copper can easily be synthesized by high-temperature solid state reaction techniques; however, such noble metal oxides containing silver are difficult to prepare in one step by solid-state reactions because  $Ag_2O$  decomposes in open systems above 150 °C before the reaction can occur. Our research focuses on the synthesis of copper and silver delafossite-type oxides via low temperature ( $< 210$  °C) and low pressure ( $< 20$  atm) hydrothermal reactions between the constituent, binary oxides, oxyhydroxides and/or hydroxides. Through control of the key parameters: temperature, pH and reactant selection, phase pure products can be obtained in high yield. Particular emphasis has been placed on how the constituent oxide's acid-base character influences whether or not a certain delafossite-type oxide can be synthesized.

## Narrow gap heavy main group semiconductors

Holger Kleinke  
*Department of Chemistry, University of Waterloo, Waterloo, ON, Canada N2L 3G1*

Recent ground-breaking success in the field of thermoelectric research is indicative for the renewed interest in the thermoelectric energy conversion. Ideally, a thermoelectric material forms a complex yet highly symmetric crystal structure with heavy constituent elements, and theory indicates that it should comprise a band gap of approximately 10 kT, i.e. 0.26 eV at 300 K. Hence the materials of interest are narrow gap, thus black, semiconductors.

With this contribution we present our results in the field of main group chalcogeno-stannates and antimonates, two classes of semiconducting Zintl phases that are usually colorful, i.e. have too large gaps for the thermoelectric energy conversion. We achieved to overcome this principal problem by working with a) mixed valent Sn atoms, b) Sn/Sb and Pb/Sb mixtures, c) polychalcogenide groups.

## Magnetic and Electronic Interactions at the Mott Transition in $Nd_{1-x}TiO_3$

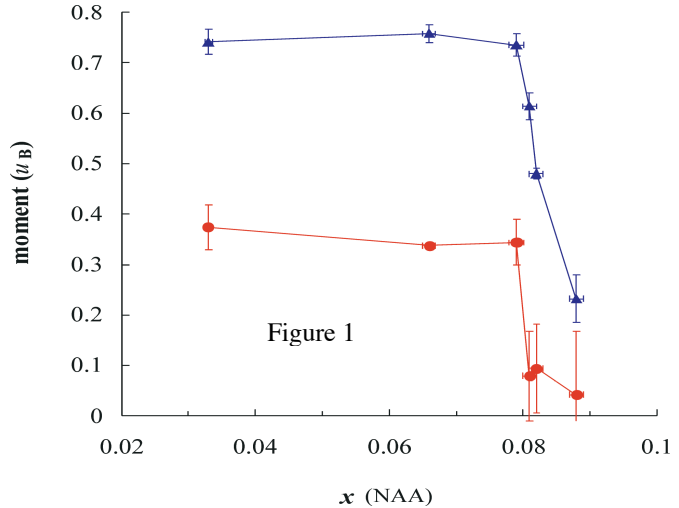
A. S. Sefat, J. E. Greedan  
*Chemistry Department, McMaster University, 1280 Main Street West, Hamilton, ON,  
L8S4M1.*

The  $Ti^{3+}$  magnetic moments in the Mott insulator  $NdTiO_3$  (Pnma space group) are antiferromagnetically (AF) ordered below 100K. It was found that having neodymium deficiencies rapidly disorders the moments by introducing  $Ti^{4+}$  and reduces the ordering temperature  $T_N$ . Small vacancy-doping ( $x=0.082$ ) was found to destroy the long-range magnetic ordering and cause the emergence of metallic properties, i.e. a Mott transition.



To explore the interplay of the magnetic and electronic interactions for the  $\text{Nd}_{1-x}\text{TiO}_3$  compositions in the intermediate region between the itinerant and the localized states, a systematic study of a series of compositions in  $0 < x < 0.15$  region has been performed.

The magnetic susceptibility of the  $\text{Nd}_{1-x}\text{TiO}_3$  compounds with  $x = 0.033(1)$ ,  $0.066(1)$ ,  $0.078(1)$ ,  $0.082(1)$ ,  $0.088(1)$  show ZFC/FC divergences below  $\sim 98\text{K}$ ,  $90\text{K}$ ,  $84\text{K}$ ,  $40\text{K}$ , and  $35\text{K}$ , respectively. Powder neutron diffraction experiments, found long-range AF order for  $x = 0.033$ ,  $0.066$ ,  $0.078$ . For the  $x = 0.082$ ,  $0.088$  compositions, broad magnetic reflections were indicative of short-range AF order. The refined magnetic moments for  $\text{Ti}^{3+}$  ( $G_x$ ) and  $\text{Nd}^{3+}$  ( $C_y$ ) remain constant up to the Mott transition and then disappear precipitously as shown in Figure 1. The magnetic susceptibility and neutron diffraction result are complemented by specific heat, resistivity, and Seebeck coefficient measurements on the same compositions.



## Resolving the distortion in the square nets of tellurium of the modulated $\text{RETe}_3$ ( $\text{RE}=\text{Ce}$ , $\text{Pr}$ and $\text{Nd}$ ) materials

Christos Malliakas and Mercuri G. Kanatzidis

*Department of Chemistry, Michigan State University, East Lansing, Michigan 48824*

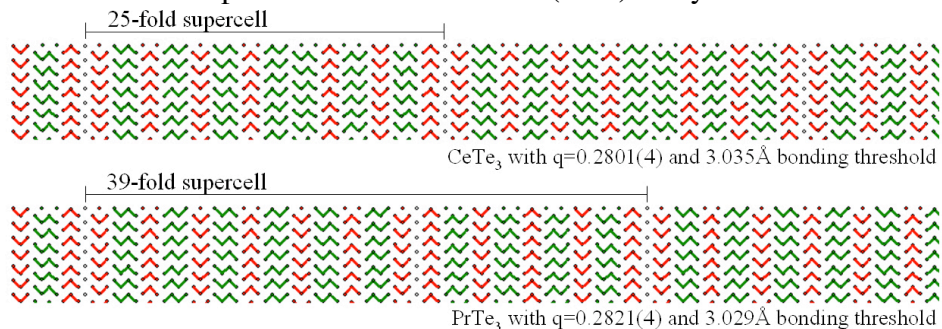
HyunJeong Kim and Simon Billinge

*Department of Physics and Astronomy, Michigan State University*

In polytellurides extended Te–Te bonding is frequently observed with flat square nets of tellurium. At first glance these nets are highly symmetric but a closer look almost always reveals these square nets to be prone to distortions and the respective compounds to exhibit commensurately or incommensurately modulated superstructures. When the formal oxidation state of all Te atoms in the net is  $-2$ , a stable square net is observed (e.g.,  $\text{NaCuTe}$ ). However, when the formal oxidation state is  $< -2$ , or when there are atomic vacancies in the square net, structural distortions are possible leading to Te–Te bonding interactions and the formation of  $\text{Te}_x^{n-}$  species within the net. These distortions are manifested through the formation of a superstructure with respect to the ideal square net. Compounds with these features can give rise to interesting physical properties such as charge density waves (CDW), anisotropic optical properties, and may even be interesting candidates for thermoelectric investigations.

The structures of the rare earth trichalcogenides  $\text{REQ}_3$  have been known since the 60s. According to these early investigations, they compounds crystallize in the so-called  $\text{NdTe}_3$  type in space group  $\text{Cmcm}$ . The structure consists of puckered  $[\text{NdTe}]$  double slabs, and layers of tellurium made of “perfect” square planar Te atoms stacked in the order  $-\text{[NdTe]}-\text{[Te]}-\text{[Te]}-$ .

We have solved the modulated structures of the RETe<sub>3</sub> compounds (RE=Ce, Pr and Nd) using both 3D conventional crystallography and the 4D superspace approach (q-vector). We have confirmed the resulting crystal structures as being representative of the total bulk crystals using synchrotron radiation and pair distribution function (PDF) analysis.



### Dielectric Property of Perovskite Oxynitrides

Young-II Kim and Patrick M. Woodward

*Department of Chemistry, The Ohio State University, Columbus, Ohio 43210*

Dielectric properties of simple and complex perovskite oxynitrides have been investigated by ac impedance spectroscopy using cold-isostatic-pressed specimens with ~55 % density. Equivalent circuit analysis of impedance spectra showed that BaTaO<sub>2</sub>N and SrTaO<sub>2</sub>N have unexpectedly high bulk dielectric constants,  $\kappa \sim 4900$  and 2900 respectively at room temperature. The dielectric constants of both compounds are frequency dependent and show a relatively weak, linear dependence upon temperature with no sign of a phase transition over the temperature range 300–180 K. The origin of those dielectric behaviors are not readily explained by the crystal structure analyses which indicated non-polar centrosymmetric crystal symmetries for BaTaO<sub>2</sub>N (*Pm-3m*) and SrTaO<sub>2</sub>N (*I4/mcm*). In the subsequent study, thin film BaTaO<sub>2</sub>N was epitaxially grown on (100) cut SrTiO<sub>3</sub> substrate with a conducting buffer layer of SrRuO<sub>3</sub> by pulsed-laser-deposition. The dielectric measurements on BaTaO<sub>2</sub>N thin film roughly reproduced the bulk property. For better understanding the origin of dielectric polarization in BaTaO<sub>2</sub>N, the extended X-ray absorption fine structure (EXAFS) spectroscopy has been performed at the Ta *L*<sub>3</sub>-edge. In contrast to the previous diffraction studies using X-ray, neutron, and electron radiations, the Ta *L*<sub>3</sub>-edge EXAFS revealed that the Ta<sup>+5</sup> coordination environment in BaTaO<sub>2</sub>N is severely distorted far from a regular octahedral picture, thus providing a clue to understand the high dielectric constant observed. Comparative results on complex oxynitride compositions, LaMg<sub>0.67-x</sub>Ta<sub>0.33+x</sub>O<sub>3-3x</sub>N<sub>3x</sub> and BaSc<sub>0.33</sub>Ta<sub>0.67</sub>O<sub>2.67</sub>N<sub>0.33</sub>, will be also presented.

## Crystal Structure of Uranyl Oxalates

Paul A. Giesting, Nathan J. Porter, and Peter C. Burns

*Dept. of Civil Engineering and Geological Sciences, University of Notre Dam*

Uranyl-organic complexation in geologic fluids can have a profound impact upon uranium solubility and transport. Studies of uranyl organic crystal structures provide a basis for understanding complexation in solution.

### Novel uranyl oxalates

The crystal structures of six novel uranyl oxalates have been determined. The compounds were synthesized by mild hydrothermal methods and their structures determined by single crystal X-ray diffraction. Three of these compounds form a compositional series:  $\text{K}(\text{UO}_2)_2(\text{C}_2\text{O}_4)_2\text{OH}(\text{H}_2\text{O})_2$  ( $\text{KUrOx}$ ),  $\text{Rb}(\text{UO}_2)_2(\text{C}_2\text{O}_4)_2\text{OH}(\text{H}_2\text{O})_{1.7}$  ( $\text{RbUrOx}$ ), and  $\text{Cs}(\text{UO}_2)_2(\text{C}_2\text{O}_4)_2\text{OH}(\text{H}_2\text{O})$  ( $\text{CsUrOx}$ ). The other three compounds differ only in structure and hydration state:  $(\text{UO}_2)_2\text{C}_2\text{O}_4(\text{OH})_2(\text{H}_2\text{O})_{2-a}$  ( $\text{UrOx2A}$ ),  $(\text{UO}_2)_2\text{C}_2\text{O}_4(\text{OH})_2(\text{H}_2\text{O})_{2-b}$  ( $\text{UrOx2B}$ ), and  $(\text{UO}_2)_2\text{C}_2\text{O}_4(\text{OH})_2(\text{H}_2\text{O})_3$  ( $\text{UrOx3}$ ). These structures demonstrate new features not previously known in this chemical system, in particular polymerization into infinite sheets and direct linkage of uranyl polyhedra. Further work on this chemical system seems likely to turn up further insights.

### Structural classification scheme for uranyl oxalates

Although a hierarchical scheme exists for classifying inorganic uranyl compounds,<sup>1</sup> no similar work has been done for organic compounds. Such a hierarchy would have practical benefits, in particular making structural information more accessible and understandable to workers studying related problems such as the environmental transport of hexavalent uranium as dissolved organic complexes. We offer a simple scheme that classifies uranyl oxalate structures by analyzing the long-range structural features and the coordination environments of uranyl ions, which leads to a structural symbol that can be used to easily identify uranyl oxalates with common structural features.

(1) Burns, P. C., Miller, M. L., and Ewing, R. C. (1996). U6+ minerals and inorganic phases: A comparison and hierarchy of crystal structures. *The Canadian Mineralogist*, 34:845.

## Exploring Anion Ordered Transition Metal Oxochloride Phases

M. Bieringer

*University of Manitoba, Department of Chemistry, Winnipeg, MB, R3T 2N2.*

Magnetic materials with large paramagnetic ion densities are desirable for a variety of applications. We are investigating 1-, 2-, and 3-dimensional magnetic systems with tailored sublattice topologies.

Commonly low dimensional magnetic sublattices are generated by separating paramagnetic ions with diamagnetic cations, e.g. insertion of diamagnetic layers into a given lattice. Alternatively the magnetic properties of solids with 3-dimensional cation lattices can be drastically changed through the introduction of multiple anions. Modifying anion sublattices introduces anisotropic magnetic exchange-interactions and can result in magnetic layers and

chains. The combination of tailored cation and anion architectures provides a powerful tool for the design and discovery of novel magnets.

In an effort to generate low-dimensional magnetic sublattices without sacrificing magnetic moment density anion ordered oxychlorides have been prepared. Systematic studies under oxidizing and reducing conditions using in-situ X-ray diffraction and thermal analysis techniques will be presented. Crystallographic structures, magnetic sublattice formation and magnetic properties will be discussed in detail. Neutron diffraction studies supplemented with magnetization data and muon spectroscopy results will be shown. In this presentation a variety of 1-dimensional and 2-dimensional systems will be contrasted with 3-dimensional structures.

### **Development of the Solid-State Microwave Synthetic Method for the Preparation of Diamond-Like Semiconductors**

Jonathan W. Lekse, Heather A. Figure, and Jennifer A. Aitken  
*Department of Chemistry, Duquesne University*

Diamond-like semiconductors (DLS) are of interest due to their technological applications and their compositional flexibility, which allows for the tailoring of physical properties. DLS have found uses in areas such as nonlinear optics and solar cells, among others. Previous synthetic work with DLS has focused primarily on high-temperature solid-state reactions, molecular beam epitaxy, directional solidification and molten metal growth. Solid-state microwave synthesis is another avenue that can be used to synthesize these materials; however, this technique is underutilized and poorly understood. In these reactions stoichiometric ratios of elemental or binary starting materials are ground together, sealed in quartz tubes and irradiated for several minutes. The reactions can reach temperatures in excess of 900°C within seconds, as initially determined by the morphology of the products, and more recently verified by an infrared temperature sensor. Solid-state microwave synthesis can be advantageous due to the short reaction times, which may stabilize metastable or kinetically stable phases not easily accessed via other methods.

Our research of the solid-state microwave synthetic method has initially focused on the known materials, AgInSe<sub>2</sub> and CuInS<sub>2</sub>. We are exploring the variables in solid-state microwave synthesis in order to utilize this method in a rational manner to prepare new diamond-like semiconductors and diamond-like semiconductors doped with magnetic ions. We have determined that reaction variables such as the irradiation time, microwave power, grinding time of the precursors and sample volume can have a profound effect on the outcome of the reactions. Adaptation of a research-grade microwave to determine reaction temperature profiles using an infrared temperature sensor and a thermocouple will be presented.

## **Combinatorial Processing and Characterization of Inorganic Materials**

James Cooper, Hongmei An, Qinxin Zhang, Guanghai Zhang, Paul J. McGinn  
*Dept of Chemical & Biomolecular Engineering, University of Notre Dame*

The combinatorial approach to materials investigations offers tremendous potential for accelerating the discovery of novel materials. This technique typically relies on parallel processing and screening in order to identify promising leads for further research. The combinatorial approach is being used for the development of novel materials for a wide variety of applications.

In our laboratories we are developing combinatorial processing and screening techniques for materials investigations in for a variety of applications including diesel soot catalysts, fuel cell electrodes, and dielectric materials for wireless communications. Combinatorial processing of materials in thin film and powder forms as practiced in our labs will be described.

Development of effective screening techniques in combinatorial investigations is often more challenging than processing issues. The use of scanning microwave microscopy for dielectric materials, scanning electrochemical microscopy and microarray characterization for fuel cell applications, and automated TGA for catalyst development will be discussed.

**Friday, May 27**

## **The Metal Flux – A Preparative Tool for the Exploration of Intermetallic Compounds**

Mercouri G. Kanatzidis

*Department of Chemistry, Michigan State University, East Lansing, MI 48824.*

This talk will highlight the use and great potential of liquid metals as exotic and powerful solvents (i.e. fluxes) for the synthesis and exploration of intermetallic phases. I will present results that demonstrate the considerable advances made in the discovery of novel and complex phases by utilizing molten metals as solvents. A representative cross-section of reported examples of flux-grown intermetallics and related solids will be discussed. The most commonly used metal fluxes in our group are Al, Ga and In and they will be surveyed and where possible, the underlying principal reasons that make the flux reactions work as well as reactivity trends among the flux metals will be discussed.

## **Square Net Distortion Engineering in the Titanium Antimonide $Ti_2Sb$**

Shahab Derakhshan<sup>a</sup>, Xiangyun Qiu<sup>b</sup>, Simon J. L. Billinge<sup>b</sup>, Holger Kleinke<sup>a</sup>

<sup>a</sup> *Department of Chemistry, University of Waterloo, Waterloo, ON, Canada N2L 3G1*

<sup>b</sup> *Department of Physics and Astronomy, Michigan State University, East Lansing, MI 48824*

Since the introduction of the Kleinke-Harbrecht structure map, our research group has focused on the crystal structure prediction, synthesis, and the experimental structure determination of new  $M_2Q$  compounds, where  $M$  is an early transition metal and  $Q$  is a pnictogen or chalcogen atom. Last year we uncovered the new binary titanium antimonide  $Ti_2Sb$  whose structure lies in a region between the  $Cu_2Sb$  and  $La_2Sb$  structure types in the structure map. Its powder diagram was reminiscent of the  $La_2Sb$  type. The La atom substructure of  $La_2Sb$  is composed of corner-sharing octahedra, elongated along the  $c$  axis. A square net with short La-La bonds is formed within the  $(ab)$  plane. Applying this model for the single crystal X-ray data revealed problematic thermal displacement parameters for the Ti atoms in this plane. Considering a distorted model composed of alternating squares and rhombs in the  $(ab)$  plane resulted in a much improved refinement. The model was subsequently proved by the real-space pair distribution function (PDF) technique utilizing both the X-ray and neutron powder diffraction data. Electronic structure calculations revealed that the driving force toward the distortion is a stabilization by the Ti-Ti interactions in the short diagonals of the rhombs.

Replacing Ti atoms by the heavier Zr atoms would move the material towards the  $La_2Sb$  structure type domain in the structure map. We successfully synthesized the series of  $Ti_{2-d}Zr_dSb$  ( $d = 0.25, 0.5, \text{ and } 0.78$ ), and our X-ray single crystal structure studies proved that by increasing  $d$  the distortion gradually disappears.

## Electronic Structure and Formation Pathway of the Transition Metal Oxide Hydride $\text{LaSrCoO}_3\text{H}_{0.7}$

C.A. Bridges, G.R Darling, M.A. Hayward, M.J. Rosseinsky  
Department of Chemistry, The University of Liverpool, Liverpool L69 7ZD, UK

A series of *in situ* and *ex situ* X-ray diffraction studies have been used to address the mechanism of hydrogen insertion to form  $\text{LaSrCoO}_3\text{H}_{0.7}$ .<sup>1,2</sup> The cobalt oxide-hydride is formed by a *chimie douce* reaction between  $\text{CaH}_2$  and  $\text{LaSrCoO}_4$ . The structure is related to the  $n=1$  member of the  $\text{A}_{n+1}\text{B}_n\text{O}_{3n+1}$  family of oxides, which is often described as an intergrowth of AO rock-salt and  $\text{ABO}_3$  perovskite layers. Oxide ions have been replaced within the perovskite layers to form chains of  $\text{CoO}_4$  squares, linked by hydride anions. *In situ* studies reveal both a relationship between the microscopic growth of the observed oxide hydride order and the anisotropic broadening of the diffraction profile, and the existence of a range of intermediate compositions. The unusual coexistence of oxide and hydride anions with a divalent transition metal cation produces questions about the electronic properties and electronic structure of the material. The influence of the hydride anion on the electronic properties has been investigated theoretically by full potential DFT band structure calculation and experimentally by determination of the Néel temperature for three-dimensional magnetic ordering. Calculations indicate that the electronic structure of  $\text{LaSrCoO}_3\text{H}$  is surprisingly similar to that of  $\text{LaSrCoO}_4$ .

- (1) Hayward, MA; Cussen, EJ; Claridge, JB; Bieringer, M; Rosseinsky, MJ; Kiely, CJ; Blundell, SJ; Marshall, IM; Pratt, FL; *Science* **295** (2002) 1882.
- (2) Poeppelmeier, K; *Science* **295** (2002) 1849.

## Chemistry of the Giant Magnetocaloric Effect Material $\text{Gd}_5\text{Si}_2\text{Ge}_2$ and Related Phases

Yurij Mozharivskyi<sup>1</sup> and Gordon J. Miller<sup>1,2</sup>

<sup>1</sup> Ames Laboratory of US DOE, Ames, Iowa 50011-3020

<sup>2</sup> Department of Chemistry, Iowa State University, Ames, Iowa 50011-3111

Magnetic refrigeration has a potential for large-scale industrial applications. The discovery of the giant magnetocaloric effect in  $\text{Gd}_5\text{Si}_2\text{Ge}_2$  around room temperature can make this possibility a reality.<sup>1</sup> The  $\text{Gd}_5\text{Si}_2\text{Ge}_2$  phase proves to have a rich structural chemistry and interesting magnetic properties, and exhibits unusual phenomena, namely structural and magnetic memory effects. Detailed analyses of the structural transitions and bonding in  $\text{Gd}_5\text{Si}_2\text{Ge}_2$  and related phases give us insights into the structure-property relationship and allow us to formulate some guiding principles for designing new magnetocaloric materials.

- (1) V. K. Pecharsky and K. A. Gschneidner, Jr., *Phys. Rev. Lett.*, **78**, 4494 (1997).

## The Crystal Chemistry of Actinyl Peroxides

P.C. Burns<sup>1,2</sup>, Karrie-Ann Kubatko<sup>1</sup>, G. Sigmon<sup>1</sup>, M. Antonio<sup>2</sup> and L. Soderholm<sup>1,2</sup>

<sup>1</sup> *Department of Civil Engineering and Geological Sciences, University of Notre Dame*

<sup>2</sup> *Chemistry Division, Argonne National Laboratory, Argonne IL, 60439*

Our initial interest in actinyl peroxide solid state chemistry stems from their potential importance for understanding the mobility of actinides in the environment. Alpha radiolysis of water associated with nuclear waste in a geological repository, or nuclear waste in storage, results in the formation of peroxide that may combine with actinyl ions to form a variety of structures. Study of this complex system has revealed considerable structural diversity and unexpected structural topologies. Under acidic to neutral solutions, phases such as the mineral studtite,  $\text{UO}_2\text{O}_2(\text{H}_2\text{O})_4$ , readily crystallize from solution. The structure of studtite contains chains of edge-sharing uranyl hexagonal bipyramids, and the shared edges correspond to peroxide groups with corresponding edge-lengths of  $\sim 1.45 \text{ \AA}$ . Adjacent chains are linked through H bonding that extends between the chains and interstitial  $\text{H}_2\text{O}$  groups. Under alkaline ambient conditions, a diverse group of actinyl peroxides have been synthesized that contain a variety of structural units, ranging from isolated actinyl triperoxide clusters through sheets and rings of polyhedra to unprecedented spherical nanoclusters. The nano-scale actinyl peroxide clusters are spherical and contain 24, 28 or 32 actinyl polyhedra. Small-angle X-ray scattering data have shown that these clusters self-assemble in solution prior to crystallizing. These clusters are polyoxometalates, and present many interesting possibilities for future study.

### **Synthesis, Photoluminescence, and Quantum-Confinement Effects of Colloidal InP Quantum Wires and Quantum Rods**

Wang, Fudong; Loomis, Richard A.; Kirmaier, Chris; Holten, Dewey; Buhro, William E.  
*Department of Chemistry, Washington University, Saint Louis, MO, USA.*

We report the solution-liquid-solid growth of soluble, narrowly dispersed InP quantum wires and rods with controllable diameters. These wires and rods are stabilized by hexadecylamine (HDA) and other conventional quantum-dot surfactants. Quantum wires are ideal 2D-confinement systems, the properties of which will be compared to those of the analogous 3D-confined dots and anisotropically 3D-confined rods. The critical length where a rod becomes a wire will be analyzed. The photoluminescence of these quantum wires and rods will also be described.



## Wide Band-Gap *p*-Type Semiconductor BaCuSF and Related Materials: Powder and Thin Films

Cheol-Hee Park,<sup>†</sup> Robert Kykyneshi,<sup>‡</sup> Janet Tate,<sup>‡</sup> and Douglas A. Keszler<sup>†</sup>

<sup>†</sup> *Department of Chemistry, Oregon State University, Corvallis, Oregon 97331-4003*

<sup>‡</sup> *Department of Physics, Oregon State University, Corvallis, Oregon, 97331-6507*

To realize transparent electronic and electro-optic devices, it is necessary to develop wide band-gap complementary semiconductors having tunable band gaps. Transparent *n*-type conductors have been used for decades in a variety of electrical applications; *p*-type conductivity, however, is not common in transparent conductors. Since the report in 1997 of *p*-type conductivity in transparent CuAlO<sub>2</sub> films, other new materials have followed. Most *p*-type transparent conductors are oxides, but carrier mobilities in these materials are typically two orders of magnitude smaller than those for *n*-type transparent conductors.

Various *p*-type transparent conducting chalcogenides have been synthesized and characterized in this lab, including the family of compounds BaCuQF (Q=S, Se, Te). The sulfide and selenide members exhibit *p*-type conductivity and band gaps that allow transmission of much of the visible spectrum. With *p*-type doping, *e.g.*, substitution of several percent K for Ba, the highest conductivities have been found to be 82 S/cm for Ba<sub>0.9</sub>K<sub>0.1</sub>CuSF and 43 S/cm for Ba<sub>0.9</sub>K<sub>0.1</sub>CuSeF. Undoped BaCuSF also exhibits strong red luminescence near 630 nm under ultraviolet excitation, and band gaps can easily be tuned by varying Q. In this presentation, results from electrical and optical characterization of both powder and thin-film samples of BaCuQF will be described.

## The Chemical Nature of Polar Intermetallics: New Insights into the Chemical Bonding and Reactivity of Zintl Phases

Arnold M. Guloy  
*University of Houston*

Exploratory synthesis of salt-like intermetallics along the Zintl border offers unique opportunities in investigating structure-bonding-property relationships among materials at the border between metals and nonmetals. The Zintl concept is used in rationalizing the synthesis, stoichiometry, and chemical bonding of complex non-classical and ‘electron-poor’ Zintl phases that exhibit unusual chemical bonding (*e.g.* unsaturated hydrocarbon, aromatic and metallocene intermetallic analogs). These compounds and other newly discovered polar intermetallics add new insight to the structural and chemical bonding peculiarities of Zintl phases and the less polar intermetallics. In addition, results of exploratory forays into the yet unexplored chemical reactivity of Zintl phases will be presented. The mild reduction and oxidation of these salt-like intermetallics provides a novel route to new materials with interesting and properties structures.

## Redox-Driven Phase Transitions

P. Subramanya Herle, O. Crosnier, H. Kleinke and L.F. Nazar

*Department of Chemistry, University of Waterloo, Waterloo Ontario Canada N2L 3G1*

This presentation will focus on redox-driven phase transitions demonstrated by transition metal phosphides and silicides. Like nitrides in some respects and antimonides in others, phosphides have recently been shown to exhibit interesting behavior that is a combination of the other Group V members. We will discuss comparative structural aspects and the "intercalation" properties of these materials. Detailed aspects of these systems will follow, with focus on the rich chemistry exhibited by the copper phosphide system exhibited by  $\text{Li}_2\text{CuP}$  and  $\text{Cu}_3\text{P}$  that ranges from "topotactic insertion" of Li similar to graphite; reversible crystalline-amorphous transformations; to reversible extrusion of bulk metal that is reassimilated in the structure. *In-situ* XRD measurements were performed to investigate the structural evolutions of the electrode materials upon changes in redox states, and were augmented by local structure information obtained from EXAFS and XANES studies. Electronic calculations performed using tight binding LMTO calculations revealed details of the electronic structure and bonding, and the nature of the redox "centers" in the phosphides. The comparative chemistry of some new layered silicides will also be discussed.

## New Phase-Change Materials For Optical Data Storage Applications

Joseph B. Wachter<sup>1</sup>, K. Chrissafis<sup>2</sup>, Christos Malliakas<sup>1</sup>, Daniel Bilc<sup>3</sup>, K. M. Paraskevopoulos<sup>2</sup>,  
S. D. Mahanti<sup>3</sup>, and Mercuri G. Kanatzidis<sup>1</sup>

<sup>1</sup> *Department of Chemistry, Michigan State University, East Lansing, MI 48824*

<sup>2</sup> *Department of Physics, Aristotle University of Thessaloniki, 54124 Thessaloniki, Greece*

<sup>3</sup> *Department of Physics, Michigan State University, East Lansing, MI 48824*

Materials with a reversible glass-crystal phase transitions are highly sought after for optical data storage applications. The best materials should have moderate melting points, low enough to be reached with a low power laser but high enough to prevent self-crystallization, a difference in optical absorption wavelength between the crystalline phase and the glass, and a rapid and stable phase transition process. The semiconductor  $\text{KSb}_5\text{S}_8$  was found to be an excellent candidate for phase-change applications.<sup>1,2</sup> Upon cooling from a melt, the material does not recrystallize but rather forms a glass. Reheating to 287°C causes the material to crystallize. The structure of the glass was probed with atomic pair distribution function analysis (PDF) to show longer-range order than ordinarily seen in glasses, possibly accounting for the material's exceptionally fast transition rates. Solid solutions were prepared with compositions  $\text{K}_{1-x}\text{Rb}_x\text{Sb}_5\text{S}_8$ ,  $\text{K}_{1-x}\text{Tl}_x\text{Sb}_5\text{S}_8$ , and  $\text{Tl}_{1-x}\text{Rb}_x\text{Sb}_5\text{S}_8$ . This allows for composition-dependent tuning of optical and thermal properties. The glasses comprised by the solid solutions have nearly 100 °C variance in crystallization and melting temperatures, so they would be well-suited for many different applications in the data storage industry because of this tailoring ability. Syntheses, structures, and physical measurements will be presented.

- (1) Kyratsi, T.; Chrissafis, K.; Wachter, J.; Paraskevopoulos, K.; Kanatzidis, M. G. *Adv. Mater.* **2003**, *15*, 1428.  
 (2) P. Berlepsch, R. Miletich and Th. Armbruster, *Z. Kristallogr.* **1999**, *214*, 57.

### Use of *s*-Block Metal Aggregates in Controlling Network Assembly.

Kenneth W. Henderson, Dugald J. MacDougall, J. Jacob Morris, and Bruce C. Noll  
*Department of Chemistry and Biochemistry, University of Notre Dame, IN, USA*

The use of transition metal-containing cage or cluster compounds to control the assembly of infinite network materials in a predictable manner is quickly emerging as a highly promising strategy. In contrast, although many classes of *s*-block metal complexes are known to have extensive molecular aggregation chemistry, their use in network assembly has not yet been realized. This deficit may be explained by the considerable problems associated with these species, such as the spherical, non-polarizable, nature of the cations; the limited preference for fixed metal geometries, and the lability of metal-ligand bonding resulting in complex dynamic solution equilibria between aggregated species. In this submission we will outline our latest work demonstrating that these issues may be overcome through the judicious choice of metal, linker and reaction conditions. We have successfully prepared a series of extended network materials with topologies controlled by linking together pre-assembled *s*-block metal cages complexes. Extended structures include 3D diamondoid networks composed of  $\text{Li}_4(\text{OR})_4$  tetrameric cubane aggregates and primitive cubic lattices formed by the fusion of  $\text{Na}_6(\text{OR})_6$  hexameric cages. A model for network prediction in this area will also be discussed.

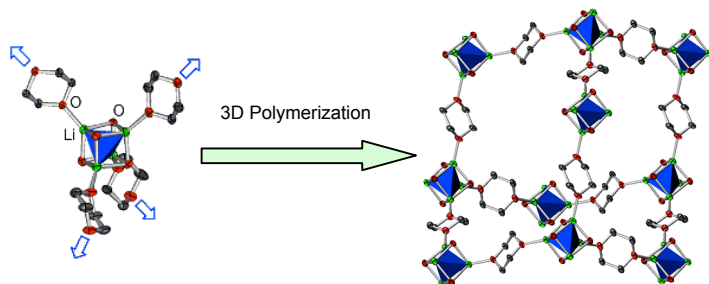


**Figure 1.**  $\text{Li}_4\text{O}_4$  tetrameric cubanes acting as tetrahedral nodes to give a diamondoid network.

### Transition Metal-Centered Zintl Anions in Solution

Jose M. Goicoechea and Slavi C. Sevov  
*Department of Chemistry and Biochemistry, University of Notre Dame*

Addition of  $d^{10}$  transition metal complexes to ethylenediamine solutions of  $\text{Ge}_9^{n-}$  ( $n = 2, 3, 4$ ) deltahedral clusters has resulted in the isolation and characterization of a wealth of new species. The transition metal can insert into the clusters and the resulting metal-centered species have been found to further aggregate to form more complex deltahedral species such as  $[(\text{Ni-Ni-Ni})@(\text{Ge}_9)_2]^{4-}$  or  $[(\text{Pd-Pd})@(\text{Ge}_{18})]^{4-}$ . The former exhibits a linear Ni-Ni-Ni filament protected by a

dimer of nine-atom germanium clusters and can be viewed as either two ten-atom [Ni@Ge<sub>9</sub>Ni] cages sharing a common vertex, or as two nine-atom [Ni@Ge<sub>9</sub>] clusters bridged by a  $\mu^6$ -Ni atom.

[Pd<sub>2</sub>@Ge<sub>18</sub>]<sup>4+</sup> exhibits a dimer of Pd atoms inside the largest single-cage deltahedron isolated to date. The cluster has a prolate shape deviating ever-so-slightly from the ideal D<sub>3d</sub> geometry expected for such a species. In addition to single crystal X-ray diffraction, these new species were also characterized by negative ion-mode ES mass-spectrometry which proved their existence in solution. The reactivity of the aforementioned clusters towards a variety of nucleophiles such as (C<sub>6</sub>H<sub>5</sub>)C≡C<sup>-</sup> will also be discussed.

### **Evidence for Electrostatic Stabilization in Thermally-Induced Growth of Alkanethiol-Gold Clusters Determined by a Unified Cluster Aggregation and Ripening Model.**

Shawn P. Resler and William E. Buhro  
*Washington University in Saint Louis*

A unified kinetic cluster aggregation and ripening model that includes the induction period, growth, and coarsening regimes was adapted from an Avrami-based nucleation and growth mechanism. The model was tested using thermally-induced growth of pre-synthesized decanethiol-capped gold (Au-DT) nanoclusters under varying Tetraoctylammonium Bromide (TOABr) concentrations as an example system. By varying the TOABr concentration in solution, a critical coagulation concentration (ccc) was elucidated at 0.62M. Existence of a ccc in Au-DT nanocluster solutions in organic solvents indicates that electrostatic stabilization is present. Fits of kinetic data from particle size distributions indicated an initial Reaction-Limited or Diffusion-Limited Cluster Aggregation (RLCA/DLCA) process (nucleation step) followed by crystal growth and aging according to an Ostwald ripening mechanism. We compare the nucleation and growth rate constants obtained from the unified model to those calculated from our data for each kinetic regime separately according to previously published cluster aggregation and coalescence models. The experimentally measured growth of cluster mass with time correlated favorably to the growth curve calculated using the model for each TOABr concentration. Additional support for the Ostwald ripening mechanism includes self-similarity of the particle size distributions in time.

### **Actinide Solution Speciation Using High-Energy X-Ray Scattering**

L. Soderholm<sup>1,2</sup>, S. Skanthakumar<sup>1</sup>, and Peter C. Burns<sup>1,2</sup>

<sup>1</sup> *Chemistry Division, Argonne National Laboratory, Argonne IL, 60439*

<sup>2</sup> *Department of Civil Engineering and Geological Sciences, University of Notre Dam*

Crystallographic structural data forms the template on which metal-ion coordination is understood. The metrical information obtained from single-crystal structural determinations is routinely used in understanding the physical properties of metal ions, including their chemical reactivity, electronic behavior and magnetic properties. Metal-ion properties in solution or in amorphous systems are more difficult to quantify because of the problems involved in extracting atom-atom correlations, which by definition are less well defined than in crystalline materials.

EXAFS spectroscopy has proved invaluable in providing some information about the near-neighbor environment in non-ordered systems but its low precision in determined coordination number, combined with its limitation to distances from the absorbing ion of less than about 5 Å often prohibit an adequate understanding of the problem at hand. High-energy (> 80 keV) X-ray scattering (HES) is proving to be an important complementary tool for probing metal-ion speciation in solution. Recent high-energy X-ray scattering experiments are providing a new picture of the metal-ion environment that includes metal-metal and metal-solvent correlations out to distances of 6 Å and longer. In selected cases the coordination environment in solution is providing insights into the metal-ion environments in the solid state.

**Saturday, May 28**

**Colloidal Semiconductor Quantum Wires: Synthesis, Spectroscopy, and Confinement Effects**

William E. Buhro

*Department of Chemistry, Washington University, St. Louis, MO 63130-4899*

The recent availability of soluble III-V and II-VI quantum wires having diameters in the range of 3 – 20 nm has afforded new opportunities to experimentally determine how quantum confinement is influenced by the geometric dimensionality of confinement. Quantum wires are ideal 2D-confinement systems, the properties of which may be compared to those of the analogous 3D-confined dots, 1D-confined wells, and anisotropically 3D-confined rods. The synthesis and spectroscopic behavior of several sets of quantum wires, grown by the solution-liquid-solid mechanism, will be described. The absorption and emission spectra of the wires are used to analyze the band gaps and photoluminescence quantum yields, which are compared to theory and to experimental data from wells, rods, and dots. The results confirm 2D quantum confinement in the wires, and establish quantitatively how the confinement in dots, rods, wires, and wells should differ.

We have observed weak room-temperature photoluminescence from the colloidal quantum wires. Our studies show that the photoluminescence quantum yields are influenced by factors previously known to influence quantum yields in quantum dots. These factors include preparative conditions, use of long-chain primary amine surfactants, post-synthesis photo-etching and photo-annealing, and introduction of wider-band-gap inorganic shells. We are also determining how single-nanowire spectroscopic behavior compares to the ensemble spectroscopic measurements. These and related studies will be described.

**Quasicrystals and Approximants in the Sc-Mg-Zn system: Prediction and Realization**

Qisheng Lin and John D. Corbett

*Department of Chemistry, Iowa State University, Ames, IA, 50010*

In searching for stable icosahedral quasicrystal phases, we have formulated a practical route for electronic tuning of approximants and quasicrystals. From the viewpoint of clusters,  $\text{Mg}_2\text{Zn}_{11}$  contains three shell 45-atom clusters that resemble Bergman clusters, generally considered as a guide to quasicrystals. Moreover, band structure calculations for  $\text{Mg}_2\text{Zn}_{11}$  reveal that 9 electrons per cell would be required (for a rigid band) to optimize the Zn–Zn bonding states and push the Fermi level into a pseudogap, on which basis quasicrystalline phases are predicated.<sup>1</sup> Here we present the results of tuning  $\text{Mg}_2\text{Zn}_{11}$  to crystalline approximants and quasicrystalline phases by replacement of part of Mg with Sc. Single crystal structures of two complex compounds, namely the 1/1 (**1**) and 2/1 approximants (**2**), were determined. The crystal **1**,  $\text{Sc}_3\text{Mg}_{0.19(2)}\text{Zn}_{17.81(2)}$ , crystallizes in *Im*3 with  $a = 13.863(2)$  Å and  $Z = 8$ , whereas crystal **2**,  $\text{Sc}_{11.2(1)}\text{Mg}_{2.5(1)}\text{Zn}_{73.22(5)}$ , occurs in *Pa*3 with  $a = 22.412(3)$  Å and  $Z = 8$ . Both crystals have a similar structure motif, that is, both contain 5-shell concentric polyhedral clusters as their building blocks. The building blocks are packed in a body-centered-cubic (*bcc*) manner in crystal **1**; in contrast, crystal **2** requires an additional double-Friauf cluster to fill in the voids formed

because of the primitive cubic packing of the 5-shell polyhedral clusters. Experimentally, a quasicrystalline phase,  $\text{Sc}_{10.8(6)}\text{Mg}_{3.2(6)}\text{Zn}_{86.1(2)}$  (according to EDX), was found with a composition close to that of crystal **2**. TB-LMTO-ASA band structure calculations on approximants are in excellent agreement with the predictions.

(1) Lin, Q.; Corbett, J.D., *Inorg. Chem.*, **2003**, *42*, 8762.

## Synthesis and Characterization of Layered Transition Metal Pnictate Nanoparticles – Precursor Materials to Pnictide Nanoparticle Arrays

Palaniappan Arumugam, Christopher Young and Stephanie L. Brock  
*Department of Chemistry, Wayne State University, Detroit, Michigan 48202*

The chemistry of nanoparticles of transition metal (TM) pnictides (pnictide = anion of group 15 elements) is not well explored, although the bulk phases show interesting magnetic and catalytic properties. A bottleneck in the exploration of size-dependent properties in these phases is the unavailability of reliable synthetic methods to prepare homogeneous nanoparticles. In our lab we have developed different methodologies to synthesize TM pnictide nanoparticles including a high temperature route employing coordinating solvents and hydrogen annealing of pnictate nanoparticles. Recently, we developed a surfactant assisted solvothermal method to synthesize nickel arsenate  $[\text{Ni}_3(\text{AsO}_4)_2 \cdot \text{H}_2\text{O}]$  nanoribbons and found that both carbothermal reduction using *in situ* TEM and hydrogen annealing on a supported substrate like mica affords periodic arrays or patterns of nickel arsenide nanoparticles. In this presentation the above methodology will be described in detail and the potential to produce other TM pnictide nanoparticle arrays starting from lamellar TM pnictate phases (particularly phosphate phases), will be discussed.

## Conducting Main Group Metal Oxides

P. M. Woodward, H. Mizoguchi, M. W. Stoltzfus  
*Department of Chemistry, Ohio State University*

Conductivity in metal oxides has been extensively studied for decades, although much of the focus has been on transition metal oxides. Metal oxides containing ions with filled d-subshells have not been studied as widely. Our interest in such compounds stems from their use as transparent conductors (doped  $\text{In}_2\text{O}_3$ ,  $\text{SnO}_2$ ,  $\text{ZnO}$  &  $\text{CdO}$ ), but they are also of interest for other applications, such as sensors and optoelectronic devices. In this presentation we will consider the interplay between local bonding interactions, crystal structure and electronic structure. The motivation for this study is a search for the structural and compositional features common to conducting main group oxides, which provides a qualitative framework for finding new compounds with attractive electrical and/or optical properties.

## Networking polyoxomolybdate-based clusters

Paul Kögerler

Ames Laboratory, Iowa State University, Ames, IA 50011

Polyoxomolybdates provide structurally versatile and rigid frameworks that can be functionalized by incorporating magnetic centers (e.g. 3d, 4f cations) or electron-rich groups.<sup>1</sup> This renders them attractive targets in the synthesis of magnetic molecules and functional molecular materials, the physical properties of which are primarily characterized by *intramolecular* electronic and magnetic interactions. An important next step is to gradually, if possible, introduce *intermolecular* interactions by interlinking the polyoxomolybdate-based cluster moieties. Recent examples for such molecules that can be linked to helical, 1, 2, or 3-dimensional coordination networks include molybdate-linked  $\{\text{Fe}_3\text{m}_3\text{-O}\}$  trimers, reduced  $\{\text{Mo}_8\text{Ag}_2\}$  clusters, or nanometer-sized spherical  $\{\text{Mo}_{72}\text{Fe}_{30}\}$ -type Keplerate clusters.<sup>2</sup> The presentation will focus on the requirements for linking such systems, the resulting networks, and the ramifications to their electronic and magnetic properties, including the time-resolved introduction of long-range magnetic ordering.

- (1) A. Müller, P. Kögerler, C. Kuhlmann, *Chem. Commn.* **1999**, 1347; A. Müller, P. Kögerler, A.W.M. Dress, *Coord. Chem. Rev.* **2001**, 222, 193.
- (2) A. Müller, S. K. Das, E. Krickemeyer, P. Kögerler, H. Bögge, M. Schmidtman, *Solid State Science* **2000**, 2, 847.

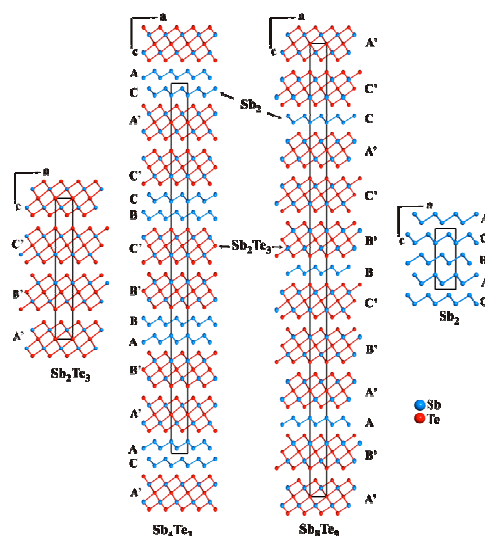
### Design in Solid State Chemistry Based on Phase Homologies: $\text{Sb}_4\text{Te}_3$ and $\text{Sb}_8\text{Te}_9$ as New Members of the Series $(\text{Sb}_2\text{Te}_3)_m \cdot (\text{Sb}_2)_n$

Pierre F. P. Poudeu and Mercuri G. Kanatzidis

Department of Chemistry, Michigan State University, East Lansing, MI 48824, USA

The concept of phase homologies has been demonstrated to be a powerful approach to design new solid state compounds [1]. Recently, the family of antimony tellurides with general formula  $(\text{Sb}_2\text{Te}_3)_m \cdot (\text{Sb}_2)_n$  has been recognized [2] to define a homologous series where the  $\text{Sb}_2\text{Te}_3$ ,  $\text{Sb}_2\text{Te}$  [3],  $\text{SbTe}$  [4] and  $\text{Sb}_2$  are currently known members. New homologues can be predicted by combining individual slabs from the structure of antimony,  $\text{Sb}_2$  [5], and slabs from the structure of  $\text{Sb}_2\text{Te}_3$  (Figure) in various ratios (i.e.  $m/n$ ). The total number of slabs in a  $\text{Sb}_2\text{Te}_3/\text{Sb}_2$  stacking sequence defines the cell parameters and the space group of each intermediate member.

$\text{Sb}_4\text{Te}_3$  and  $\text{Sb}_8\text{Te}_9$  are two new members of the  $(\text{Sb}_2\text{Te}_3)_m \cdot (\text{Sb}_2)_n$  family that were prepared starting from compositions calculated using the general formula. Both compounds as predicted by the homology crystallize in the trigonal space group  $R\bar{3}m$  with  $a = 4.2754(6)$  Å,  $c = 83.5640(2)$  Å





for  $\text{Sb}_4\text{Te}_3$  and  $a = 4.2738(5) \text{ \AA}$ ,  $c = 102.689(9) \text{ \AA}$  for  $\text{Sb}_8\text{Te}_9$ . In  $\text{Sb}_4\text{Te}_3$ , the  $\text{Sb}_2\text{Te}_3$ -type and  $\text{Sb}_2$ -type slabs alternate in pairs i.e. “two to two” to form a structure with 42 atomic layers (42R). This, contrast with the alternation of single  $\text{Bi}_2\text{Te}_3$ - and  $\text{Bi}_2$ - slabs, i.e. “one to one” found in the structure of  $\text{Bi}_4\text{Te}_3$  [6]. In the structure of  $\text{Sb}_8\text{Te}_9$ ,  $\text{Sb}_2\text{Te}_3$ -like and  $\text{Sb}_2$ -like slabs are arranged in the sequence “three to one” to form a structure with 51 atomic layers (51R).  $(\text{Sb}_2\text{Te}_3)_m(\text{Sb}_2)_n$  compounds are p-type semiconductors.

[1] A. Mrozek, M. G. Kanatzidis, *Acc. Chem. Res.*, 2003, **36**, 111-119.

[2] L. E. Shelimova, O. G. Karpinskii, M. A. Kretova, V. I. Kosyakov, V. A. Shestakov, V. S. Zemskov, F. A. Kuznetsov, *Inorg. Mater.*, 2000, **36**, 768.

[3] V. Agafonov, N. Rodier, R. Ceolin, R. Bellissent, C. Bergman, J. P. Gaspard, *Acta Crystallogr.*, 1991, **C47**, 1141.

[4] M. M. Stasova, O. G. Karpinskii, *Zh. Strukt. Khim.*, 1967, **8**, 654.

[5] D. Schiferl, *Rev. Sci. Instr.*, 1977, **48**, 24.

[6] K. Yamana, K. Kihara, T. Matsumoto, *Acta Crystallogr.*, 1979, **B35**, 147.

## The Magnetic Properties of Compounds with Clusters and low-D structures

Timothy Highbanks, Lindsay E. Roy, and Lucas Sweet

*Department of Chemistry, Texas A&M University, College Station, TX 77842-3012*

The magnetic moments of lanthanide atoms originate in their unpaired  $4f$ -electrons and consequently magnetic coupling involving Ln compounds involves an indirect mechanism that relies on interaction via  $6s$  and, especially,  $5d$  electron density. In the context of magnetically dilute alloys, the  $d$ -electron mediated exchange coupling has gives rise to the well-known “RKKY” coupling. The effective coupling envisioned in the dilute (RKKY) limit is not particularly useful in predicting or rationalizing the magnetic properties of compounds with much higher lanthanide contents. Work in our laboratory has demonstrated that spin-density functional (SDFT) calculations allow us to understand  $5d$ - $4f$  exchange coupling in quasimolecular and low-dimensional solids such as  $\text{Gd}_2\text{Cl}_3$ . An attempt to account for the calculated magnetic energies of competing “spin patterns” using an Ising model is unsuccessful, indicating that the latter model is inappropriate. The qualitative features can be interpreted using a perturbative molecular orbital (PMO) model that focuses the influence of the  $4f^7$ - $d$  exchange interaction on the  $d$ -based molecular orbitals. Fundamental to the  $d$ -electron mediated exchange mechanism is the intra-atomic  $4f^7$ - $d$  exchange interaction. The qualitative interpretation scheme developed on the  $\text{Gd}_2\text{Cl}_3$  benchmark system leads to a prediction that certain discrete molecular clusters might exhibit strong ferromagnetic coupling and therefore the possibility of finding large molecular magnetic moments that persist to ambient temperature and above. Also promising is the possibility of introducing  $4f^n$  ( $n \neq 7$ ) Ln centers will confer robust magnetic anisotropy on such molecules. Such molecules might then constitute a fascinating new class of single-molecule-magnets. Experimental and computational results pointing in this direction will be presented.

## List of Posters

- (1) Don Seo, Arizona State University  
*“Unified Understanding of Magnetic Exchange Interactions in Molecules and Solids: Spin Polarization as Perturbation within Density Functional Theory (DFT)”*
- (2) Nora Iancu, Qiangbin Wang, and Don Seo, Arizona State University  
*“Convenient Preparations of CdSe and CdSe@ZnS Quantum Dots (QDs) in Microwave-Assisted Low-Temperature Reaction Conditions: Utilization of B<sub>2</sub>Se<sub>3</sub>”*
- (3) Qiangbin Wang, Nora Iancu and Don Seo, Arizona State University  
*“Preparation of Mesoporous Silica Monoliths with Embedded CdSe@ZnS Core/Shell Quantum Dots (QDs) via New Non-Acidic Sol-Gel Route”*
- (4) M. J. Manos, R. G. Iyer, E. Quarez, J.H. Liao, M. G. Kanatzidis, Michigan State University  
*“{Sn[Zn<sub>4</sub>Sn<sub>4</sub>S<sub>17</sub>]}<sup>b</sup>: An Robust Open Framework Based on Metal-linked Penta-Supertetrahedral [Zn<sub>4</sub>Sn<sub>4</sub>S<sub>17</sub>]<sup>10-</sup> Clusters possessing ion-exchange properties”*
- (5) Sang-Hwan Kim and Don Seo, Arizona State University  
*“Structure Determination of a Ferromagnetic Mn<sub>2</sub>Ga<sub>3</sub> and Elucidation of its Structure-Magnetism Correlations”*
- (6) Kristy A. Gregg, Susanthri C. Perera, Samuel Shinozaki, Gavin Lawes, Stephanie L. Brock, Wayne State University  
*“Morphological Control and Characterization of MnP Nanoparticles”*
- (7) Tori Ziemann and Dr. Peter Burns, University of Notre Dame  
*“The Crystal Chemistry of Neptunium Sulfates and Phosphates”*
- (8) Karrie-Ann Kubatko, Peter C. Burns & Alexandra Navrotsky, University of Notre Dame and UC Davis  
*“Chemical Thermodynamics of Select Uranyl Phases”*
- (9) Tetsuhiro Katsumata, Akihiro Takase, Yoshiyuki Inaguma and John E. Greedan, Gakushuin University and McMaster University  
*“Magnetic and dielectric properties for perovskite-type oxyfluoride, PbFeO<sub>2</sub>F”*
- (10) Alex Norquist, Haverford College  
*“Acentric Materials”*
- (11) Heather Cuthbert and John Greedan, McMaster University  
*“Unexpected Magnetic Properties of the 4d and 5d Transition Metal Oxides, SrLaRuNiO<sub>6</sub> and La<sub>3</sub>Re<sub>2</sub>O<sub>10</sub>”*
- (12) A.D. Lozano-Gorrín, J.E. Greedan, Gianluigi Botton, Guillaume Radtke and P. Núñez, McMaster University and Universidad de La Laguna  
*“Studies of the Co<sup>3+</sup> Spin State and Oxygen Order/Disorder in the Defect Perovskites Ba<sub>2</sub>In<sub>2-x</sub>Co<sub>x</sub>O<sub>5</sub>”*
- (13) George H. Chan and Jim Ibers, Northwestern University  
*“Syntheses, Structure, and Physical Properties of ALnMQ<sub>3</sub> (A = alkali metal; Ln = Rare-earth or Y; M = Transition Metal; Q = S, Se, Te)”*
- (14) Nathan J. Takas, Austin M. Savatt and Jennifer A. Aitken, Duquesne University  
*“Characterization and Reactivity of Na<sub>3</sub>PO<sub>3</sub>S in the Solid-State”*

- (15) Paul H. Tobash and Svilen Bobev, University of Delaware  
*“Crystal Growth, Structural and Magnetic Property Studies on a Family of Ternary Rare-Earth Phases  $RE_2InGe_2$  ( $RE = Sm, Gd, Tb, Dy, Ho, Yb$ )”*
- (16) Laura M. Castro-Castro and John D. Corbett, Iowa State University  
*“Advances in the Synthesis of Yttrium and Lutetium Chalcogenides”*
- (17) Hongtao Yu and Stephanie L. Brock, Wayne State University  
*“Synthesis of Crystalline, Soluble  $MoS_2$  Nanocrystals”*
- (18) Keerthi Senevirathne, Stephanie L. Brock, Wayne State University  
*“Synthesis and Characterization of Discrete Nanoparticles of  $Ni_2P$ ”*
- (19) Bin Li and John D. Corbett, Iowa State University  
*“Synthesis, Structure, and Bonding of  $Na_3MIn_2$  ( $M = Au, Ag$ ): Participation of Na in the Anionic Network”*
- (20) Jing-Cao Dai and John D. Corbett, Iowa State University  
*“ $BaAu_{0.4}Tl_{1.6}$ ,  $BaAu_{0.35(4)}In_{1.65(4)}$  and  $BaHg_{0.92(2)}In_{1.08(2)}$ : three new intermetallics with  $CeCu_2$ -type structures”*
- (21) Wendy L. Burns, Northwestern University  
*“Syntheses and Structures of f-Electron Selenite Hydroselenites”*
- (22) Ming-Hui Ge and Jing-Tai Zhao, Shanghai Institute of Ceramics  
*“ $[CH_3(CH_2)_{11}NH_3^+][H_2PO_4^-]$ : Its crystal structure and unusual photoluminescent property”*
- (23) Kennedy K. Kalebaila and Stephanie L. Brock, Wayne State University  
*“Synthesis and Characterization of High Surface Area Germanium Sulfide Aerogels”*
- (24) Jacques Barbier, Nicolas Penin, Anton Dabkowski and Lachlan M. Cranswick, McMaster University and Chalk River Laboratories  
*“The non-centrosymmetric melilite-type borates  $Bi_2ZnB_2O_7$  and  $CaBiGaB_2O_7$ ”*
- (25) Gerasimos S. Armatas, Nan Ding and Mercuri G. Kanatzidis, Michigan State University  
*“Mesostructured Semiconductors via Supramolecular Assembly of  $[Ge_4Q_{10}]_4$  ( $Q=S, Se$ ) Adamantane Clusters with  $Ru^{2+}$  and Cationic Surfactants”*
- (26) Valentina Ganzha-Hazen and Stephanie L. Brock, Wayne State University  
*“Solvothermal syntheses of  $Cu_3P$  via reactions of amorphous redphosphorous with a variety of copper sources”*
- (27) Jared P. Smit, Peter C. Stair, and Kenneth R. Poeppelmeier, Northwestern University  
*“Structure and Cation Distribution of  $Mg_2CrV_3O_{11}$ ,  $Mg_2GaV_3O_{11}$ , and  $Mg_2InV_3O_{11}$ ”*
- (28) Ian Saratovsky, Jean-François Gaillard, and Kenneth R. Poeppelmeier, Northwestern University  
*“Structure of manganese oxide produced by *Leptothrix discophora* SP6”*
- (29) Sujith Perera, Nadiya Zelenski, and Edward G. Gillan, University of Iowa  
*“Rapid solid-state synthesis of crystalline, photocatalytic active titanium oxides”*
- (30) Jong Lak Choi and Edward G. Gillan, University of Iowa  
*“Solvothermal Routes to Crystalline Metal Nitrides via Metal Azide Precursor Decomposition”*
- (31) Dharmika Herath and Stephanie L. Brock, Wayne State University  
*“Synthesis and Characterization of New Clathrate I Type Pnictogen Halide Materials”*

- (32) Lucas Sweet and Tim Hughbanks, Texas A&M University  
*"Synthesis, Structure and Magnetic Properties of Rare Earth Cluster Compounds"*
- (33) Jianxiao Xu, Heather L. Cuthbert, John E. Greedan, Holger Kleinke, University of Waterloo and McMaster University  
*"Synthesis, Structure and Physical Properties of the new layered Cu<sup>II</sup> oxide Na<sub>2</sub>Cu<sub>2</sub>TeO<sub>6</sub> with a distorted honeycomb lattice"*
- (34) Navid Soheilnia, Jon Giraldi, Holger Kleinke, University of Waterloo  
*"Thermoelectric Properties of n-type Nb<sub>3</sub>Sb<sub>d</sub>Te<sub>7-d</sub>"*
- (35) Angang Dong and William E. Buhro, Washington University  
*"Solution-Based Zinc Chalcogenide Semiconductor Nanowires: Preparation and Properties"*
- (36) Michael R. Marvel and Kenneth R. Poeppelmeier, Northwestern University  
*"Solid State Oxide Fluoride Anions"*
- (37) Digamber Porob and Paul Maggard, North Carolina State University  
*"Synthesis and characterization of Bi<sub>4</sub>Ti<sub>3</sub>O<sub>12</sub>-AMO<sub>3</sub> (A=Bi, La; M=Cr, Mn, Fe, Co, Ni) series of compounds"*
- (38) Danielle L. Gray and Jim Ibers, Northwestern University  
*"A Uranium Assisted Synthesis of Ba<sub>4</sub>Fe<sub>2</sub>I<sub>5</sub>S<sub>4</sub> and CsTi<sub>5</sub>Te<sub>8</sub>"*
- (39) Bangbo Yan, Paul Maggard, North Carolina State University  
*"Insertion of Metal-Organic Coordination Polymers into V<sub>2</sub>O<sub>5</sub>: Hydrothermal Syntheses and Characterizations of [M(py<sub>z</sub>)]<sub>0.5</sub>V<sub>2</sub>O<sub>5</sub> (M = Co, Ni)"*
- (40) Susan E. Lattner, Florida State University  
*"Synthesis of new carbide phases from mixed rare earth/transition metal fluxes"*
- (41) Nan Ding and Mercuri G. Kanatzidis, Michigan State University  
*"From [Cd<sub>4</sub>Sn<sub>3</sub>Se<sub>13</sub>]<sup>6-</sup> to [Cd<sub>60</sub>Sn<sub>48</sub>Se<sub>184</sub>]<sup>56-</sup>: Acid-Induced 3D to 3D Single-Crystal Transformation"*
- (42) Matthew A. Gave, Christos Malliakas, and Mercuri G. Kanatzidis, Michigan State University  
*"Impressive Structural Diversity in the System Tl/Bi/P/S"*
- (43) Huajun Zhou, Bruno Cloix, and Abdou Lachgar, Wake Forest University  
*"One-dimensional Coordination Polymers Based on Octahedral Cluster Anion [Nb<sub>6</sub>Cl<sub>12</sub>(CN)<sub>6</sub>]<sup>4-</sup> and Phenoxo-bridged Dimer [Mn<sub>2</sub>(7-Me-salen)<sub>2</sub>]<sup>2+</sup>"*
- (44) Hyunjin Ko, Christopher J. Kurtz, Gordon J. Miller, Iowa State University  
*"Electronic Structures and Magnetic Orderings in MM'As Compounds (M, M' = Cr, Mn, Fe)"*
- (45) Katie L. McNerny and Jennifer A. Aitken, Duquesne University  
*"Preparation of Diamond-like Semiconductors with Potentially Interesting Nonlinear Optical Properties"*
- (46) Britt A. Vanchura II, Christos Malliakas, and Mercuri G. Kanatzidis, Michigan State University  
*"Successes and Setbacks in the Synthesis of Borides Using a Molten Metal Flux"*
- (47) Jun-Ho Kim and Mercuri G. Kanatzidis, Michigan State University  
*"Synthesis and Thermoelectric Properties of CdBi<sub>4</sub>S<sub>7</sub>"*
- (48) Mi-Kyung Han and Gordon J. Miller, Iowa State University  
*"LaFe<sub>13-x</sub>Si<sub>x</sub> with the NaZn<sub>13</sub> Structure Type: La(Fe<sub>x</sub>Si<sub>1-x</sub>)<sub>13</sub>"*

- (49) Erin M. Sorensen, Heather K. Izumi, John T. Vaughey, Charlotte L. Stern, and Kenneth R. Poeppelmeier, Northwestern University and Argonne National Laboratory  
*“Ag<sub>4</sub>V<sub>2</sub>O<sub>6</sub>F<sub>2</sub>: An New Electrochemically Active Phase”*
- (50) Janet E. Kirsch, Heather K. Izumi, Charlotte L. Stern, and Kenneth R. Poeppelmeier, Northwestern University  
*“Synthesis and Characterization of the Face-Sharing Biocahedral [Mo<sub>2</sub>O<sub>6</sub>F<sub>3</sub>]<sup>3-</sup> Anion”*
- (51) Lindsay E. Roy and Timothy Highbanks, Texas A&M University  
*“Computational and Conceptual Tools for Understanding Magnetic Ordering in Reduced Lanthanide Compounds”*
- (52) Sumohan Misra and Gordon J. Miller, Iowa State University  
*“Structural Characterization and Magnetic Measurements of Gd<sub>5-x</sub>Y<sub>x</sub>Tt<sub>4</sub> (Tt = Si, Ge)”*
- (53) Meghan Knapp and Patrick Woodward, Ohio State University  
*“Structure and Properties of Perovskites Exhibiting Cation ordering of the A and B Sites”*
- (54) Aurélié Guéguen, Eric Quarez, Kuei-Fang Hsu, and Mercouri G. Kanatzidis, Michigan State University  
*“Exploratory synthesis of lead substitution in the homologous family CsPb<sub>m</sub>Bi<sub>3</sub>Te<sub>5+m</sub>”*
- (55) Shawna R. Brown, Susan M. Kauzlarich, G. Jeff Snyder, and Franck Gascoin, University of California at Davis and Jet Propulsion Laboratory  
*“Investigation of Zn Doping onto the Mn site of the Yb<sub>14</sub>MnSb<sub>11</sub> System”*
- (56) Xiuni Wu and Mercouri G. Kanatzidis, Michigan State University  
*“Ternary Yb Compounds Grown from Al Flux”*
- (57) Pesak Rungrojchaipon, Ekaterina V. Anokhina, and Allan J. Jacobson, University of Houston  
*“Crystal structure and characterization of Ta<sub>2</sub>WO(PO<sub>4</sub>)<sub>4</sub>”*
- (58) Tae-Soo You and Gordon J. Miller, Iowa State University  
*“Structural and Electronic Comparisons in Polar Intermetallic Compounds : Experimental and Theoretical Studies of MGe<sub>2</sub>, MGaGe and MZnGe (M=Eu or Sr)”*
- (59) YongBok Go, Xiqu Wang, Ekaterina V. Anokhina, and Allan J. Jacobson, University of Houston  
*“The Influence of Reaction Temperature and pH on the Coordination modes of the 1,4-benzenedicarboxylate (BDC) ligand: A Case Study of the Ni(II)-1,4-BDC-2,2'-Bipyridine System”*
- (60) Matthew J. O'Malley, Patrick M. Woodward, Henk Verweij, Ohio State University  
*“Identification of New Lithium Ruthenium Ternary Oxide: Conductivity and Crystal Structure Determination”*
- (61) Iliya Todorov and Slavi C. Sevov, University of Notre Dame  
*“Use of Mixed A/AE and A/RE Cations as a Way to Novel Zintl Phases”*
- (62) Marie Vougo-Zanda, Ekaterina V. Anokhina, and Allan J. Jacobson, University of Houston  
*“Hydrothermal Synthesis and Structure of Al(OH)(C<sub>12</sub>H<sub>6</sub>O<sub>4</sub>)·1.7(H<sub>2</sub>O)”*
- (63) In Chung and Mercouri G. Kanatzidis, Michigan State University  
*“Synthesis and Characterization of the New Selenophosphate Ternary Compounds: K<sub>2</sub>P<sub>2</sub>Se<sub>6</sub>, Rb<sub>4</sub>P<sub>6</sub>Se<sub>12</sub> and Cs<sub>2</sub>P<sub>2</sub>Se<sub>8</sub>”*
- (64) M. A. Chondroudi, J. R. Salvador, C. Malliakas, Xiuni Wu, M. G. Kanatzidis, Michigan State University  
*“Rare-earth intermetallic phases of the type RECu<sub>6+x</sub>In<sub>6-x</sub> (RE= Ce, Nd, Ce, Nd, Sm, Gd, Dy, Ho, Er, Yb) and LaCu<sub>7</sub>In<sub>6</sub> from liquid Indium”*

- (65) S. Skanthakumar, L. Soderholm, Peter C. Burns, M.R. Antonio, and Tori Ziemann, Argonne National Laboratory and University of Notre Dame  
*“Cation-Cation Interactions in Neptunyl(V) Systems”*
- (66) C. Lanier, L.D. Marks, K.R. Poeppelmeier, Northwestern University  
*“Reduction of  $Mg_3V_2O_8$  to  $Mg_3V_2O_6$ : Insight into Catalysis”*
- (67) Matthew W. Stoltzfus, Pat Woodward, and Bruce Bursten, Department of Chemistry, Ohio State University  
*“Lone pair distortions involving  $ns^2$  cations in ternary metal oxides”*
- (68) Dugald J. MacDougall, J. Jacob Morris, Bruce C. Noll, Kenneth W. Henderson, Department of Chemistry and Biochemistry, University of Notre Dame  
*“Tetrameric Cage Aggregates of Lithium Organyloxides as Secondary Building Units: Controlling Assembly in Zero One Two and Three Dimensions”*
- (69) Jeffrey A. Rood, J. Jacob Morris, Dugald J. MacDougall, Bruce C. Noll, Kenneth W. Henderson, Department of Chemistry and Biochemistry, University of Notre Dame  
*“Self-Assembly of Two and Three Dimensional Networks by Hexameric Sodium Aryloxides”*
- (70) J. Jacob Morris, Bruce C. Noll, Kenneth W. Henderson, Department of Chemistry and Biochemistry, University of Notre Dame  
*“Control of Lithium Aggregate Assemblies Through Solvent Effects”*

# Abstracts

## Poster Presentations

### **Unified Understanding of Magnetic Exchange Interactions in Molecules and Solids: Spin Polarization as Perturbation within Density Functional Theory (DFT)**

Don Seo

*Department of Chemistry and Biochemistry, Arizona State University, Tempe, AZ 85287-1604*

One difficulty in understanding magnetic interactions is that the current theories are not originated from the same theoretical framework among different magnetic systems. For organic diradicals, configuration interactions (CI) or unrestricted Hartree-Fock (UHF) methods are used for total energy calculations of different spin states, and yet qualitative “Different Orbitals for Different Spins (DODS)” concept is employed in general for the interpretation of the calculational results. For transition metal complexes, despite the great success of the broken-symmetry DFT method, the semi-quantitative understanding of the results has been mainly based on the models that were derived by explicit treatments of CI. Metallic magnetism is currently investigated using spin-polarized DFT band calculations with a reasonable predictability, and yet the interpretation of the calculation outcomes remains qualitative except the case of Stoner theory derived from the linear response theory.

To provide a coherent picture to the problem, we have created a new theoretical formalism for understanding magnetic interactions, by developing a new perturbational orbital theory that employs spin-polarization density as a perturbation in the density functional formalism. Within the local density approximation, we show that the new theory provides a conceptual machinery that allows us to understand systematically and (semi)quantitatively the outcome of calculations and even predict relative stability of different magnetic states solely based on the shapes and one-electron energies of Kohn-Sham orbitals. Within the unified theoretical framework, we now attempt to explain spin polarization in atoms, Hay-Thibeault-Hoffmann theory for dimeric metal complexes, DODS concept for organic diradicals, Stoner condition for metallic ferromagnetism, Slater antiferromagnetism, non-rigid band behavior of half metals and Mott-Hubbard behavior of half-filled systems.

### **Convenient Preparations of CdSe and CdSe@ZnS Quantum Dots (QDs) in Microwave-Assisted Low-Temperature Reaction Conditions: Utilization of B<sub>2</sub>Se<sub>3</sub>**

Nora Iancu, Qiangbin Wang and Don Seo

*Department of Chemistry and Biochemistry, Arizona State University, Tempe, AZ 85287-1604*

The II-V semiconducting QDs are one of the most studied nanomaterials in recent years due to their unique optical tunability, and their ever-increasing research and applications prompt further efforts in synthesis aimed at improved affordability, scalability, versatility and reproducibility. By utilizing amine-soluble B<sub>2</sub>Se<sub>3</sub> as a versatile Se source, we have developed a new synthetic method that provides CdSe QDs (5 ~ 16 nm in diameter) at low temperatures from 70 to 200 °C. The preparations are carried out by heating a mixture of CdCl<sub>2</sub> and B<sub>2</sub>Se<sub>3</sub> dissolved in oleyl amine as a coordinating solvent without a need of a Schlenk line and solvent-refluxing unit. The original process has been extended to utilize non-coordinating “polar” solvents such as 1,3-dimethyl-3-imidazolidinone (DMI) and N-methyl pyrrolidinone (NMP), and this allows us to replace the original oleyl amine capping molecules by various other long-chain molecules such as tri-octyl phosphine oxide (TOPO), octadecylthiol (ODT) and 3-mercaptopropyl-trimethoxysilane (MPS)). CdSe@ZnS core/shell structures also can be prepared in a single-step process in which the shell formation occurs simultaneously with the replacement of capping molecules but without the undesired core-particle growth. This work presents also the first successful use of microwave-assisted heating for highly luminescent size-controlled II-V QDs with a good reproducibility.

## Preparation of Mesoporous Silica Monoliths with Embedded CdSe@ZnS Core/Shell Quantum Dots (QDs) via New Non-Acidic Sol-Gel Route

Qiangbin Wang, Nora Iancu and Don Seo

Department of Chemistry and Biochemistry, Arizona State University, Tempe, AZ 85287-1604

Because of their superior optical tunability and photostability, II-V semiconducting quantum dots (QDs) may replace organic dye molecules in some optical applications. Especially, incorporation of the photostable QDs in silica glasses may provide better performance over the recently developed tunable dye lasers prepared by the sol-gel method. Because of their decomposition in acidic media, however, CdSe QDs have remained one of the challenging materials to be incorporated in silica composites via conventional sol-gel routes. By utilizing ammonia as a catalyst, we now show that highly transparent silica monoliths can be prepared with embedded QDs without suppressing the QDs' desired optical properties. In our mild preparation process, the core CdSe QDs are coated at first with a ZnS shell *simultaneously*, as 3-mercaptopropyltrimethoxysilane (MPS) replaces oleylamine, the original capping molecules. The low-temperature reaction condition avoids undesired core-particle growth during the coating, and the resultant MPS-capped CdSe@ZnS QDs are highly photoluminescent and well soluble in alcohols. Under optimized reaction conditions, co-condensation of the silanes of the capping molecules with additional tetramethyl orthosilicate (TMOS) results in highly transparent mesoporous silica monoliths that are embedded with well-dispersed CdSe@ZnS core/shell QDs.

## {Sn[Zn<sub>4</sub>Sn<sub>4</sub>S<sub>17</sub>]}<sup>6-</sup>: An Robust Open Framework Based on Metal-linked Penta-Supertetrahedral [Zn<sub>4</sub>Sn<sub>4</sub>S<sub>17</sub>]<sup>10-</sup> Clusters possessing ion-exchange properties

M. J. Manos, R. G. Iyer, E. Quarez, J.H. Liao, M. G. Kanatzidis

Department of Chemistry, Michigan State University, East Lansing MI 48842-1793

Chalcogenides with open frameworks can uniquely combine zeolitic microporous properties including solid acid, ion-exchange or absorption with semiconducting properties such as electronic, optical and photonic. Some chalcogenides with open frameworks are based on so-called super-tetrahedral clusters, denoted as  $T_n$  (where  $n$  is the number of metal layers).<sup>1</sup> Other frameworks are based on different units ranging from simple tetrahedra to so-called penta-supertetrahedral clusters denoted as  $Pn$ .<sup>1a</sup> The P1 series of discrete clusters  $A_{10}M_4M_4S_{17}$  ( $A = K, Cs$ ;  $M = Zn, Cd, Fe, Co$ ;  $M_4 = Sn, Ge$ ) were recently reported from our group.<sup>2</sup> This cluster type (P1) is an assembly of four  $MQ_4$  (T1) and one  $QM_4$  (anti-T1) structural units, where  $M$  is the metal ion and  $Q$  is the chalcogen atom (Figure 1a). The  $[M_4M_4S_{17}]^{10-}$  clusters have four terminal S atoms which are potential binding sites to other clusters or metal centers, and thus can offer themselves as building blocks for framework materials. Herein we report  $A_5 \cdot xK_{1+x}Sn[Zn_4Sn_4S_{17}](A = K^+, Rb^+, Cs^+, NH_4^+, H^+; x = 0, 4, 5)$ , the first examples of compounds consisting of P1  $[Zn_4Sn_4S_{17}]^{10-}$  clusters linked with  $Sn^{4+}$  centers (Figure 1b).<sup>3</sup> They feature a new type of open framework with excellent chemical stability. Further, we report the surprising finding that one fifth of the  $K^+$  ions play an important templating role in stabilizing the framework. The  $A^+$  ions fill relatively large voids and exhibit remarkably facile ion-exchange properties similar to those of small pore zeolites.

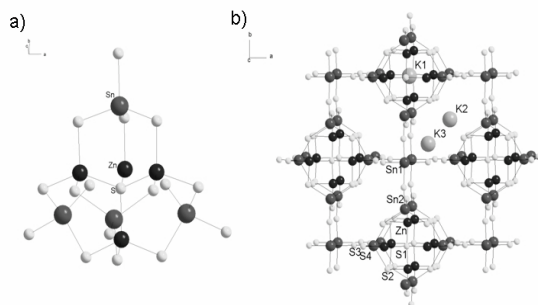


Figure 1

1. a) X. Bu, N. Zheng, P. Feng, *Chem. Eur. J.* **2004**, *10*, 3356 and references therein; b) H. Li, A. Laine, M. O'Keefe, O. M. Yaghi, *Science* **1999**, *283*, 1145.
2. a) O. Palchik, R. G. Iyer, J.H. Liao, M. G. Kanatzidis, *Inorg. Chem.* **2003**, *42*, 5052; b) O. Palchik, R. G. Iyer, J. H. Liao, M. G. Kanatzidis, *Z. Anorg. Allg. Chem.* **2004**, *630*, 2237.
3. M. J. Manos, R. G. Iyer, E. Quarez, J.H. Liao, M. G. Kanatzidis, *Angew. Chem. Int. Ed. Engl.* **2005** (in press).



## Structure Determination of a Ferromagnetic Mn<sub>2</sub>Ga<sub>5</sub> and Elucidation of its Structure-Magnetism Correlations

Sang-Hwan Kim and Don Seo

*Department of Chemistry and Biochemistry, Arizona State University, Tempe, AZ 85287-1604*

*p*-Metal-rich intermetallics generally do not show a ferromagnetism because (1) their structure formation is clearly influenced by chemical bonding between the magnetic atoms and the surrounding *p*-metals (strong *sp-d* orbital interactions), leading to a (pseudo-)bandgap at the Fermi level, and (2) the well-defined Stoner condition implies the absence of spin polarization for those compounds exhibiting a small density of states at the Fermi level. Mn<sub>2</sub>Ga<sub>5</sub> is intriguing, because it shows a strong ferromagnetism at room temperature although its composition lies clearly in the *p*-metal-rich regime. From our LMTO-ASA and FPLO (full potential local orbital) calculations, we have found that the electronic band structure of the Mn<sub>2</sub>Ga<sub>5</sub> exhibits a remarkable two-dimensional superdegeneracy near the Fermi level in the entire *a*\**b*\*-plane, and that the superdegeneracy causes the ferromagnetism (Stoner condition) despite the optimized Mn–Ga and Ga–Ga bonds in the structure. Fixed spin moment (FSM) calculation results for the Mn<sub>2</sub>Ga<sub>5</sub> are also consistent with the Stoner theory. The detailed orbital analysis shows that the superdegeneracy is originated from the orbital phase relationships between Mn (*d*<sub>xz</sub>, *d*<sub>yz</sub>) and Ga orbitals as well as from the unique Ga–Mn–Ga bond angles along the *c*-axis.

## Morphological Control and Characterization of MnP Nanoparticles

Kristy A. Gregg, Susanthri C. Perera, Samuel Shinozaki, Gavin Lawes, Stephanie L. Brock

*Department of Chemistry, Wayne State University, Detroit, MI 48202*

Nanoparticles have opened a new avenue in materials science for investigating fundamentally interesting and technologically important properties. As bulk materials are scaled down to the nano-size regime, the electronic, optical, and magnetic behaviors become both size and shape dependant. Transition metal pnictides are a class of materials that exhibit a wide range of properties depending on composition including ferromagnetism, semiconductivity, superconductivity, and magneto-optical phenomenon. Here we will report the effect of particle size and shape on the ferromagnetic properties of MnP. The particles are prepared by employing trioctylphosphine (TOP) in a dual role as both a coordinating solvent and a source of phosphorus, and Mn<sub>2</sub>(CO)<sub>10</sub> as a manganese precursor. The shape of the nanoparticles can be altered by incorporating a co-solvent, trioctylphosphine oxide (TOPO), and by varying the post annealing time. Magnetic properties of spheres cubes, and rods will be compared and discussed in the context of prevailing theories of nanomagnetism.

## The Crystal Chemistry of Neptunium Sulfates and Phosphates

Tori Ziemann and Dr. Peter Burns

*Department of Civil Engineering and Geological Sciences, University of Notre Dame*

The crystal chemistry of higher-valence actinides is extraordinarily diverse due to an array of stable oxidation states and the diversity of coordination geometries typical of these cations. Substantial progress has been made in advancing understanding of the crystal chemistry of U<sup>+6</sup>, for which there are now about 350 known inorganic structures (Burns, 2004). Much less is known concerning the crystal chemistry of Np<sup>+5</sup> and Np<sup>+6</sup>, although similarities in coordination polyhedra exist between structures containing U<sup>+6</sup>, Np<sup>+5</sup>, and Np<sup>+6</sup> (Burns et al., 1997). In almost all cases, the crystal chemistry of these compounds is impacted by the presence of approximately linear actinyl dioxo ions (neptunyl or uranyl ions) that are further coordinated by four to six ligands, giving square, pentagonal and hexagonal bipyramids. We are investigating the crystal chemistry of environmentally relevant Np phases. Hydrothermal syntheses of Np<sup>+5</sup> sulfates have resulted in several new structure types, including infinite chains, sheets, and frameworks of polyhedra. In several of these structures O atoms of neptunyl ions coordinate other neptunyl ions (which is often described as a cation-cation interaction). Such interactions occur in less than 2% of known structures with uranyl ions, thus many of the Np<sup>+5</sup> sulfates have structures with novel connectivity. The Np<sup>+5</sup> and Np<sup>+6</sup> phosphates synthesized to date have structures that are more closely related to naturally occurring U<sup>+6</sup> compounds.

Burns, P.C. Materials Research Society Symposium Proceedings 802 (2004) 89 –100.

Burns, P.C. et al. Journal of Nuclear Materials

## Chemical Thermodynamics of Select Uranyl Phases

Karrie-Ann Kubatko<sup>1</sup>, Peter C. Burns<sup>1</sup> & Alexandra Navrotsky<sup>2</sup>

<sup>1</sup>Department of Civil Engineering and Geological Sciences, University of Notre Dame

<sup>2</sup>Thermochemistry Facility, University of California at Davis

Despite significant recent progress in the description of phases relevant to remediation and storage of actinides in the environment, evaluation of thermodynamic parameters for these phases is still largely lacking. Presently, the thermodynamic database for uranyl phases is limited, contradictory, and even suggests thermodynamic instability of ubiquitous species. In an effort to expand the thermodynamic database of uranyl phases, high-temperature oxide melt drop-solution calorimetry was utilized. Calorimetric data will be presented for one uranyl peroxide, three uranyl carbonates, ten uranyl oxide hydrates, one uranyl silicate and nine uranyl phosphates. Subsequent thermodynamic calculations were used to obtain the enthalpies of drop-solution,  $H_{ds}$ , enthalpies of formation from the binary oxides,  $H_{f-ox}$ , and enthalpies of formation from the elements in their pure reference state,  $H_f^\circ$ .

Energetic trends of the uranyl phases relative to the binary oxides ( $-H_{f-ox}$ ) appear to be dominated by the acid-base character of the binary oxides and additional favorable interactions arising from hydration and/or changes in cation environments. The calorimetric investigation of the uranyl peroxide,  $UO_2(O_2)(H_2O)_4$ , indicate that while thermodynamically unstable in systems containing no peroxide, in the presence of peroxide it is thermodynamically favored relative to even the most stable uranyl oxide hydrates and uranyl silicate. Given the long-term significance of alpha radiation and the thermodynamic stability of  $UO_2(O_2)(H_2O)_4$  in peroxide-bearing systems, it is likely that  $UO_2(O_2)(H_2O)_4$  will persist at the surface of spent nuclear fuel in contact with water in a nuclear waste repository. Uranyl peroxides may dominate at the expense of more common uranyl phases, such as uranyl oxide hydrates and uranyl silicates, which have also been found as alteration phases on spent fuel in laboratory studies.

## Magnetic and dielectric properties for perovskite-type oxyfluoride, $PbFeO_2F$

Tetsuhiro Katsumata, Akihiro Takase, Yoshiyuki Inaguma and John E. Greedan\*

Faculty of Science, Gakushuin Univ., Tokyo, Japan

\*Brockhouse Institute for Materials Research, McMaster University, Hamilton, Canada

There has been much interest in materials which are simultaneously ferromagnetic and ferroelectric because these properties are expected to be coupled and therefore tunable by external magnetic and/or electric fields. The perovskite-type oxyfluoride,  $PbFeO_2F$  is considered to be such a candidate material. While the synthesis of  $PbFeO_2F$  at high temperature under high pressure has been reported, the dielectric property has not been investigated yet. In this study, we synthesize the  $PbFeO_2F$  and investigate the crystal structure, magnetic and dielectric properties.

The stoichiometric mixture of starting materials,  $PbF_2$ ,  $PbO$  and  $Fe_2O_3$ , was dried under vacuum at approximately 200 °C for 12 hours. The dried mixture was then sealed in a Au capsule and allowed to react in a cubic multianvil-type high-pressure apparatus at 6 GPa and 925 °C for 30 min. The magnetic susceptibility and dielectric constant was measured by a SQUID magnetometer and a precision LCR meter, in the temperature range from 2 K to 300 K and from 8 K to 300 K, respectively. The structures at 20, 150, 100, 200, 250 and 300 K were investigated by a powder X-ray diffraction.

The dielectric constant of  $PbFeO_2F$  is approximately 250 at room temperature and decreases gradually below 100 K. However, the cubic perovskite-type structure was maintained at 20 K. Temperature dependent magnetic susceptibility indicates that this compound is antiferromagnetic.

## Acentric Materials

Alex Norquist

Haverford College

Materials that possess crystallographic noncentrosymmetry are of great interest to researchers owing to their ability to some or all of the following desirable physical properties, enantiomorphism, optical activity (circular dichroism), piezoelectricity, pyroelectricity, and second-order nonlinear optical activity (second-order harmonic generation (SHG)). The presence of these technologically advantageous properties is solely dependent upon symmetry. Unfortunately, the *a priori* synthesis of noncentrosymmetric materials is extremely difficult. One strategy for the

directed synthesis of noncentrosymmetric materials is the use of enantiomerically pure chiral molecules as structure directors. Two new noncentrosymmetric sulfated molybdates has been synthesized through the use either [(R)-2-methylpiperazine] or [(S)-2-methylpiperazine],  $\text{MoO}_3$ ,  $\text{H}_2\text{SO}_4$ , and  $\text{H}_2\text{O}$  were subjected to mild hydrothermal conditions, resulting in the growth of single crystals of [(R)- $\text{C}_5\text{H}_{14}\text{N}_2$ ][(MoO<sub>3</sub>)<sub>3</sub>(SO<sub>4</sub>)]H<sub>2</sub>O and [(S)- $\text{C}_5\text{H}_{14}\text{N}_2$ ][(MoO<sub>3</sub>)<sub>3</sub>(SO<sub>4</sub>)]H<sub>2</sub>O. These materials crystallize in the noncentrosymmetric space group  $P2_12_12_1$  (No. 19), which exhibits the enantiomorphic crystal class 222 ( $D_2$ ). The second harmonic generation activities were measured on sieved powders.

### Unexpected Magnetic Properties of the 4d and 5d Transition Metal Oxides, $\text{SrLaRuNiO}_6$ and $\text{La}_3\text{Re}_2\text{O}_{10}$

Heather Cuthbert and John Greedan

*Department of Chemistry, McMaster University*

The magnetic properties of oxides involving the 4d and 5d transition metals have been much less explored, in comparison to the 3d metals. The crystal chemistry and structures of the 4d and 5d oxides are often different, due to the more extended nature of the 4d and 5d orbitals, the occurrence of higher oxidation states and the tendency to form metal-metal bonds. These factors can also have a detrimental effect on the resulting magnetic behaviour of these compounds. However, novel magnetic properties are also possible.

The crystal structure of the double perovskite,  $\text{SrLaRuNiO}_6$ , consists of a three-dimensional lattice of corner-sharing  $\text{RuO}_6$  and  $\text{NiO}_6$  octahedra with  $\text{Sr}^{2+}$  and  $\text{La}^{3+}$  ions occupying the interstices. The ordering of the B-site cations,  $\text{Ru}^{5+}$  ( $4d^3$ ,  $S = 3/2$ ) and  $\text{Ni}^{2+}$  ( $3d^8$ ,  $S = 1$ ) can have a profound effect on the resulting magnetic properties. Apparent long range order below appears below 150K but not of the ferromagnetic type expected for a  $d^3/d^8$  interaction. This result will also be probed using neutron diffraction.

The second title compound,  $\text{La}_3\text{Re}_2\text{O}_{10}$ , has a very different crystal structure. It consists of isolated  $\text{Re}_2\text{O}_{10}$  dimer units of two edge-shared  $\text{ReO}_6$  octahedra, interconnected by  $\text{La}^{3+}$  ions into a three-dimensional framework. The short Re-Re bond distance (2.484(1) Å) is indicative of a metal-metal bond, which pairs electrons and destroys magnetism. However, electron counting results in one unpaired electron per  $\text{Re}_2\text{O}_{10}$  dimer unit. The resulting magnetic behaviour of  $\text{La}_3\text{Re}_2\text{O}_{10}$  is also remarkable in that interdimer short range ordering effects appear below 150K in spite of the fact that the nearest Re – Re interdimer distance is 5.574 Å.

### Studies of the $\text{Co}^{3+}$ Spin State and Oxygen Order/Disorder in the Defect Perovskites $\text{Ba}_2\text{In}_{2-x}\text{Co}_x\text{O}_5$

A.D. Lozano-Gorrín,<sup>§</sup> J.E. Greedan,<sup>§</sup> Gianluigi Botton,<sup>§</sup> Guillaume Radtke<sup>§</sup> and P. Núñez<sup>Y</sup>

<sup>§</sup>*Brockhouse Institute for Materials Research, McMaster University, Hamilton, Ontario, Canada L8S 4M1*

<sup>Y</sup>*Departamento de Química Inorgánica, Universidad de La Laguna, 38206-La Laguna, Tenerife, Spain*

New oxides of general formula  $\text{Ba}_2\text{In}_{2-x}\text{Co}_x\text{O}_5$  ( $0.50 \leq x \leq 1.70$ ) have been synthesized and characterized by means of X-ray powder diffraction, magnetic susceptibility<sup>1</sup> and high resolution electron energy loss spectroscopy (EELS). From the X-ray data an ideal cubic perovskite-type structure,  $Pm\bar{3}m$ , is found. This implies a high (1/6) concentration of vacancies randomly distributed on the oxygen site, and an average 5-fold coordination of the Co ions. The spin state of  $\text{Co}^{3+}$  is well known to be very sensitive to the coordination number and therefore, the crystal field, in oxides and high spin (HS), low spin (LS) and intermediate spin states (IS) are found.<sup>2</sup> All of the compositions above appear to be spin glasses and it is possible that a distribution of Co spin states is present. The magnetic data, while not completely unambiguous, suggest the HS state for all x. The  $\text{Co}^{3+}$  spin state was investigated by high temperature magnetic susceptibility and high resolution EELS, and preliminary analysis of the Co L-edge data are also consistent with HS. The issue of order/disorder of the O ions was investigated using neutron powder diffraction and these results will also be presented.

[1] A.D. Lozano-Gorrín, P. Núñez, M.A. López de la Torre, J. Romero de Paz, R. Sáez-Puche, *J. Solid State Chem.*, **165**, 254-260 (2002).

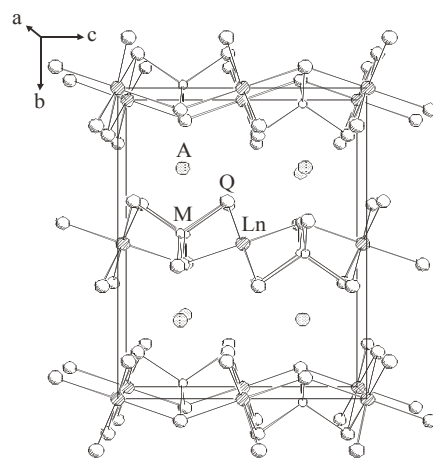
[2] M.A. Senaris-Rodríguez, J.B. Goodenough, *J. Solid State Chem.*, **116**, 224 (1995).

## Syntheses, Structure, and Physical Properties of $ALnMQ_3$ ( $A$ = alkali metal; $Ln$ = Rare-earth or Y; $M$ = Transition Metal; $Q$ = S, Se, Te)

George H. Chan and Jim Ibers

Northwestern University

Over the last few years, about 50 alkali-metal/rare-earth/transition-metal/chalcogenides,  $ALnMQ_3$ , have been synthesized in our group.<sup>1-5</sup> These isostructural compounds crystallize in the layered  $KZrCuS_3$  structure type with four formula units in space group  $Cmcm$  of the orthorhombic system. The structure of these compounds is composed of  $LnQ_6$  octahedra and  $MQ_4$  tetrahedra that share edges to form  $^2_4[LnMQ_3]$  layers. These layers stack perpendicular to  $[010]$  and are separated by  $A^+$  cations. Each cation is coordinated by eight  $Q$  atoms in a bicapped trigonal prismatic arrangement. This is an ideal structure type for the assessment of the effects of chemical substitution on the magnetic and optical properties of these  $ALnMQ_3$  compounds. A summary of this substitutional chemistry will be presented.



- (1) Mitchell, K.; Haynes, C. L.; McFarland, A. D.; Van Duyne, R. P.; Ibers, J. A. *Inorg. Chem.* **2002**, *41*, 1199-1204.
- (2) Mitchell, K.; Huang, F. Q.; McFarland, A. D.; Haynes, C. L.; Somers, R. C.; Van Duyne, R. P.; Ibers, J. A. *Inorg. Chem.* **2003**, *42*, 4109-4116.
- (3) Mitchell, K.; Huang, F. Q.; Caspi, E. N.; McFarland, A. D.; Haynes, C. L.; Somers, R. C.; Jorgensen, J. D.; Van Duyne, R. P.; Ibers, J. A. *Inorg. Chem.* **2004**, *43*, 1082-1089.
- (4) Yao, J.; Deng, B.; Sherry, L. F.; McFarland, A. D.; Ellis, D. E.; Van Duyne, R. P.; Ibers, J. A. *Inorg. Chem.* **2004**, *43*, 7735-7740.
- (5) Chan, G. H.; Van Duyne, R. P.; Ibers, J. A., unpublished work.

## Characterization and Reactivity of $Na_3PO_3S$ in the Solid-State

Nathan J. Takas, Austin M. Savatt and Jennifer A. Aitken

Department of Chemistry and Biochemistry, Duquesne University, Pittsburgh, PA

Our work is currently focused on the use of sodium monothiophosphate as a precursor for the development of more complex oxythiophosphates, a family of compounds ripe for development. The anhydrous salt of sodium monothiophosphate was first formed in 1940 by Zintl and Bertram.<sup>1</sup> The following decades, however, did not greatly contribute to the understanding of this substance's physical properties. This poster will describe the thermal properties of  $Na_3PO_3S$ , including data obtained by DTA experiments under vacuum and static air atmospheres, as well as TGA experiments. PXRD of the meta-stable, high-temperature  $\beta$ -phase will be discussed, along with observations regarding the unusual stability of this polymorph.  $\beta$ - $Na_3PO_3S$  exhibits second harmonic generation, frequency doubling of light, and has been determined to be phase matchable.

The reaction of  $Na_3PO_3S$  with several metal chlorides has been successful in producing novel oxythiophosphates. These metathetical reactions have also been achieved in the solid-state at ambient temperatures. Characterization of these new materials will be discussed.

- (1) Zintl, E.; Bertram, A. *Z. Anorg. u. Allgem. Chem.* **1940**, *245*, 16.

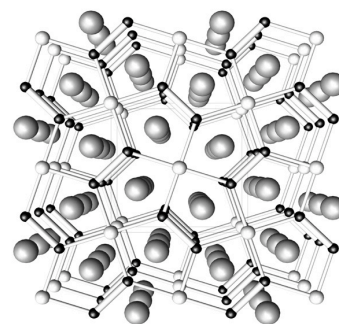
## Crystal Growth, Structural and Magnetic Property Studies on a Family of Ternary Rare-Earth Phases $\text{RE}_2\text{InGe}_2$ (RE = Sm, Gd, Tb, Dy, Ho, Yb)

Paul H. Tobash and Svilen Bobev

*Department of Chemistry and Biochemistry, University of Delaware, Newark, DE 19716*

Binary rare-earth silicides and germanides have been extensively studied in the past due to their unique structural and physical properties. These phases crystallize in a number of different crystal structure types, largely dependent on the nature of the rare-earth element, the stoichiometry, and the reaction conditions. The purpose of the present work was to study the variations of the polyanionic network of some rare-earth based germanides, with particular focus on RE-T-Ge compounds (RE = rare-earth, T = early *p*-block element such as Al, Ga, and In).

The title compounds were discovered over the course of exploring the possibility to utilize excess of In metal to serve as a media for facilitating crystal growth.  $\text{RE}_2\text{InGe}_2$  phases (RE = Sm, Gd, Tb, Dy, Ho, Yb) crystallize in the tetragonal  $\text{Mo}_2\text{BFe}_2$  type (space group  $P4/mbm$ , Pearson's symbol  $tP10$ ), an ordered ternary variant of the  $\text{U}_3\text{Si}_2$  structure, as confirmed by single-crystal X-ray diffraction studies. The structure can be viewed as infinite  $[\text{InGe}_2]$  layers, stacked along the *c*-axis, and separated by layers of rare-earth atoms. Magnetic susceptibility measurements as a function of the temperature and the field indicate that most of the compounds exhibit Curie-Weiss paramagnetic behavior at ambient conditions, and order antiferromagnetically at temperatures below  $\sim 60$  K.



Crystal structure of  $\text{RE}_2\text{InGe}_2$ ,  
viewed down the *c*-axis

## Advances in the Synthesis of Yttrium and Lutetium Chalcogenides

Laura M. Castro-Castro and John D. Corbett

*Department of Chemistry, Iowa State University, Ames, IA 50011*

Our efforts to identify and characterize new metal-rich binary yttrium and lutetium chalcogenides and ternary  $\text{RMTe}$  (R=Y, Lu; M=Ru, Os, Rh, Ir, Pd, Pt, Cu, Ag, Bi) have resulted in the synthesis and crystal structure determination of several new compounds. Our presentation includes the new ternary metal-rich phases  $\text{Y}_6\text{AgTe}_2$   $Pnma$  (No. 62)  $a = 21.865(3)$ ,  $b = 4.0733(6)$ ,  $c = 11.5058(2)$ ,  $\text{Sc}_6\text{PdTe}_2$  type;  $\text{Lu}_6\text{AgTe}_2$   $Pnma$  (no. 62)  $a = 21.0225(3)$ ,  $b = 3.9877(6)$ ,  $c = 11.1897(2)$ ,  $\text{Sc}_6\text{PdTe}_2$  type;  $\text{Y}_6\text{BiTe}_2$   $Cmc2_1$  (no. 36)  $a = 4.0770(5)$ ,  $b = 21.375(3)$ ,  $c = 11.5236(1)$ ; and  $\text{Y}_6\text{PtTe}_2$   $I222$  (no. 23)  $a = 3.9690(1)$ ,  $b = 9.5767(3)$ ,  $c = 15.6464(4)$ . Similarly, we introduce the new binary phases  $\text{Y}_7\text{Te}_2$   $Pnma$  (no. 62)  $a = 21.3282(5)$ ,  $b = 4.0562(9)$ ,  $c = 11.401(2)$ ,  $\text{Sc}_6\text{PdTe}_2$  type;  $\text{Y}_{1.044}\text{Te}$   $I4/m$  (no. 87)  $a = 4.3022(2)$ ,  $c = 18.2798(2)$  and  $\text{YSe}_2$   $P321$  (no. 150)  $a = 3.8454(8)$ ,  $c = 6.5306(3)$ .

## Synthesis of Crystalline, Soluble $\text{MoS}_2$ Nanocrystals

Hongtao Yu and Stephanie L. Brock

*Department of Chemistry, Wayne State University, Detroit MI, 48202*

Nano size  $\text{MoS}_2$  crystals have been synthesized via the reaction of  $\text{Mo}(\text{CO})_6$  with elemental sulfur in trioctylphosphine oxide (TOPO) at elevated temperature ( $300^\circ\text{C}$ - $330^\circ\text{C}$ ). The as-obtained nanocrystals are crystalline, and soluble in a variety of organic solvents, including toluene, hexane, and pyridine. The size distribution (several tens of nanometers to several nanometers) can be further narrowed by size selective precipitation. Structure and morphology of the nanocrystals is determined by powder X-ray diffraction and transmission electron microscopy.

## Synthesis and Characterization of Discrete Nanoparticles of $\text{Ni}_2\text{P}$

Keerthi Senevirathne, Stephanie L. Brock

*Department of Chemistry, Wayne State University, Detroit MI, 48202*

Transition metal phosphides are an important class of materials because of their unique magnetic, electronic, optical and catalytic properties. In particular, supported nickel phosphide has been reported to be a good catalyst for hydrodesulfurization (HDS) and hydrodenitrogenation (HDN), which are the processes that remove sulfur and nitrogen from gasoline. The focus of this study is to develop a synthetic route to produce discrete nanoparticles

of Ni<sub>2</sub>P with high surface areas. Here we report the synthesis of spherical Ni<sub>2</sub>P nanoparticles using a surfactant-aided solution-phase method with bis (1,5-cyclooctadiene) nickel (0) as the nickel source and trioctylphosphine (TOP) as the phosphorus source. The structure, particle size, and surface area will be presented and discussed in light of potential catalytic applications.

### Synthesis, Structure, and Bonding of Na<sub>3</sub>MIn<sub>2</sub> (M = Au, Ag): Participation of Na in the Anionic Network

Bin Li and John D. Corbett

*Ames Laboratory-DOE and Department of Chemistry, Iowa State University, Ames, Iowa 50011, USA*

Two compounds Na<sub>3</sub>MIn<sub>2</sub> (M = Au, Ag) were synthesized via a typical high-temperature reactions in Ta tubes. The structures were determined by single-crystal X-ray diffraction methods in space group Fd-3m. Both compounds crystallize in NiTi<sub>2</sub>-type structure. The partial gold-indium structure contains tetrahedral stars [In<sub>4</sub>Au<sub>4/2</sub>] (TS) as the building units which are connected to a three-dimensional framework via sharing the vertexes of TS, the Na atoms filling the resulting cages. Based on TB-LMTO-ASA calculations, the detailed electronic structure of Na<sub>3</sub>AuIn<sub>2</sub> has been studied through the analyses of density of states, energy bands and integrated crystal overlap Hamiltonian populations. A substantial participation of sodium in the overall bonding of the structure is found instead of a complete electron transfer from the cations onto anionic framework assumed by Zintl-Klemm concepts.

### BaAu<sub>0.4</sub>Tl<sub>1.6</sub>, BaAu<sub>0.35(4)</sub>In<sub>1.65(4)</sub> and BaHg<sub>0.92(2)</sub>In<sub>1.08(2)</sub>: three new intermetallics with CeCu<sub>2</sub>-type structures

Jing-Cao Dai and John D. Corbett

*Ames Laboratory-DOE and Department of Chemistry, Iowa State University, Ames, Iowa 50010*

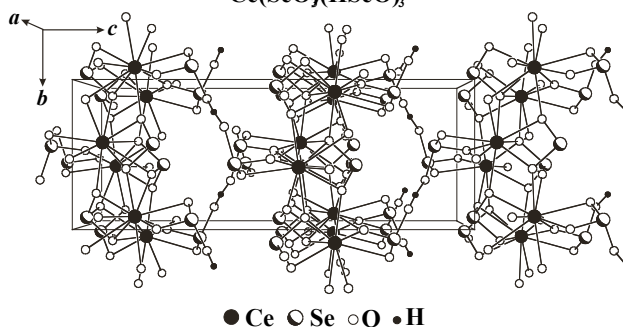
The title compounds were prepared by high temperature solid synthesis techniques. Single crystal X-ray diffraction shows that the three compounds crystallize in orthorhombic CeCu<sub>2</sub>-type structure, *Imma*, *Z* = 4 (*a* = 5.140(1), 5.145(1), 8.580(2), *b* = 8.317(2), 8.373(2), 5.104(1), and *c* = 8.809(2), 8.715(2), 8.461(2) for BaAu<sub>0.4</sub>Tl<sub>1.6</sub> (**1**), BaAu<sub>0.35(4)</sub>In<sub>1.65(4)</sub> (**2**) and BaHg<sub>0.92(2)</sub>In<sub>1.08(2)</sub> (**3**), respectively). The structure can be directly described as a 3D 4-linked honeycomb-like network (4<sup>2</sup>6<sup>3</sup>8 net) of [Tr]<sub>∞</sub><sup>2-</sup> (Tr = Tl or In) polyanion with encapsulated Ba<sup>2+</sup> cations. The Tr are randomly replaced by 20% Au in **1**, 18(2)% Au in **2**, and 46(1)% Hg in **3**. The band calculations (EHTB) demonstrate that three compounds are electron-poor phases and metallic. The structure for **1** crystallizes in this CeCu<sub>2</sub>-type rather than in related hexagonal *P6<sub>3</sub>/mmc* BaTl<sub>2</sub> (CaIn<sub>2</sub>-type) or hexagonal *P6/mmm* BaAu<sub>2</sub> (AlB<sub>2</sub>-type), and stabilization of this electron-poorer phase result arises from partial substitution of smaller Au atoms on the polyanion network. Relativistic effects for the heavier Au and Hg are responsible for lattice parameters decreases in these three compounds.

### Syntheses and Structures of *f*-Electron Selenite Hydroselenites

Wendy L. Burns

*Northwestern University*

The selenite hydroselenites Ce(SeO<sub>3</sub>)(HSeO<sub>3</sub>), Tb(SeO<sub>3</sub>)(HSeO<sub>3</sub>)A<sub>2</sub>H<sub>2</sub>O, and Cs[U(SeO<sub>3</sub>)(HSeO<sub>3</sub>)]A<sub>3</sub>H<sub>2</sub>O were synthesized by hydrothermal means at 453 K from the reaction of CeO<sub>2</sub>, Tb<sub>4</sub>O<sub>7</sub>, or UO<sub>2</sub> with SeO<sub>2</sub>. Ce(SeO<sub>3</sub>)(HSeO<sub>3</sub>), which is isostructural to Pr(SeO<sub>3</sub>)(HSeO<sub>3</sub>), crystallizes in the orthorhombic space group *Pca*2<sub>1</sub>. Tb(SeO<sub>3</sub>)(HSeO<sub>3</sub>)A<sub>2</sub>H<sub>2</sub>O, which is isostructural to *Ln*(SeO<sub>3</sub>)(HSeO<sub>3</sub>)A<sub>2</sub>H<sub>2</sub>O (*Ln* = Nd, Sm), crystallizes in the orthorhombic space group *P2<sub>1</sub>2<sub>1</sub>2<sub>1</sub>*. Cs[U(SeO<sub>3</sub>)(HSeO<sub>3</sub>)]A<sub>3</sub>H<sub>2</sub>O crystallizes in the monoclinic space group *P2<sub>1</sub>/n*. There is extensive hydrogen bonding in all three crystal structures.



## **[CH<sub>3</sub>(CH<sub>2</sub>)<sub>11</sub>NH<sub>3</sub><sup>+</sup>][H<sub>2</sub>PO<sub>4</sub><sup>-</sup>]: Its crystal structure and unusual photoluminescent property**

Ming-Hui Ge<sup>1</sup> and Jing-Tai Zhao

*Shanghai Institute of Ceramics, Chinese Academy of Sciences, Shanghai 200050, China*

<sup>1</sup> *Presently at Ames Laboratory – DOE and Department Chemistry, Iowa State University*

Alkylammonium phosphates are solid materials composed of hydrogen-bonded networks of anionic [H<sub>x</sub>PO<sub>4</sub>]<sup>x-3</sup> phosphate centers (x = 0 – 3) and alkylammonium cationic molecules. The alkylammonium phosphates readily form in most solvents. Despite this, only about ten crystal structures have been reported. There are some interesting properties reported in alkylammonium phosphates[1,2]. The dodecylammonium dihydrogen phosphate was discovered to undergo several polymorphic phase transitions before ultimately transforming to a smectic liquid crystal mesophase[2]. Furthermore, there are not any optical properties reported about these materials. Here we report the structure of dodecylamine dihydrogen phosphate (DDP, [CH<sub>3</sub>(CH<sub>2</sub>)<sub>11</sub>NH<sub>3</sub><sup>+</sup>][H<sub>2</sub>PO<sub>4</sub><sup>-</sup>]) determined by single crystal X-ray diffraction analysis and its unusual photoluminescent property. DDP is composed of dihydrogen phosphate arranged in layers. The dodecylammonium cations are interdigitated between the phosphate layers. Its structure contains the longest carbon chains reported in alkylammonium phosphates so far. More interestingly, DDP is observed to emit bright white light with short afterglow with excitation of UV at about 237nm. The luminescence mechanism is being studied.

[1] Oliver S.R.J., Ozin G.A. (1998) *J. Mater. Chem.*, **8**(4), 1081- 1085

[2] Ozin G.A. (1997) *Acc. Chem. Res.*, **30**, 17-27

## **Synthesis and Characterization of High Surface Area Germanium Sulfide Aerogels**

Kennedy K. Kalebaila and Stephanie L. Brock

*Department of Chemistry, Wayne State University, Detroit, Michigan, 48202*

Aerogels are a unique class of solid materials that consist of a highly porous internal structure, a low solid content (1-10%), and nanoscale building blocks. Aerogels exhibit extremely high specific surface areas, low thermal conductivities, low sound velocities, and can have high catalytic activity, depending on the composition. These properties make aerogels well-suited for applications as catalysts/catalyst supports, sensors and thermal insulators. The chemistry of aerogel formation is well developed for oxide systems such as SiO<sub>2</sub>, TiO<sub>2</sub>, V<sub>2</sub>O<sub>5</sub>, and MnO<sub>2</sub>. However, despite the wide range of functional properties associated with the aerogel architecture, there has been very little work on non-oxide forms, except for carbon.

We are interested in extending the chemistry of aerogels to metal chalcogenide (S, Se, Te) materials, as many of these are technologically relevant semiconductors that might be expected to demonstrate unique photophysical and photocatalytic properties if prepared as porous nanostructures. Recently, we have demonstrated CdS aerogel formation by a 2-pot process involving nanoparticle synthesis, aggregation to form a gel-network, and supercritical fluid extraction. In this work, we will evaluate the ability to use simple thiolysis (1-pot) reactions to go from a molecular precursor to the gel stage, thus reducing the number of steps to aerogel formation. Here we report the application of thiolysis reactions to formation of GeS<sub>2</sub> aerogels (supercritically dried materials) and xerogels (bench-top dried materials), and evaluate the influence of the synthetic methodology on morphology and surface area. The generality of this method will be discussed and compared to the multistep process developed previously in our lab.

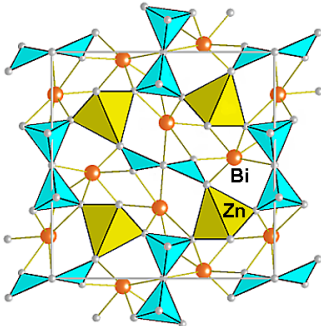
## **The non-centrosymmetric melilite-type borates Bi<sub>2</sub>ZnB<sub>2</sub>O<sub>7</sub> and CaBiGaB<sub>2</sub>O<sub>7</sub>**

Jacques Barbier<sup>1</sup>, Nicolas Penin<sup>1</sup>, Anton Dabkowski<sup>1</sup> and Lachlan M. Cranswick<sup>2</sup>

<sup>1</sup> *Department of Chemistry and Brockhouse Institute for Materials Research, McMaster University, Hamilton, Ontario L8S 4M1, Canada.* <sup>2</sup> *Neutron Program for Materials Research, National Research Council Canada, Chalk River Laboratories, Chalk River, Ontario K0J 1J0, Canada.*

As part of exploratory research on ternary bismuth borates, the novel non-centrosymmetric compounds Bi<sub>2</sub>ZnB<sub>2</sub>O<sub>7</sub> and CaBiGaB<sub>2</sub>O<sub>7</sub> have been synthesized by solid-state reactions at temperatures between 600 and 800°C at 1 atm pressure. These compounds are the first synthetic diborate members of the large melilite family, A<sub>2</sub>T<sub>3</sub>O<sub>7</sub>, in which layers of A cations alternate with T<sub>3</sub>O<sub>7</sub> tetrahedral layers, as in the åkermanite (Ca<sub>2</sub>MgSi<sub>2</sub>O<sub>7</sub>) - gehlenite (Ca<sub>2</sub>Al<sub>2</sub>SiO<sub>7</sub>) series. The crystal structures of Bi<sub>2</sub>ZnB<sub>2</sub>O<sub>7</sub> and CaBiGaB<sub>2</sub>O<sub>7</sub> have been determined by powder X-ray diffraction and

refined by the Rietveld method using powder neutron diffraction data.  $\text{CaBiGaB}_2\text{O}_7$  adopts the regular tetragonal melilite structure (P-4<sub>2</sub>m space group,  $a = 7.4669(3) \text{ \AA}$ ,  $c = 4.8344(2) \text{ \AA}$ ,  $Z = 2$ ) containing  $\text{B}_2\text{O}_7$  tetrahedral dimers.



The refinement of split eight-coordinated sites for the  $\text{Ca}^{2+}$  and  $\text{Bi}^{3+}$  inter-layer cations suggests the presence of additional disorder.  $\text{Bi}_2\text{ZnB}_2\text{O}_7$  adopts a novel orthorhombic melilite superstructure (Pba2 space group,  $a = 10.8268(4) \text{ \AA}$ ,  $b = 11.0329(4) \text{ \AA}$ ,  $c = 4.8848(2) \text{ \AA}$ ,  $Z = 4$ ) containing both tetrahedral  $\text{B}_2\text{O}_7$  and triangular  $\text{B}_2\text{O}_5$  dimers (see figure). The  $\text{Bi}^{3+}$  cations occupy two distinct inter-layer sites with strongly asymmetric six-fold coordination environments. The measurement of second harmonic generation efficiencies ( $d_{\text{eff}}$ ) of powder samples has yielded values of 4.0 ( $\text{Bi}_2\text{ZnB}_2\text{O}_7$ ) and 1.6 ( $\text{CaBiGaB}_2\text{O}_7$ ) relative to a  $\text{KH}_2\text{PO}_4$  standard. Single crystals of  $\text{Bi}_2\text{ZnB}_2\text{O}_7$  have been successfully grown by the Czochralski technique using  $\text{Bi}_2\text{O}_3$ -rich melts.

### Mesostructured Semiconductors via Supramolecular Assembly of $[\text{Ge}_4\text{Q}_{10}]_4$ (Q=S, Se) Adamantane Clusters with $\text{Ru}^{2+}$ and Cationic Surfactants

Gerasimos S. Armatas, Nan Ding and Mercouri G. Kanatzidis

Department of Chemistry, Michigan State University East Lansing, Michigan 48824

The mesoporous silicates of the MCM-n family with ordered pore structure, reported by the Mobil group using long-chain organic liquid-crystal templates, have spawned a new era in open framework materials and has captured the imagination of many materials scientists. In general, the synthetic approaches involve the organized polymerization of the basic tetrahedral  $[\text{SiO}_4]_4^-$  anion in the presence of various surfactants [1]. Bulk materials that combine mesoscale features, however, are also important, because they may impart electronic properties and optical properties to the framework. The introduction of noble metals in these frameworks is highly attractive because they could impart useful catalytic functionality in ways that may not be possible with the mesoporous silicates. Such characteristics may be expected in non-oxidic materials such as the chalcogenides. Nevertheless, chalcogenide analogs to mesostructured silicates are still scarce because their rational synthetic routes remain a challenge, although progress in this area has been reported recently [2]. The incorporation of catalytically relevant ions in a mesostructured framework is an intriguing prospect as it could lead to novel mesoporous materials with catalytic functionality built in.

We report the use of  $\text{Ru}^{2+}$  ion as a linking agent for  $[\text{Ge}_4\text{Q}_{10}]^{4+}$  (where Q= S, Se) adamantane clusters to form ordered mesostructured materials through electrostatically driven co-assembly with cationic surfactants. The adamantane  $[\text{Ge}_4\text{Q}_{10}]^{4+}$  anions has proven to be highly suitable in preparing mesostructured sulfide and selenide solids. These clusters are hydrolytically more stable and they can bind metal ions to form polymeric covalent chalcogenide frameworks. The elemental composition of *surfact*- $\text{RuGeQ}$  was determined with energy dispersive microprobe analysis (SEM/EDS), elemental C, H, N, and TGA analysis. The pore organization of *surfact*- $\text{RuGeQ}$  phases was readily observed by powder X-ray diffraction and transmission electron microscopy. Depending upon surfactant and cluster used in the synthesis, the periodicity of the nano-structured composites can be transformed from regular hexagonal symmetry to lamellar, or to a worm-like three-dimensional framework structure. The optical absorption properties of the mesostructured chalcogenides were investigated with solid-state diffuse reflectance UV-vis/near-IR spectroscopy. All solids possess well-defined, sharp optical absorptions associated with band gap transitions ( $E_g$ ) in the energy range 1.5–2.3 eV.

[1] Kresge, C. T.; Leonowicz, M. E.; Roth, W. J.; Vartuli, J. C.; Beck, J. S. *Nature* **1992**, 359, 710-712.

[2] (a) Trikalitis, P. N.; Bakas, T.; Kanatzidis, M. G. *J. Am. Chem. Soc.* **2005**, 127, 3910-3920. (b) Trikalitis, P. N.; Rangan, K. K.; Kanatzidis, M. G. *J. Am. Chem. Soc.* **2002**, 124, 2604-2613. (c) Trikalitis, P. N.; Rangan, K. K.; Bakas, T.; Kanatzidis M. G. *Nature* **2001**, 410, 671.



## **Solvothermal syntheses of Cu<sub>3</sub>P via reactions of amorphous redphosphorous with a variety of copper sources**

Valentina Ganzha-Hazen and Stephanie L. Brock

*Department of Chemistry, Wayne State University, Detroit, MI*

Jennifer Ann Aitkin

*Department of Chemistry and Biochemistry, Duquesne University, Pittsburgh, PA.*

The solvothermal synthesis of Cu<sub>3</sub>P is investigated. Compared to other methods, solvothermal chemistry can be much easier, safer, and more efficient to a previous preparation reported the use of reactive yellow phosphorous. Here, we reported the solvothermal synthesis of Cu<sub>3</sub>P were using less reactive, more easily handled red phosphorous with copper halides (copper(I) iodide, copper(I) chloride, copper(II) chloride) and with pure copper metal in water. Pure phase Cu<sub>3</sub>P was obtained at 200°C in water over 1-2 day of reaction and no ethylenediamine or ammonia was required. The influence of the copper source and copper : phosphorous ratio on the purity of the resulting products will be discussed. Products were characterized using powder X-ray diffraction, scanning electron microscopy, DTA and optical band gap spectroscopy.

## **Structure and Cation Distribution of Mg<sub>2</sub>CrV<sub>3</sub>O<sub>11</sub>, Mg<sub>2</sub>GaV<sub>3</sub>O<sub>11</sub>, and Mg<sub>2</sub>InV<sub>3</sub>O<sub>11</sub>**

Jared P. Smit, Peter C. Stair, and Kenneth R. Poeppelmeier

*Northwestern University, Evanston, IL 60201*

Multicomponent vanadates are known to catalyze a variety of hydrocarbon oxidation reactions. In particular, magnesium vanadates have been shown to be selective for the oxidative dehydrogenation of propane and butane. The introduction of a third metal into the magnesium vanadium framework is of interest owing to the creation of potentially interesting catalytic materials. The flux growth, crystal structure and cation distribution of the ternary oxides Mg<sub>2</sub>CrV<sub>3</sub>O<sub>11</sub>, Mg<sub>2</sub>GaV<sub>3</sub>O<sub>11</sub>, and Mg<sub>2</sub>InV<sub>3</sub>O<sub>11</sub> are presented. Mg<sub>2</sub>CrV<sub>3</sub>O<sub>11</sub>, Mg<sub>2</sub>GaV<sub>3</sub>O<sub>11</sub>, and Mg<sub>2</sub>InV<sub>3</sub>O<sub>11</sub> are isostructural and crystallize in the triclinic space group P-1. The distribution of cations is disordered with respect to Mg<sup>2+</sup>, Cr<sup>3+</sup>, Ga<sup>3+</sup>, In<sup>3+</sup> in the respective compounds.

## **Structure of manganese oxide produced by *Leptothrix discophora* SP6**

Ian Saratovsky (NU, Chemistry), Jean-François Gaillard (NU, Civil and Environmental Engineering), and Kenneth R. Poeppelmeier (NU, Chemistry)

In environmental systems the oxidation of Mn(II) is primarily catalyzed by biological processes. Manganese oxides (MnO<sub>x</sub>) formed by biological processes are ubiquitous throughout aquatic environments. However, their structures are often difficult to determine owing to intimate association with a complex nucleation medium, small particle size, lack of long-range order, and diversity of structure types. Natural MnO<sub>x</sub> minerals can provide good reference compounds for the study of biogenic MnO<sub>x</sub>. However, natural samples often contain multiple MnO<sub>x</sub> phases or polymorphs of a particular MnO<sub>x</sub> phase. As such, spectroscopic comparison of natural MnO<sub>x</sub> to biogenic MnO<sub>x</sub> is not ideal as it can produce ambiguous phase identification. Syntheses of well-characterized MnO<sub>x</sub> model compounds have proven crucial for spectroscopic comparison to biogenic specimens and have afforded structure identification of biogenic MnO<sub>x</sub> produced by *Leptothrix discophora* SP-6.

## **Rapid solid-state synthesis of crystalline, photocatalytic active titanium oxides**

Sujith Perera, Nadiya Zelenski, and Edward G. Gillan

*Department of Chemistry and the Optical Science and Technology Center, University of Iowa*

Though titanium dioxide (TiO<sub>2</sub>) is a well known compound with numerous industrial applications, recent interest is growing in the photocatalytic applications of TiO<sub>2</sub>, which shows photocatalytic activity under UV light illumination. Several researchers have attempted to modify TiO<sub>2</sub> to achieve visible light photocatalytic activity by doping other elements into TiO<sub>2</sub>. Conventionally TiO<sub>2</sub> is synthesized by the “sol-gel” method, which is time consuming and needs post annealing treatment to obtain a crystalline compound. Previous work by several research groups has shown that solid-state metathesis reactions successfully can synthesize crystalline inorganic materials in a rapid manner (~1sec). The reaction is driven by production of a very stable alkali halide by-product and includes a large exothermic energy release, allowing the reaction to self propagate and make crystalline products in a rapid manner. This presentation describes our success in using solid-state metathesis reactions to rapidly form crystalline thermodynamically stable

rutile TiO<sub>2</sub> using TiCl<sub>3</sub> and Na<sub>2</sub>O<sub>2</sub> precursors. Cooling the reaction system by adding excess NaCl as a heat sink, results in a mixture of kinetically stable and more photocatalytically active anatase with rutile. Also addition of NaCl results in a decrease in TiO<sub>2</sub> particle sizes. The photocatalytic activity of synthesized TiO<sub>2</sub> using methylene blue under UV light will be discussed. By changing the oxide precursor to Na<sub>2</sub>O, a low Ti oxidation state Ti<sub>2</sub>O<sub>3</sub> also was synthesized. Preliminary studies of synthesis of transition metal doped Ti<sub>1-y</sub>M<sub>y</sub>O<sub>2</sub> (y ~ 0.1) (M= Cr, Mn, Fe, Co, Ni) by mixing MCl<sub>x</sub> with TiCl<sub>3</sub> starting material in desired stoichiometric ratio also will be presented.

### **Solvothermal Routes to Crystalline Metal Nitrides via Metal Azide Precursor Decomposition**

Jong Lak Choi and Edward G. Gillan

*Department of Chemistry and the Optical Science and Technology Center, University of Iowa*

In contrast to well-studied metal and metal chalcogenide solution syntheses, current low-temperature methodologies for the synthesis of metal nitrides still leave much room for improvement. The biggest challenge for metal nitride synthesis involves finding a nitrogen source that is thermally unstable enough to yield crystalline metal nitrides at low temperatures (< 400 °C). Metal azides have an established foothold in explosives and air-bag systems and, under the proper conditions, they are useful in metal nitride synthesis. Our group has previously reported on an azido thermal metathesis route to GaN from GaCl<sub>3</sub> and NaN<sub>3</sub> under moderate temperature non-aqueous solvothermal conditions. This presentation describes extensions of this methodology to other metal nitrides, such as InN, Cu<sub>3</sub>N, Ni<sub>3</sub>N and W<sub>2</sub>N. Several of these products are metastable and decompose to the elements by 500 °C and Ni<sub>3</sub>N is a known room-temperature ferromagnet. Critical synthetic parameters for these metal nitride reactions will be presented. Moreover, the synthetic pathway to crystalline nitride product, Cu<sub>3</sub>N, through azide intermediates will be presented and compositional information of Cu<sub>3</sub>N synthesized under different conditions will be compared as well.

### **Synthesis and Characterization of New Clathrate 1 Type Pnictogen Halide Materials**

Dhammika Herath and Stephanie L. Brock

*Department of Chemistry, Wayne State University, Detroit, Michigan 48202.*

Clathrates are periodic solids in which tetrahedrally coordinated atoms form cages that surround a guest atom. These guest atoms can scatter phonons but not electrons, thus lowering the thermal conductivity without reducing the electron conductivity. Thus, many clathrate phases, such as Ge<sub>30</sub>Ga<sub>16</sub>Sr<sub>8</sub>, have been found to be good thermoelectric materials. Thermoelectric materials conduct heat from one side of the solid to the other side by passing an electric current. They are used for refrigeration and energy recovery in special applications. Ge<sub>38</sub>E<sub>8</sub>I<sub>8</sub> (E = P, As, Sb) and Sn<sub>24</sub>E<sub>19.3</sub>I<sub>8</sub> (E = As, P) both belong to the clathrate 1 class, with I-acting as guests. In order to assess the compositional versatility of these materials we are exploring the synthesis of solid-solutions, Ge-Sn-E-I, using Ge<sub>38</sub>E<sub>8</sub>I<sub>8</sub> and Sn<sub>24</sub>E<sub>19.3</sub>I<sub>8</sub> (E = As, P) as starting materials in different molar ratios, or from reaction of the elements. X-ray diffraction (XRD) and Energy Dispersive Spectroscopy (EDS) techniques were used for characterization. Here we describe the structure and compositions of these materials and the effect of heating temperature and Ar pressure on their formation and purity.

### **Synthesis, Structure and Magnetic Properties of Rare Earth Cluster Compounds**

Lucas Sweet and Tim Hughbanks

*Texas A&M University*

Polynuclear lanthanide coordination complexes and network solids containing “normal” Ln<sup>3+</sup> ions are magnetically uninteresting because the coupling necessary to achieve magnetic ordering is generally very weak. The contraction of lanthanide 4*f* orbitals strongly limits direct and indirect *f-f* coupling with adjacent ions. In contrast, lanthanide elements are of great interest for researchers concerned with intermetallic compounds. Exchange between 4*f* electrons can be quite substantial in reduced compounds. We are currently targeting lanthanide-rich materials with *discrete* clusters, such as those with the R<sub>7</sub>X<sub>12</sub>Z structure-type. Preliminary magnetic results of the closed-shell system R[R<sub>6</sub>I<sub>12</sub>Co] (R= Gd, Er) show Curie-Weiss behavior, which show signs of antiferromagnetic coupling at 85 K. However, when transition metals (Z) Mn or Fe are the cluster center, the compounds exhibit behavior consistent with strong intracluster ferromagnetic coupling of the Gd 4*f*<sup>7</sup> moments along with intercluster antiferromagnetic coupling. To study both the intracluster and cross-linked interactions, we carried out density functional calculations (DFT-

BLYP) on a model cluster compound. In our search for new compounds which contain rare earth clusters, three new compounds have been discovered, CsR(R<sub>6</sub>CoI<sub>12</sub>)<sub>2</sub> (R = Er and Gd) and K(Ce<sub>6</sub>MnI<sub>9</sub>). CsGd(Gd<sub>6</sub>CoI<sub>12</sub>)<sub>2</sub> crystallizes in the  $Pa\bar{3}$  space group while CsEr(Er<sub>6</sub>CoI<sub>12</sub>)<sub>2</sub> crystallizes in the  $R\bar{3}$  space group. K(Ce<sub>6</sub>MnI<sub>9</sub>) crystallizes in the  $R\bar{3}$  space group and has a connectivity described by the formulation  $K(\text{Ce}_6\text{Mn})\text{I}_{\frac{6}{2}^{\text{a-i}}}\text{I}_{\frac{6}{2}^{\text{i-i}}}\text{I}_{\frac{6}{2}^{\text{i-a}}}$ .

### **Synthesis, Structure and Physical Properties of the new layered Cu<sup>II</sup> oxide Na<sub>2</sub>Cu<sub>2</sub>TeO<sub>6</sub> with a distorted honeycomb lattice**

Jianxiao Xu<sup>a</sup>, Heather L. Cuthbert<sup>b</sup>, John E. Greedan<sup>b</sup>, Holger Kleinke<sup>a</sup>

<sup>a</sup> Department of Chemistry, University of Waterloo, Waterloo, ON, Canada N2L 3G1

<sup>b</sup> Department of Chemistry and the Brockhouse Institute for Materials Research, McMaster University, Hamilton, ON, Canada L8S 4M1

A new quaternary layered transition-metal oxide, Na<sub>2</sub>Cu<sub>2</sub>TeO<sub>6</sub>, has been synthesized under air using stoichiometric (with respect to the cationic elements) mixtures of Na<sub>2</sub>CO<sub>3</sub>, CuO and TeO<sub>2</sub>. Na<sub>2</sub>Cu<sub>2</sub>TeO<sub>6</sub> crystallizes in the monoclinic space group C2/m with  $a = 5.7059(6)$  Å,  $b = 8.6751(9)$  Å,  $c = 5.9380(6)$  Å,  $\beta = 113.740(2)^\circ$ ,  $V = 269.05(5)$  Å<sup>3</sup> and  $Z = 2$ , as determined by single crystal X-ray diffraction. The structure is composed of  ${}^2_z[\text{Cu}_2\text{TeO}_6]$  layers with the Na atoms located in the octahedral voids between the layers. Na<sub>2</sub>Cu<sub>2</sub>TeO<sub>6</sub> is a green nonmetallic compound, in agreement with the electronic structure calculation and electrical resistance measurement. The magnetic susceptibility shows Curie-Weiss behavior between 300 K and 600 K with an effective moment of 2.07(8) μ<sub>B</sub> per Cu<sup>2+</sup> ion and  $T_c = -156(22)$  K. A broad maximum at 160 K is interpreted as arising from short range two-dimensional antiferromagnetic correlations. The Cu<sup>2+</sup> sublattice topology is that of a distorted honeycomb lattice, and  $J^{\text{intra}}/k_B = -114(5)$  K was estimated from  $T(\text{max})$  using published constants. An analysis of the "Fisher" heat capacity suggests a transition to long range antiferromagnetic order below 80 K.

### **Thermoelectric Properties of *n*-type Nb<sub>3</sub>Sb<sub>d</sub>Te<sub>7-d</sub>**

Navid Soheilnia, Jon Giraldo, Holger Kleinke

Department of Chemistry, University of Waterloo, Waterloo, ON, Canada N2L 3G1

We recently succeeded in modifying and optimizing the electronic structure and physical properties of *p*-type Mo<sub>3</sub>Sb<sub>5</sub>Te<sub>2</sub> for thermoelectric applications. Our efforts to obtain *n*-type semiconducting material with molybdenum were not successful. Since the structure and number of valence electrons per formula unit are the same for Mo<sub>3</sub>Sb<sub>5</sub>Te<sub>2</sub> and Nb<sub>3</sub>Sb<sub>2</sub>Te<sub>5</sub>, we investigated the series Nb<sub>3</sub>Sb<sub>d</sub>Te<sub>7-d</sub> ( $d = 2 - 2.5$ ). The investigation revealed Sb/Te ordering, i.e. a symmetry reduction, and physical properties comparable with Mo<sub>3</sub>Sb<sub>5</sub>Te<sub>2</sub> and the desired *n*-type semiconducting properties.

### **Solution-Based Zinc Chalcogenide Semiconductor Nanowires: Preparation and Properties**

Angang Dong and William E. Buhro

Department of Chemistry, Washington University, St. Louis, Missouri 63130-4899

The solution-liquid-solid (SLS) method has been successfully used to grow both zinc telluride (ZnTe) and zinc selenide (ZnSe) nanowires. By using different sized catalyst nanoparticles, the diameters of ZnTe nanowires can be well controlled in the range of 5-13 nm, with corresponding lengths up to several micrometers. Due to the relatively large exciton Bohr radius (~6 nm) and small diameters, the excitonic features of ZnTe nanowires show a blue shift in the absorption spectra by comparison to bulk ZnTe. Furthermore, the size dependence of the band gaps in ZnTe quantum wires has been investigated. Our preliminary results indicate that ZnTe nanowires show a similar degree of quantum confinement as do CdSe nanowires. In the case of ZnSe, the diameters of the nanowires can be tailored in the range of 10-14 nm. Absorption measurements show that ZnSe nanowires exhibit a weak quantum-confinement effect, which is reasonable considering the relatively small exciton Bohr radius (~3 nm) and large diameters of the ZnSe wires. In addition, the as-synthesized ZnTe and ZnSe quantum wires can be further transformed into Ag<sub>2</sub>Te and Ag<sub>2</sub>Se nanowires, respectively by cation-exchange reactions at room temperature.

## Solid State Oxide Fluoride Anions

Michael R. Marvel and Kenneth R. Poeppelmeier  
*Department of Chemistry, Northwestern University*

Owing to their application as nonlinear optical materials and piezoelectrics, noncentrosymmetric (NCS) compounds have been intensely studied. NCS materials can be designed from oxide fluoride anions due to their inherent acentricity. In order to rationally engineer new NCS materials from acentric oxide fluoride anions, their structure-directing properties must be understood. The first step in achieving such an understanding is crystallizing the anions without orientational disorder. Increasing the asymmetry of the coordination environment around the anion is one way of imposing crystallographic order. The  $[\text{NbOF}_5]^{2-}$  anion has been crystallographically ordered in a new compound,  $\text{CsNaNbOF}_5$ . Multiple, asymmetric contacts to the anion are necessary to distinguish the anion's oxide and fluoride ligands.

## Synthesis and characterization of $\text{Bi}_4\text{Ti}_3\text{O}_{12}\cdot\text{AMO}_3$ (A=Bi, La; M=Cr, Mn, Fe, Co, Ni) series of compounds

Digamber Porob and Paul Maggard

*Department of Chemistry, North Carolina State University, Raleigh - NC*

Multiferroic materials exhibiting simultaneous semiconducting, ferroelectric, and ferromagnetic properties present opportunities for potential application in information storage, spintronics and sensors. Extensive studies have been conducted on  $\text{Bi}_4\text{Ti}_3\text{O}_{12}\cdot n\text{BiMO}_3$  (M=Fe, Mn; n=1,2) system in which a ferroelectric ( $\text{Bi}_4\text{Ti}_3\text{O}_{12}$ ) is combined with either  $\text{BiFeO}_3$  (ferroelectric, antiferromagnetic) or  $\text{BiMnO}_3$  (ferroelectric, ferromagnetic). These materials exhibit simultaneous ferroelectric and antiferromagnetic properties.  $\text{LaMO}_3$  series of perovskite oxides with M = Cr, Mn, Fe, Co, Ni display interesting magnetic properties. Hence these oxides can be combined with  $\text{Bi}_4\text{Ti}_3\text{O}_{12}$  to generate novel multiferroic materials. We have investigated the  $\text{Bi}_4\text{Ti}_3\text{O}_{12}\cdot\text{LaMO}_3$  and  $\text{Bi}_4\text{Ti}_3\text{O}_{12}\cdot\text{BiMO}_3$  (M=Cr, Mn, Fe, Co, Ni) series using both hydrothermal and flux methods.

The hydrothermal synthesis were carried out at temperatures in the range of 200-240°C for 24-48h using Titanium *n*-butoxide ( $\text{Ti}(\text{OC}_4\text{H}_9)_4$ ), metal nitrates and 3M KOH solution. Syntheses by flux method were carried out using metal oxides in eutectic mixtures of  $\text{Na}_2\text{SO}_4+\text{K}_2\text{SO}_4$  and  $\text{NaCl}+\text{KCl}$  at temperatures in the range of 700-1000°C. The products obtained had distinct plate like morphology and good homogeneity. X-ray diffraction studies confirmed the formation of the typical layered Aurivillius phases. Detailed crystal structure analysis along with magnetic and electric property studies will be presented.

## A Uranium Assisted Synthesis of $\text{Ba}_4\text{Fe}_2\text{I}_5\text{S}_4$ and $\text{CsTi}_5\text{Te}_8$

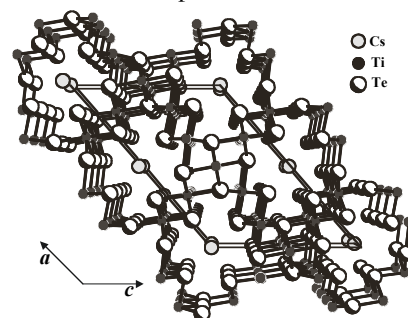
Danielle L. Gray and Jim Ibers

*Department of Chemistry, Northwestern University, Evanston, IL 60208-3113, U.S.A.*

The new metal chalcogenides,  $\text{Ba}_4\text{Fe}_2\text{I}_5\text{S}_4$  and  $\text{CsTi}_5\text{Te}_8$ , were synthesized with the aid of uranium turnings.  $\text{Ba}_4\text{Fe}_2\text{I}_5\text{S}_4$  was synthesized serendipitously at 1173 K by the reaction of FeS, BaS, S, and U with  $\text{BaI}_2$  as a flux.  $\text{Ba}_4\text{Fe}_2\text{I}_5\text{S}_4$  crystallizes with two formula units in space group  $I4/m$  of the tetragonal system in a cell of dimensions  $a = 13.7583(13)$  Å,  $c = 5.1261(7)$  Å. The structure contains what we believe is the first example of infinite chains of edge-sharing  $\text{FeS}_4$  tetrahedra.  $\text{CsTi}_5\text{Te}_8$  was synthesized while trying to resynthesize  $\text{CsTiUTe}_5^1$  at 1173 K by the reaction of U,  $\text{Cs}_2\text{Te}_3$ , Ti, Te with CsCl as a flux.  $\text{CsTi}_5\text{Te}_8$  crystallizes with two formula units in space group  $C2/m$  of the monoclinic system in a cell of dimensions  $a = 19.2442(2)$  Å,  $b = 3.8912(5)$  Å,  $c = 13.4135(16)$  Å, and  $\beta = 130.969(1)^\circ$ . The structure contains a network of  $\text{TiTe}_6$  octahedra penetrated by Cs-containing channels. This structure is similar to that of  $\text{CsCr}_5\text{S}_8$ ,<sup>2</sup> although the channels differ.

1. Cody, J. A.; Ibers, J. A. *Inorg. Chem.* **1995**, *34*, 3165-3172.

2. Huster, J. Z. *Anorg. Allg. Chem.* **1978**, *447*, 89-96.



Structure of  $\text{CsTi}_5\text{Te}_8$

## Insertion of Metal-Organic Coordination Polymers into V<sub>2</sub>O<sub>5</sub>: Hydrothermal Syntheses and Characterizations of [M(py<sub>z</sub>)]<sub>0.5</sub>V<sub>2</sub>O<sub>5</sub> (M = Co, Ni)

Bangbo Yan, Paul Maggard

*Department of Chemistry, North Carolina State University, Raleigh, NC*

Layered compounds are of great interest because of their broad applications in heterogeneous catalysis, ion exchange and rechargeable batteries. There is particular interest in the insertion of small organic molecules or conducting organic polymers into V<sub>2</sub>O<sub>5</sub> layers in order to synthesize organic-inorganic composite materials. We have been interested in the synthesis of intercalation compounds using metal/organic coordination compounds as guests through a charge-density matching approach. Single crystal structure analysis of the hydrothermally synthesized compounds [M(py<sub>z</sub>)]<sub>0.5</sub>V<sub>2</sub>O<sub>5</sub> (M = Co, Ni) reveals their structure is comprised of [V<sub>2</sub>O<sub>5</sub>]<sup>-</sup> layers separated by [M(py<sub>z</sub>)]<sup>2+</sup> (py<sub>z</sub> = pyrazine) chains. Similar to the layers in V<sub>2</sub>O<sub>5</sub>, the [V<sub>2</sub>O<sub>5</sub>]<sup>-</sup> layer consists of distorted VO<sub>5</sub> square pyramids linked by edge- and corner-sharing O atoms. Their thermal stabilities and magnetic properties are also studied.

## Synthesis of new carbide phases from mixed rare earth/transition metal fluxes

Susan E. Latturmer

*Department of Chemistry and Biochemistry, Florida State University*

Considering the unusual superconducting properties of magnetic RENi<sub>2</sub>B<sub>2</sub>C structures and the strong magnetism of ternary phases such as Nd<sub>2</sub>Fe<sub>14</sub>C, it is evident that intermetallic carbide phases containing rare earth and transition metals have the potential for interesting and useful properties. Synthesis in molten metal eutectics comprised of early rare earth metals combined with late transition metals (such as the 70 mol% La / 30 mol% Ni mixture, mp 520 °C) is being explored and has produced a number of interesting materials. In addition to well-formed crystals of known lanthanum-rich phases such as La<sub>5</sub>Ni<sub>2</sub>Sn and La<sub>10</sub>Ni<sub>3+d</sub>Si<sub>6</sub>, new carbide phases have been crystallized out of the molten metal eutectic. These include La<sub>22</sub>Fe<sub>6</sub>C<sub>36</sub>, which is a superstructure of a known ternary phase and features iron atoms bound to three C<sub>2</sub> units (the short 1.3 Å carbon-carbon bond is similar to that of ethylene). A new quaternary structure, La<sub>21</sub>Fe<sub>8</sub>M<sub>7</sub>C<sub>12</sub> (M = Bi or Sn), has also been isolated from reactions in La/Ni eutectic flux. The cubic structure features tetrahedra of iron atoms capped on each edge by carbon; these Fe<sub>4</sub>C<sub>6</sub> tetrahedra are surrounded by a La/(Bi or Sn) network. Cerium analogs of these materials have also been synthesized and their magnetic properties are being investigated.

## From [Cd<sub>4</sub>Sn<sub>3</sub>Se<sub>13</sub>]<sup>6-</sup> to [Cd<sub>60</sub>Sn<sub>48</sub>Se<sub>184</sub>]<sup>56-</sup>: Acid-Induced 3D to 3D Single-Crystal Transformation

Nan Ding and Mercouri G. Kanatzidis

*Department of Chemistry, Michigan State University, East Lansing, Michigan 48824*

During the past decades a continued development in crystalline chalcogenides<sup>[1]</sup> with 3D open-frameworks has been under way. The main impetus is because of the potential to combine zeolitic with optoelectronic properties in a single material. Another motivating factor for us has been to use the structures of the crystalline chalcogenides as starting models for the chalcogenide-based (e.g. [Sn<sub>2</sub>Se<sub>4</sub>]<sup>4+</sup>, [Sn<sub>2</sub>Se<sub>6</sub>]<sup>4+</sup>, [Ge<sub>4</sub>S<sub>10</sub>]<sup>4+</sup>) mesostructured chalcogenides<sup>[2]</sup> which have long-range order but are locally disordered. Recently, we reported the open-framework compound K<sub>6</sub>Cd<sub>4</sub>Sn<sub>3</sub>Se<sub>13</sub> which shows good ion-exchange properties with other alkali metal cations such as Li<sup>+</sup>, Na<sup>+</sup> and Rb<sup>+</sup>.<sup>[3]</sup> Surprisingly, in an attempt to proton-exchange, a 3D to 3D single crystal transformation was discovered. The new crystal H<sub>x</sub>K<sub>56-x</sub>Cd<sub>60</sub>Sn<sub>48</sub>Se<sub>184</sub> has a completely different structure from K<sub>6</sub>Cd<sub>4</sub>Sn<sub>3</sub>Se<sub>13</sub>. Interestingly, such transformation also happens under a mild hydrothermal condition when Lewis acid such as Ca<sup>2+</sup>, Mg<sup>2+</sup> is used in the synthesis of K<sub>6</sub>Cd<sub>4</sub>Sn<sub>3</sub>Se<sub>13</sub>. This new compound has a robust anionic framework which can stand strong acid up to pH ~ 1.0. Nevertheless, since there is a quite large free space in this framework, ion-exchange can be readily achieved with alkali metal cations such as Na<sup>+</sup>, Rb<sup>+</sup> and Cs<sup>+</sup> under mild conditions. The mechanism of the single crystal transformation, the synthesis of M<sub>x</sub>K<sub>56-2x</sub>Cd<sub>60</sub>Sn<sub>48</sub>Se<sub>184</sub> (M = Ca, Mg) and the results of ion-exchange reactions will be presented.

1. (a) Li, H.; Laine, A.; O'Keeffe, M.; Yaghi, O. M. *Science* **1999**, 283, 1145. (b) Feng, P.; Bu, X.; Zheng, N. *Acc. Chem. Res.* C ASAP web article.

- (a) Trikalitis, P. N.; Rangan, K. K.; Bakas, T.; Kanatzidis, M.G. *Nature* **2001**, *410*, 671. (b) Riley, A.E.; Tolbert, S. H. *J. Am. Chem. Soc.* **2003**, *125*, 4551. (c) MacLachlan, M. J.; Coombs, N.; Ozin, G. A. *Nature* **1999**, *397*, 681.
- Ding, N.; Chung, D.-Y.; Kanatzidis, M.G. *Chem. Comm.* **2004**, 1170.

### Impressive Structural Diversity in the System Tl/Bi/P/S

Matthew A. Gave, Christos Malliakas, and Mercouri G. Kanatzidis

*Michigan State University, East Lansing, MI*

An impressive example of structural diversity is found in the class of compounds containing Tl/Bi/P/S. Targeted syntheses of  $\text{Tl}_3\text{Bi}_3(\text{PS}_4)_4$  [I],  $\text{Tl}_4\text{Bi}_2(\text{P}_2\text{S}_6)(\text{PS}_4)_2$  [II], and  $\text{Tl}_3\text{Bi}(\text{PS}_4)_2$  [III] were possible by slightly varying the reaction conditions. [I] was formed when a 1:1 ratio of the metals reacted with excess  $\text{P}_x\text{S}_y$  flux. Bright red, needle-like crystals were isolated and found to crystallize in a complex 3D structure built from  $[\text{PS}_4]^{3-}$  anions in the monoclinic space group  $P2_1/c$  with  $a = 20.8189(7)$  Å,  $b = 13.2281(3)$  Å, and  $c = 22.2029(7)$  Å and  $\beta = 117.896(2)^\circ$ . An amorphous glass of [I] was also produced by rapid quenching of the melt. [II] was formed in the reaction of a stoichiometric ratio of the elements with an additional equivalent of phosphorous. The resulting bright red, needle-like crystals were found to crystallize in the monoclinic space group  $C2/c$  with  $a = 22.934(4)$  Å,  $b = 6.6902(12)$  Å and  $c = 18.482(3)$  Å and  $\beta = 121.303(3)^\circ$ . The structure is formed from lamellae of  $[\text{Bi}_2(\text{PS}_4)_2(\text{P}_2\text{S}_6)]^{4-}$  which are separated by  $\text{Tl}^+$  cations. [III] was formed by direct combination of the elements and was found to crystallize in the monoclinic space group  $P2_1/c$  with  $a = 25.4189(5)$  Å,  $b = 6.6731(11)$  Å,  $c = 17.9513(3)$  Å and  $\beta = 110.676(3)^\circ$ . The structure contains only  $[\text{PS}_4]^{3-}$  and is built from helical  $[\text{Bi}(\text{PS}_4)_2]^{3-}$  chains that run down the b-axis and are separated by  $\text{Tl}^+$  cations. All compounds were found to be wide band-gap semiconductors with optical band-gaps in the range of 1.8 – 1.9 eV.

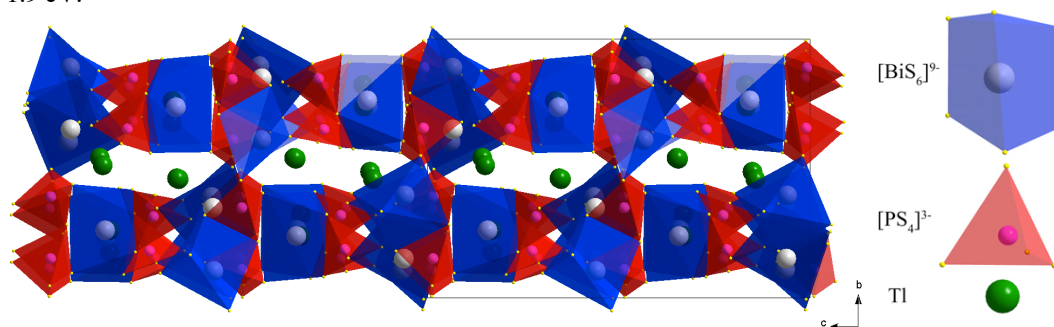


Figure 1: The structure of  $\text{Tl}_3\text{Bi}_3(\text{PS}_4)_4$  viewed down the a-axis.

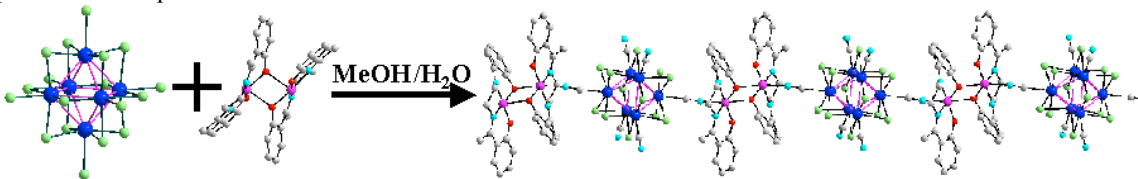
### One-dimensional Coordination Polymers Based on Octahedral Cluster Anion $[\text{Nb}_6\text{Cl}_{12}(\text{CN})_6]^{4-}$ and Phenoxo-bridged Dimer $[\text{Mn}_2(7\text{-Me-salen})_2]^{2+}$

Huajun Zhou, Bruno Cloix, and Abdou Lachgar

*Department of Chemistry, Wake Forest University, Winston-Salem, NC 27109*

Reactions between octahedral niobium cluster compounds containing  $[\text{Nb}_6\text{Cl}_{12}(\text{CN})_6]^{4-}$  cluster units and  $[\text{Mn}_2(7\text{-Me-salen})_2(\text{OAc})_2]\text{ClO}_4$  at room temperature afforded two one-dimensional (1D) compounds with different chemical and structural features depending on the solvent used and counteranions:  $[\text{Mn}_2(7\text{-Me-salen})_2(\text{MeOH})_2]\{[\text{Mn}_2(7\text{-Me-salen})_2][\text{Nb}_6\text{Cl}_{12}(\text{CN})_6]\} \cdot 2\text{MeOH}$  (**1**) and  $[\text{Mn}(7\text{-Me-salen})(\text{MeOH})(\text{H}_2\text{O})_2][\text{Mn}_2(7\text{-Me-salen})_2][\text{Nb}_6\text{Cl}_{12}(\text{CN})_6] \cdot 8\text{MeOH} \cdot 2\text{H}_2\text{O}$  (**2**). The compounds have been characterized by single crystal X-ray diffraction, IR, magnetic susceptibility, TGA, and elemental analysis. In both compounds the  $[\text{Nb}_6\text{Cl}_{12}(\text{CN})_6]^{4-}$  cluster units is linked to two phenoxo-bridged dimers  $[\text{Mn}_2(7\text{-Me-salen})_2]^{2+}$  through two apical CN ligands located in *trans* positions leading to the formation of anionic chains  $\{[\text{Mn}_2(7\text{-Me-salen})_2][\text{Nb}_6\text{Cl}_{12}(\text{CN})_6]\}^{2-}$ . However, in (**1**) an additional solvated dimeric unit  $[\text{Mn}_2(7\text{-Me-salen})_2(\text{MeOH})_2]^{2+}$  acts as counterion to balance the anionic charge on the chain, while in (**2**) a solvated monomeric unit  $[\text{Mn}(7\text{-Me-salen})(\text{MeOH})(\text{H}_2\text{O})]^{+}$  serves as counterion. Compound **1** crystallizes in the triclinic space group  $P\bar{1}$  with  $a = 12.535(1)$  Å,  $b = 13.460(1)$  Å,  $c = 16.048(1)$  Å,  $\beta = 74.184(1)^\circ$ ,

$\alpha = 80.020(1)^\circ$ ,  $\beta = 84.637(1)^\circ$ , and  $Z = 1$ . Compound **2** also crystallizes in the triclinic space group  $P\bar{1}$  with the cell dimensions of  $a = 12.478(3) \text{ \AA}$ ,  $b = 13.933(3) \text{ \AA}$ ,  $c = 16.682(4) \text{ \AA}$ ,  $\alpha = 98.679(4)^\circ$ ,  $\beta = 99.997(4)^\circ$ ,  $\gamma = 94.828(4)^\circ$ , and  $Z = 1$ . Details of synthesis, crystal structures, magnetic properties and thermal behavior of these two compounds will be presented.



### Electronic Structures and Magnetic Orderings in $MM'As$ Compounds ( $M, M' = Cr, Mn, Fe$ )

Hyunjin Ko, Christopher J. Kurtz, Gordon J. Miller

*Department of Chemistry, Iowa State University, Ames, IA 50011*

The class of ternary  $MM'X$  ( $M, M' = 3d$  or  $4d$  metals;  $X =$  non-metal element) intermetallic compounds exhibits unusual magnetic properties. These intermetallic compounds crystallise exclusively in three structures: tetragonal (the  $Fe_2As$ -type,  $P4/nmm$ ), hexagonal (the  $Fe_2P$ -type,  $P-62m$ ), or orthorhombic (the  $Co_2P$ -type,  $Pnma$ ) structures. Among the large family of these solid solutions, the transition metal arsenide system is particularly interesting due to the fact that its deviation in the crystallographic and magnetic structural transitions are a function of the metal and As content.

To understand the electronic properties of these systems, we have carried out electronic structure calculations within density functional theory (DFT) using tight-binding linear muffin tin orbital (TB-LMTO) method with local spin density approximation (LSDA). To incorporate the effect of electron concentration changes on the magnetic ordering of these systems, model structures with magnetic unit cells (double unit cell in crystallographic  $c$  direction) were constructed.

### Preparation of Diamond-like Semiconductors with Potentially Interesting Nonlinear Optical Properties

Katie L. McNerny and Jennifer A. Aitken

*Department of Chemistry and Biochemistry, Duquesne University, Pittsburgh, PA*

Diamond-like semiconductors have a number of technologically useful properties. Specifically these materials are of interest because they crystallize in a noncentrosymmetric space group, thus leading to a nonzero second-order nonlinear optical susceptibility. Quaternary sulfides of the formula  $I_2-II-IV-VI_4$  (where the larger number represents the number of valence electrons for a group of elements and the subscripted number indicates the number of that element in the formula) are expected to exhibit useful optical properties such as second harmonic generation (SHG). This property leads to a phenomenon in which the output frequency of a beam of light through the crystalline material is exactly twice that as the input. Therefore we were motivated to prepare new quaternary sulfides such as  $Li_2CdGeS_4$  and  $Li_2CdSnS_4$  and study the structure-optical property relationships of the materials.

These materials were synthesized using high temperature solid-state synthesis in which stoichiometric amounts of reactants were heated in a furnace at  $800^\circ C$  in a vacuum sealed quartz tube. It is predicted that regrinding the material followed by additional heating along with changing the ratios of reactants will maximize the purity of the sample. Efforts towards this goal will be presented. The resulting materials were characterized using powder X-ray diffraction, differential thermal analysis, diffuse reflectance spectroscopy in the UV/Vis/NIR region and scanning electron microscopy coupled with energy dispersive spectroscopy.

### Successes and Setbacks in the Synthesis of Borides Using a Molten Metal Flux

Britt A. Vanchura II, Christos Malliakas, and Mercouri G. Kanatzidis

*Department of Chemistry, Michigan State University, East Lansing, MI 48824*

The assembly of clusters in boron-rich compounds often produces interesting crystal structures and physical properties. The successful synthesis of  $RE_{1.8}Si_8C_2(B_{12})_3$ <sup>[1]</sup> ( $RE = Y, Sc, Dy, Er, Tb, \text{ and } Tm$ ) and  $b-SiB_3$ <sup>[2]</sup> has spurred our lab into exploring other  $RE/Si/C/B$ ,  $RE/TM/B$ , and  $TM/TM/B$  systems using molten gallium as a flux. While yet

to produce another new boron-rich compound in these systems, the gallium flux has aided in the crystallization of HoB<sub>12</sub> and MnB with the CrB-type structure. In trying to optimize our syntheses we often observed the formation of stable gallides and silicides. In order to compare and contrast the behavior of molten gallium with fluxes of related metals, we also examined molten aluminum and Al/Cu mixtures. The well-established success of aluminum as a flux and recent reports of copper flux syntheses led us to try a 50/50 wt% Al/Cu mixture as a flux at moderate temperatures. This flux produced a boron-rich compound that crystallizes in an orthorhombic cell with approximate composition AlB<sub>18</sub> and cell parameters  $a \approx 8.857$   $b \approx 8.857$   $c \approx 5.080$ . The structure contains interconnected boron icosahedra with aluminum atoms filling the voids between the icosahedra. Complete crystal structures for HoB<sub>12</sub>, MnB, AlB<sub>18</sub>, and some new gallides and silicides will be presented.

[1] J.R. Salvador, D. Bilc, S.D. Mahanti, M.G. Kanatzidis, *Angew. Chem. Int. Ed.* **2002**, *41*, 844

[2] J.R. Salvador, D. Bilc, S.D. Mahanti, M.G. Kanatzidis, *Angew. Chem. Int. Ed.* **2003**, *42*, 1929

### Synthesis and Thermoelectric Properties of CdBi<sub>4</sub>S<sub>7</sub>

Jun-Ho Kim and Mercuri G. Kanatzidis

*Department of Chemistry and Center for Fundamental Materials Research, Michigan State University*

Since the Bi<sub>2</sub>Te<sub>3-x</sub>Se<sub>x</sub> and Bi<sub>2-x</sub>Sb<sub>x</sub>Te<sub>3</sub> alloys showed high thermoelectric (TE) figures of merit  $ZT$ , new perspective thermoelectric materials have been devoted to alkali metal bismuth chalcogenides such as CsBi<sub>4</sub>Te<sub>6</sub> and b-K<sub>2</sub>Bi<sub>8</sub>Se<sub>13</sub>. The thermoelectric properties are defined as figure of merit  $ZT = S^2\sigma T/k$ , where  $S$  is the Seebeck coefficient,  $\sigma$  is the electrical conductivity,  $T$  is the temperature and  $k$  is the thermal conductivity. Herein, the study of thermoelectric materials has focused on the compounds with complex structure and composition that optimize  $ZT$  by virtue of increasing thermopower and decreasing thermal conductivity. In comparison with alkali metal bismuth chalcogenides, the silver analogues (e.g. AgBi<sub>3</sub>S<sub>5</sub>) produce lower band gap energies due to the more covalent bonding contribution in their structures that can lead to higher electrical conductivity. Extending to transition metal bismuth chalcogenides such as with Cd, one finds the compounds CdBi<sub>2</sub>S<sub>4</sub>, CdBi<sub>4</sub>S<sub>7</sub>, Cd<sub>2</sub>Bi<sub>6</sub>S<sub>11</sub>, Cd<sub>3</sub>Bi<sub>8</sub>S<sub>15</sub>, and CdBi<sub>2</sub>Se<sub>4</sub>, all of which have not been intensively studied or characterized. Therefore we became interested to study these phases from the thermoelectric point of view. Here we present one of these compounds, CdBi<sub>4</sub>S<sub>7</sub>, with synthesis, structure, physicochemical and thermoelectric properties.

### LaFe<sub>13-x</sub>Si<sub>x</sub> with the NaZn<sub>13</sub> Structure Type: La(Fe<sub>x</sub>Si<sub>1-x</sub>)<sub>13</sub>

Mi-Kyung Han and Gordon J. Miller

*Department of Chemistry, Iowa State University, Ames, Iowa 50011*

La(Fe<sub>x</sub>Si<sub>1-x</sub>)<sub>13</sub> with NaZn<sub>13</sub> structure-type are an important series of compounds in the study of possible materials for efficient magnetic refrigeration. A systematic study of the compositional variation in La(Fe<sub>x</sub>Si<sub>1-x</sub>)<sub>13</sub> demonstrates that depending on the fraction of the nonmagnetic element (Si), the La(Fe<sub>x</sub>Si<sub>1-x</sub>)<sub>13</sub> system exhibits a structural transformation from cubic to a tetragonal derivative of the NaZn<sub>13</sub>-structure type. For example, under our experimental conditions, the LaFe<sub>13-x</sub>Si<sub>x</sub> system crystallizes in the cubic structure for the range  $1 \leq x \leq 2.6$ , and it shows the tetragonal structure within the range  $3.2 \leq x \leq 5$ .

Single crystal X-ray diffraction at various temperatures was performed in order to examine the origin of the large magnetic entropy change. It shows a large volume change at the Curie temperature. To understand the mechanism for such a large volume change at the Curie temperature, detailed theoretical and experimental works have been carried out to investigate the coupling between magnetism and lattice in LaFe<sub>13-x</sub>Si<sub>x</sub> system. Tight-binding LMTO calculations have been performed to study the effects of a third element on stabilizing the structure and controlling the transformation of cubic NaZn<sub>13</sub>-type structures to the tetragonal derivative, and to study for relationships between their chemical bonding, structure, and properties.



### **Ag<sub>4</sub>V<sub>2</sub>O<sub>6</sub>F<sub>2</sub>: An New Electrochemically Active Phase**

Erin M. Sorensen,<sup>†</sup> Heather K. Izumi,<sup>†</sup> John T. Vaughey,<sup>‡</sup> Charlotte L. Stern,<sup>†</sup> and Kenneth R. Poeppelmeier<sup>†</sup>

<sup>†</sup>*Department of Chemistry, Northwestern University, Evanston, Illinois 60208-3113,*

<sup>‡</sup>*Chemical Engineering Division, Argonne National Laboratory, Illinois 87185-0755*

Low temperature hydrothermal techniques were used to synthesize single crystals of Ag<sub>4</sub>V<sub>2</sub>O<sub>6</sub>F<sub>2</sub>. This previously unreported oxide fluoride phase was characterized by single crystal X-ray diffraction and IR spectroscopy and was also evaluated as a primary lithium battery cathode. Ag<sub>4</sub>V<sub>2</sub>O<sub>6</sub>F<sub>2</sub> (SVOF) exhibits two characteristic regions within the discharge curve, an upper plateau at 3.5 V from the reduction of silver, and a lower sloped region around 2.3 V from reduction of the vanadium oxide fluoride framework. The material has a nominal capacity of 251 mAh/g, with 148 mAh/g above 3 V. The upper discharge plateau at 3.5 V is nearly 300 mV over the silver reduction potential of the commercial primary battery material, Ag<sub>2</sub>V<sub>4</sub>O<sub>11</sub> (SVO).

### **Synthesis and Characterization of the Face-Sharing Bioctahedral [Mo<sub>2</sub>O<sub>6</sub>F<sub>3</sub>]<sup>3-</sup> Anion**

Janet E. Kirsch, Heather K. Izumi, Charlotte L. Stern, and Kenneth R. Poeppelmeier

*Department of Chemistry, Northwestern University, Evanston, Illinois 60208-3113*

The molybdenum(VI) oxide fluoride anion [Mo<sub>2</sub>O<sub>6</sub>F<sub>3</sub>]<sup>3-</sup>, isolated in the new compound [Cu(3-apy)<sub>4</sub>]<sub>3</sub>(Mo<sub>2</sub>O<sub>6</sub>F<sub>3</sub>)<sub>2</sub> (3-apy = 3-aminopyridine), has been characterized by experimental and computational techniques. Single-crystal X-ray diffraction studies show that each Mo<sup>6+</sup> center in the confacial bioctahedral [Mo<sub>2</sub>O<sub>6</sub>F<sub>3</sub>]<sup>3-</sup> anion forms three short terminal metal–ligand bonds and three long metal–ligand–metal bridging interactions. Historically, crystallographic similarities between oxide and fluoride ligands have made straightforward assignments of the ligand sites difficult in oxide fluoride compounds; however, aspects of the electronic structure, as well as geometry comparisons of bond lengths and angles in [Mo<sub>2</sub>O<sub>6</sub>F<sub>3</sub>]<sup>3-</sup> with the similarly-distorted [MoO<sub>3</sub>F<sub>3</sub>]<sup>3-</sup> anion, all suggest that the six terminal ligand positions of the face-sharing bioctahedra are occupied exclusively by oxide ligands while fluorides occupy the three bridging sites.

### **Computational and Conceptual Tools for Understanding Magnetic Ordering in Reduced Lanthanide Compounds**

Lindsay E. Roy and Timothy Hughbanks

*Department of Chemistry, Texas A&M University, College Station, TX 77843-3012*

While compounds containing 4*f* elements provide a rich territory for investigation of magnetic properties, compounds containing the metal in the 3+ oxidation state are magnetically uninteresting because the interionic coupling achieved is generally weak. However, enhanced magnetic ordering *is* attainable in compounds which the lanthanide centers are reduced, or contain significant diffuse 5*d* and/or 6*s* orbital density, as seen in rare-earth intermetallics. A major goal of this research is to develop bonding schemes with sufficiently transparent qualitative features that experimentalists might be able to “design in” magnetic interactions in hopes of optimizing their potential properties. In our efforts to establish relationships between structure, bonding, and magnetic properties of rare-earth compounds and solids, we have already provided a perturbative-theoretic treatment of the metal bonding orbitals based on the *d*-electron mediated *f*-*f* exchange concept for benchmark rare-earth clusters and solids, including models of GdI<sub>2</sub>, Gd[Gd<sub>6</sub>I<sub>12</sub>Fe], and Gd<sub>2</sub>Cl<sub>3</sub>, using density functional theory (DFT). Continuing with our analysis, we provide in this contribution a detailed look at Gd<sub>2</sub>Cl<sub>3</sub>, with the aid of density functional calculations, to guide our development of a spin-pattern model that can be implemented in tight binding theory. Gd<sub>2</sub>Cl<sub>3</sub> is particularly useful because this semiconducting system exhibits antiferromagnetic ordering with published neutron diffraction results. Herein we will present DFT results which predict the two lowest spin patterns give the same spin arrangement in the basal atoms as the neutron diffraction experiment. Also presented will be a correlation between DFT and extended Hückel (eH), with eH parameters chosen to mimic *d*-electron exchange (de)stabilization when interacting with the *f*-moment of (un)like-spin. Cases where there are partially filled bands, such in Gd<sub>4</sub>I<sub>5</sub>C, will also be presented to determine the nature of the magnetic ordering in metallic chains.

## Structural Characterization and Magnetic Measurements of $Gd_{5-x}Y_xTt_4$ ( $Tt = Si, Ge$ )

Sumohan Misra and Gordon J. Miller

*Department of Chemistry, Iowa State University, Ames, Iowa 50011-3111*

The Magnetocaloric effect is defined as the heating or cooling of a magnetic material due to the application of a magnetic field. This finds its application in magnetic refrigeration which is becoming a promising technology to replace the conventional gas-compression refrigeration due to its high efficiency, energy saving and environmental concerns. With the discovery of the giant magnetocaloric effect, giant magnetoresistance and colossal magnetostriction in the  $Gd_5Si_xGe_{4-x}$  alloys, the rare-earth – group 14 metal systems at the 5:4 stoichiometry have become subjects of broad interest.

Recently we began a systematic investigation of the effect of replacing Gd with Y on the structural features and magnetic properties in both Si and Ge systems. Room temperature crystal structures of  $Gd_{5-x}Y_xTt_4$  ( $Tt = Si, Ge$ ) with  $x$  varying from 1 to 4 have been studied by means of X-ray single crystal diffraction. The magnetization-temperature behaviors of these systems were also studied and will be presented.

## Structure and Properties of Perovskites Exhibiting Cation ordering of the A and B Sites

Meghan Knapp and Patrick Woodward

*Ohio State University*

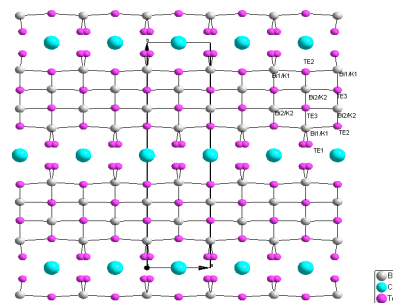
The stoichiometry of ternary oxide perovskites ( $ABO_3$ ) can be extended to apply to oxides with multiple A and or B site cations. These cations can be arranged randomly or in an ordered fashion. Rock-salt ordering of the B-cations has been well documented for double perovskites ( $A_2BB'O_6$ ). Ordering of the A-cation is not as widely observed. Several studies have examined ordering of a single A-cation with vacancies at the same site. This study investigates the cause of ordering of multiple A-cations. Previous studies of  $NaLaMgWO_6$  and  $KLaMgWO_6$  have shown that the  $Mg^{2+}$  and  $W^{6+}$  cations order on the B-site while  $Na^+/K^+$  and  $La^{3+}$  order on the A-site. Each type of A-cation forms a layer perpendicular to one of the pseudo-cubic perovskite axes. However, an analogous structure with a single B-cation,  $(Na,La)TiO_3$ , shows no A ordering. Compounds were prepared with varying relative sizes of A-cations (Na, K, Li, La, Bi, Y), varying tolerance of the A-cation, and varying degrees of ordering at the B-site (Mg, W, Sc, Sb, Nb, Ti, and Zr). Compounds were prepared by traditional ceramic methods and analyzed primarily by laboratory powder diffraction. Refinements of these structures indicate that each of these factors plays a role in the degree of ordering, and that ordering of the A-cation is typically accompanied by an extension of the c-axis, which is perpendicular to the A-layers. Layering of the A-cations is accompanied by shifts of the B-cations to compensate for the differences in size and charge of the two A-cations. These structures are therefore being studied for possible dielectric properties, particularly those with  $Bi^{3+}$  at the A-cation site. Trivalent bismuth has two 6s electrons which can act as a stereo-active lone pair, displacing the bismuth from its position. Analysis of the bismuth analogs shows less of a tendency for ordering than lanthanum and a preference for the pyrochlore structure over the perovskite structure.

## Exploratory synthesis of lead substitution in the homologous family $CsPb_mBi_3Te_{5+m}$

Aurélie Guéguen, Eric Quarez, Kuei-Fang Hsu, and Mercuri G. Kanatzidis

*Department of Chemistry, Michigan State University, East Lansing MI 48824, USA*

The discovery of new thermoelectric materials with superior properties is one of the main challenges in solid state chemistry and physics. One promising candidate for such applications is  $CsBi_4Te_6$  identified in our laboratory [1]. Recently, our effort to produce new materials that resemble to  $CsBi_4Te_6$ , led to the discovery of the homologous series of materials  $CsPb_mBi_3Te_{5+m}$  [2, 3, 4]. The four members of the series ( $m=1, 2, 3$  and 4) were obtained by introducing various equivalents of  $PbTe$  into the layered framework of  $CsBi_4Te_6$  [4]. The  $CsPb_mBi_3Te_{5+m}$  compounds show low thermal conductivity compared to that of  $Bi_2Te_3$  and  $CsBi_4Te_6$ . Preparing analogs of such



compounds can be a way to tune the thermoelectric properties. We are currently investigating the substitution of Pb in  $\text{CsPb}_m\text{Bi}_3\text{Te}_{5+m}$  by other elements such as silver, potassium, sodium, and barium.

So far, our attempts with potassium substitution yielded the new compound  $\text{Cs}_{0.74}\text{K}_{0.76}\text{Bi}_{3.5}\text{Te}_6$ . Single crystal X-Ray diffraction study indicated that this compound is isostructural to  $\text{CsPbBi}_3\text{Te}_6$  ( $m=1$ ) with cell parameters  $a = 6.3810$  (9) Å,  $b = 28.3263$  (41) Å,  $c = 4.4134$ (6) Å in the  $Cmcm$  space group (see figure). By analogy with  $\text{CsPbBi}_3\text{Te}_6$ , the formula of  $\text{Cs}_{0.74}\text{K}_{0.76}\text{Bi}_{3.5}\text{Te}_6$  can be rewritten as  $(\text{Cs}_{0.74}/\text{K}_{0.26})(\text{K}_{0.5}/\text{Bi}_{0.5})\text{Bi}_3\text{Te}_6$ . Preliminary electrical conductivity and thermopower measurements indicate n-type behavior. Further experiments aimed at preparing other analogs in the homologous series will be presented.

[1] D. K. Chung, T. Hogan, P. Brazis, M. Rocci-Lane, C. R. Kannewurf, M. Bastea, C. Uher, M. G. Kanatzidis, *Science*, **2000**, 287, 1024

[2] K. F. Hsu, D. Y. Chung, S. Lal, T. Kyratsi, T. Hogan, M. G. Kanatzidis, *J. Am. Chem. Soc.*, **2002**, 124, 2410

[3] K. F. Hsu, S. Lal, T. Hogan, M. G. Kanatzidis, *Chem. Comm.*, **2002**, 1380

[4] K. F. Hsu, D. K. Chung, S. Lal, T. Hogan, M. G. Kanatzidis, *Mat. Res. Soc. Symp. Proc.*, **2002**, 691, 269

### Investigation of Zn Doping onto the Mn site of the $\text{Yb}_{14}\text{MnSb}_{11}$ System

Shawna R. Brown,<sup>1</sup> Susan M. Kauzlarich,<sup>1</sup> G. Jeff Snyder,<sup>2</sup> Franck Gascoin<sup>2</sup>

<sup>1</sup>Department of Chemistry, University of California, One Shields Ave., Davis, CA 95616

<sup>2</sup>Jet Propulsion Laboratory, California Technical Institute, 4800 Oak Grove Drive, Pasadena, CA 91109-8099

Thermoelectric research has seen a renewed interest in the past decade which has been spurred by increased environmental, energy and aerospace issues. Preliminary measurements of the transition metal Zintl phase compound,  $\text{Yb}_{14}\text{MnSb}_{11}$ , have revealed high figure of merit at elevated temperatures (900-1275 K).  $\text{Yb}_{14}\text{Mn}_{1-x}\text{Zn}_x\text{Sb}_{11}$  with  $x = 0.17, 0.33, 0.50, 0.67,$  and  $0.83$  have been synthesized in an attempt to further improve the figure of merit of  $\text{Yb}_{14}\text{MnSb}_{11}$  and to study the doping behavior of the system. Adding Zn into the system will create additional disorder in the crystal and will decrease the number of vibrational modes, thus lowering the thermal conductivity. A low thermal conductivity is imperative for a better thermoelectric efficiency. Recent microprobe, single crystal diffraction, DSC/TG, resistivity and MPMS measurements on these doped crystals will be presented.

### Ternary Yb Compounds Grown from Al Flux

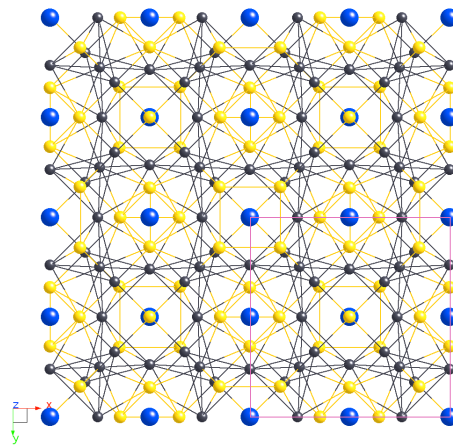
Xiuni Wu and Mercouri G. Kanatzidis

Department of Chemistry, Michigan State University, East Lansing, MI, 48824, USA

Structure of  $\text{Yb}_8\text{Cu}_{18.22}\text{Al}_{47.78}$  viewed along  $c$  axis Some Yb-based intermetallic compounds have shown interesting intermediate valence characteristics due to the hybridization between 4f and conduction electrons.<sup>1</sup> The electronic valence transition that can be induced as a function of temperature, may cause unusual charge transport and thermal expansion properties.<sup>2</sup> However, the Yb intermetallic compounds are harder to synthesize because of the high vapor pressure of Yb. By applying the method of Al flux, we are able to synthesize high quality single crystals of Yb intermetallic compounds at temperatures  $< 1000^\circ\text{C}$ . Here we present the synthesis of three ternary compounds  $\text{Yb}_8\text{Cu}_{18.22}\text{Al}_{47.78}$ ,  $\text{YbNi}_3\text{Al}_9$  and  $\text{Yb}_3\text{Ni}_5\text{Al}_{19}$  grown from Al flux. These materials have been structurally characterized by single crystal X-ray diffraction analysis. Magnetic properties and thermopower measurements have also been conducted and will be reported.

1. Kishimoto, Y.; Kawasaki, Y.; Ohno, T. *Phys. Lett. A* **2003**, 317, 308.

2. Salvador, J. R.; Guo, F.; Hogan, T.; Kanatzidis, M. G. *Nature*, **2003**, 425, 702.



Structure of  $\text{Yb}_8\text{Cu}_{18.22}\text{Al}_{47.78}$  viewed along  $c$  axis

### Crystal structure and characterization of Ta<sub>2</sub>WO(PO<sub>4</sub>)<sub>4</sub>

Pesak Rungrojchaipon, Ekaterina V. Anokhina, and Allan J. Jacobson

*Department of Chemistry, University of Houston, Houston, TX 77204*

Tantalum hydrogen phosphate  $\beta$ -TaH(PO<sub>4</sub>)<sub>2</sub> has been synthesized by reaction between tantalum oxide and polyphosphoric acid at 380 °C. The  $\beta$  phase has a three dimensional structure that is stable to remarkably high temperature (~600 °C) presumably due to strong hydrogen bonding. Preliminary AC impedance measurements give a conductivity of  $2.04 \times 10^{-6}$  S/cm at 200 °C in 5% H<sub>2</sub> with an activation energy of 0.56 eV. In further studies aimed at enhancing the conductivity by aliovalent doping, we have investigated systematically the synthesis of compounds in the TaH(PO<sub>4</sub>)<sub>2</sub> – W<sub>2</sub>P<sub>2</sub>O<sub>11</sub> system at 380 °C. As a result of the study, a new phase, Ta<sub>2</sub>WO(PO<sub>4</sub>)<sub>4</sub>, was identified and subsequently the molybdenum analog Ta<sub>2</sub>MoO(PO<sub>4</sub>)<sub>4</sub> was also prepared. The structures were determined initially by powder X-ray diffraction and subsequently by single crystal X-ray diffraction techniques. The compounds were further characterized by FTIR, thermogravimetric analysis, and scanning electron microscopy (SEM) equipped with energy dispersive spectroscopy (EDS).

### Structural and Electronic Comparisons in Polar Intermetallic Compounds : Experimental and Theoretical Studies of MGe<sub>2</sub>, MGaGe and MZnGe (M=Eu or Sr)

Tae-Soo You and Gordon J. Miller

*Department of Chemistry, Iowa State University, Ames, Iowa 50011*

EuGe<sub>2</sub> is a so-called Zintl phase compound that shows metallic character instead of typical semiconducting character. To understand the origin of this electronic behavior and physical character one or two elements substituted compounds, MGe<sub>2</sub>, MGaGe and MZnGe (M=Eu or Sr), were synthesized by high-temperature reaction of the pure elements in welded Ta tubes and studied in comparison with EuGe<sub>2</sub>. In addition isoelectronic compounds of MGaGe, a series of MA<sub>1-x</sub>Si<sub>x</sub> (M = Eu or Sr) compounds with AlB<sub>2</sub>-type structure, were prepared by Ar arc-melting for the structural and electronic property comparison.

The electronic structures of these compounds have been calculated using the TB-LMTO (tight-binding, linear muffin-tin orbital) method to understand the structural and electronic relationships between chemical bonding and physical properties. Analysis from DOS (densities of states) and COHP (crystal orbital Hamilton populations) allowed understanding the orbital interactions in the electronegative elements frameworks within each compound. Single-crystal and powder x-ray diffraction measurements have been conducted to determine crystal structures of compounds.

### The Influence of Reaction Temperature and pH on the Coordination modes of the 1,4-benzenedicarboxylate (BDC) ligand: A Case Study of the Ni(II)-1,4-BDC-2,2'-Bipyridine System

YongBok Go, Xiqu Wang, Ekaterina V. Anokhina, and Allan J. Jacobson

*Department of Chemistry, University of Houston, Houston TX 77204*

A systematic investigation of the influence of reaction temperature and pH in the hydrothermal synthesis of NiCl<sub>2</sub>-BDC-2,2'-bipy system resulted in a series of compounds with different composition and dimensionality: Ni(BDC)(2,2'-bipy)·0.75H<sub>2</sub>BDC (**1**), Ni<sub>2</sub>(BDC)(HBDC)<sub>2</sub>(2,2'-bipy)<sub>2</sub> (**2**), Ni<sub>3</sub>(BDC)<sub>3</sub>(2,2'-bipy)<sub>2</sub> (**3**), Ni(BDC)(2,2'-bipy)(H<sub>2</sub>O) (**4**) and Ni(BDC)(2,2-bipy)<sub>2</sub>·2H<sub>2</sub>O (**5**) [BDC = 1,4-benzenedicarboxylate, 2,2'-bipy = 2,2'-bipyridine]. Compound **1** which has a channel structure containing guest H<sub>2</sub>BDC molecules was formed at the lowest pH. The guest H<sub>2</sub>BDC molecules are connected by hydrogen bonds and form extended chains. At a slightly higher pH, a dimeric molecular compound **2** is formed with a lower number of protonated carboxylate groups per nickel atom and per BDC ligand. A higher temperature reaction, at the same pH leads to the transformation of both **1** and **2** into a two-dimensional layered trinuclear compound **3** built from corner-sharing nickel octahedra. As the pH is increased, a one-dimensional polymer **4** is formed with a water molecule coordinated to Ni<sup>2+</sup>. Bis-monodentate and bis-chelating BDC ligands alternate along the chain to give a crankshaft rather than a regular zigzag arrangement. Further increase of pH leads to a one-dimensional chain compound **5** which has two chelating 2,2'-bipy ligands.

## Identification of New Lithium Ruthenium Ternary Oxide: Conductivity and Crystal Structure Determination

Matthew J. O'Malley, Patrick M. Woodward, Henk Verweij

*Ohio State University*

The purpose of this study is to determine the crystal structure and conductivity of a newly discovered lithium ruthenium ternary oxide, not reported in the current  $\text{Li}_2\text{O}:\text{RuO}_2$  phase diagram. Our objective is to obtain an accurate crystal structure of this new phase via Rietveld refinements as well as obtaining values of conductivities over a range of temperatures. Currently our results indicate that the previously unreported lithium ruthenium oxide structure has a composition of  $\text{Li}_x\text{RuO}_4$ . Further analysis is needed to more accurately determine the ratio of lithium to ruthenium; techniques to be used are likely to include ICP (inductively coupled plasma) and neutron diffraction. Based on Rietveld refinements, it appears that the  $\text{Li}_x\text{RuO}_4$  structure contains edge sharing  $\text{RuO}_6$  octahedra bound in such a manner as to form a helical chain of ruthenium centers. The connectivity of the structure is likely to lead to a degree of electron conductivity through the ruthenium helix, and therefore conductivity measurements shall be obtained. Upon completion of this study, our new phase should be added to the  $\text{Li}_2\text{O}:\text{RuO}_2$  phase diagram which currently only contains  $\text{Li}_8\text{RuO}_6$  and  $\text{Li}_2\text{RuO}_3$  phases on the lithium rich region of the phase diagram. Also evidence for the removal of  $\text{Li}_8\text{RuO}_6$  from the phase diagram completely has been observed and supported by compositional studies.

## Use of Mixed A/AE and A/RE Cations as a Way to Novel Zintl Phases

Iliya Todorov and Slavi C. Sevov

*Department of Chemistry and Biochemistry, University of Notre Dame*

We have recently discovered heavy-metal aromatic pentagonal rings of  $\text{Sn}_5^{6-}$  and  $\text{Pb}_5^{6-}$  analogous to the cyclopentadienyl anion  $\text{C}_5\text{H}_5^-$ . The new species were found in the Zintl Phases  $\text{Na}_8\text{BaPb}_6$ ,  $\text{Na}_8\text{BaSn}_6$ , and  $\text{Na}_8\text{EuSn}_6$ . The rings are stacked exactly on top of each other in eclipsed fashion and form columns. The alkaline- or rare-earth cations are found exactly halfway between the ring planes in a ferrocene-like geometry. The same columns of rings and cations were later found also in  $\text{Li}_6\text{Eu}_5\text{Sn}_9$ ,  $\text{Li}_{8+x}\text{CaSn}_{6.33}$ ,  $\text{Li}_{8+x}\text{EuSn}_{6.33}$  and  $\text{Li}_5\text{Ca}_7\text{Sn}_{11}$ . In addition to the columns the isostructural  $\text{Li}_{9-x}\text{EuSn}_{6+x}$  and  $\text{Li}_{9-x}\text{CaSn}_{6+x}$  contain isolated tin atoms and bent tin trimers while  $\text{Li}_5\text{Ca}_7\text{Sn}_{11}$  and  $\text{Li}_6\text{Eu}_5\text{Sn}_9$  contain flat zig-zag hexamers and flat zig-zag infinite chains of tin, respectively. The columns of pentagonal rings disappear in the most reduced compounds, namely the isostructural  $\text{LiMgEu}_2\text{Sn}_3$  and  $\text{LiMgSr}_2\text{Sn}_3$ , which contain only flat zig-zag infinite chains and isolated tin atoms.

With these examples in mind, the next logical step was to look for similar isoelectronic pentagonal rings made of elements of two different groups, i.e. groups 13 (Tr = Triel) and 15 (Pn = Pnictide). This gives additional flexibility to the system since the oxidation numbers can be varied without changing the geometry of the cluster. So far no heteroatomic species have been found. Instead, the exploratory research in the A-Ae-Ga-Sb systems produced a number of Zintl phases with extended structures based on corner- or/and edge- sharing tetrahedra of antimony centered by gallium. The structures also contain single atom anions and dimers of antimony. Characterized structurally so far are  $\text{Li}_4\text{Ba}_5\text{GaSb}_6$ ,  $\text{Na}_2\text{Ba}_4\text{Ga}_2\text{Sb}_6$ , and  $\text{NaCa}_{10}\text{GaSb}_9$ .

## Hydrothermal Synthesis and Structure of $\text{Al}(\text{OH})(\text{C}_{12}\text{H}_6\text{O}_4)\cdot 1.7(\text{H}_2\text{O})$

Marie Vougo-Zanda, Ekaterina V. Anokhina, and Allan J. Jacobson

*Department of Chemistry, University of Houston, Houston TX 77204*

The hydrothermal synthesis and structural characterization of the novel organic-inorganic framework aluminum 2, 6-naphthalate (NDC),  $\text{Al}(\text{OH})(\text{C}_{12}\text{H}_6\text{O}_4)\cdot 1.7(\text{H}_2\text{O})$ , **1** is reported. The pure polycrystalline phase was obtained and characterized by thermogravimetric analysis, infrared spectroscopy, and X-ray powder diffraction. The structure is monoclinic with space group *C* c,  $a = 24.589 \text{ \AA}$ ,  $b = 7.547 \text{ \AA}$ ,  $c = 6.546 \text{ \AA}$ ,  $\beta = 106.75^\circ$ ,  $V = 1163.2 \text{ \AA}^3$ . The three-dimensional structure has the same topological framework as the previously reported aluminum 1, 4-benzenedicarboxylate (BDC),  $\text{Al}(\text{OH})(\text{C}_8\text{H}_4\text{O}_4)\cdot 0.7(\text{C}_8\text{H}_6\text{O}_4)$ , **2**. The frameworks are built up by interconnecting Al – OH – Al chains with the appropriate dicarboxylate (NDC **1** or BDC **2**) anions to form large diamond shaped one-dimensional channels filled with guest molecules which can be removed upon heating. In compound **1** the guest molecule is found to be  $\text{H}_2\text{O}$  while compound **2** contains additional  $\text{H}_2\text{BDC}$  molecules occupying disordered

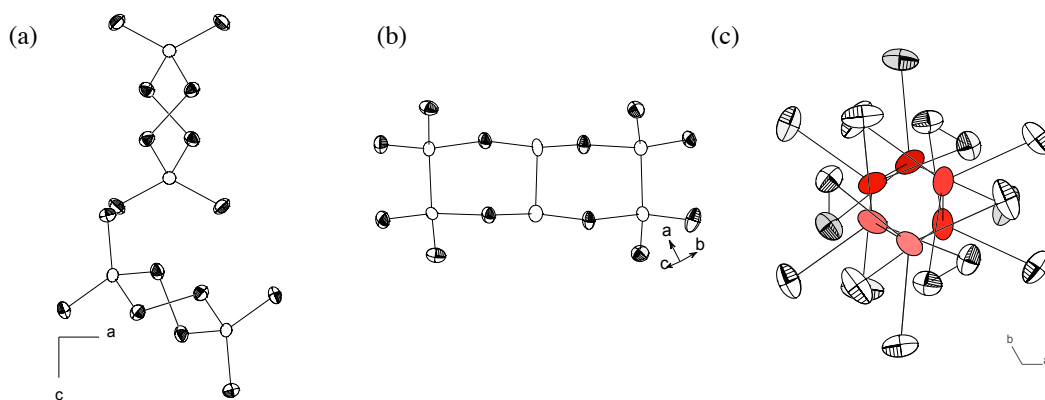
positions in the channel. When the guest molecules (H<sub>2</sub>O **1** or H<sub>2</sub>BDC **2**) are removed, the measured BET surface area for compounds **1** and **2** are respectively 7.7 m<sup>2</sup>/g and 1431 m<sup>2</sup>/g. The reason for the difference will be discussed.

### Synthesis and Characterization of the New Selenophosphate Ternary Compounds: K<sub>2</sub>P<sub>2</sub>Se<sub>6</sub>, Rb<sub>4</sub>P<sub>6</sub>Se<sub>12</sub> and Cs<sub>2</sub>P<sub>2</sub>Se<sub>8</sub>

In Chung and Mercouri G. Kanatzidis

*Department of Chemistry, Michigan State University, East Lansing, MI 48824*

Our investigations on the chalcophosphate systems are aimed at exploring the structural variability of chalcophosphate anions and their corresponding phases and also explore their potential. A core issue in this chemistry is how many different selenophosphate anions are possible and can they be incorporated into interesting materials? The new selenophosphate anions  $\infty^1[\text{P}_2\text{Se}_6]^{2-}$ ,  $[\text{P}_6\text{Se}_{12}]^{4-}$  and  $[\text{P}_2\text{Se}_8]^{2-}$  have been synthesized and characterized. The chiral compound K<sub>2</sub>P<sub>2</sub>Se<sub>6</sub> features helical  $\infty^1[\text{P}_2\text{Se}_6]^{2-}$  chains, where ethane-like [P<sub>2</sub>Se<sub>6</sub>] units are condensed to polymeric  $\infty^1[\text{P}_2\text{Se}_6]^{2-}$  chain via Se-Se bonds. Interestingly, the K<sub>2</sub>P<sub>2</sub>Se<sub>6</sub> shows reversible glass-crystal phase-change transition. Phosphorus-rich polar compound Rb<sub>4</sub>P<sub>6</sub>Se<sub>12</sub> includes the very rare *trans*-decalin-like [P<sub>6</sub>Se<sub>12</sub>]<sup>4-</sup> anion. Three P-P bonds are parallel and P atoms have mixed formal charges of 2+ and 4+. Cs<sub>2</sub>P<sub>2</sub>Se<sub>8</sub> represents the unconventional twist boat conformation of [P<sub>2</sub>Se<sub>8</sub>]<sup>2-</sup> anion.



The structure of (a) Cs<sub>2</sub>P<sub>2</sub>Se<sub>8</sub>, (b) Rb<sub>4</sub>P<sub>6</sub>Se<sub>12</sub> and (c) K<sub>2</sub>P<sub>2</sub>Se<sub>6</sub>. Alkali atoms are omitted for clarity,

### Rare-earth intermetallic phases of the type RECu<sub>6+x</sub>In<sub>6-x</sub> (RE= Ce, Nd, Ce, Nd, Sm, Gd, Dy, Ho, Er, Yb) and LaCu<sub>7</sub>In<sub>6</sub> from liquid Indium

M. A. Chondroudi, J. R. Salvador, C. Malliakas, Xiuni Wu, M. G. Kanatzidis

*Department of Chemistry, Michigan State University, East Lansing MI 48824*

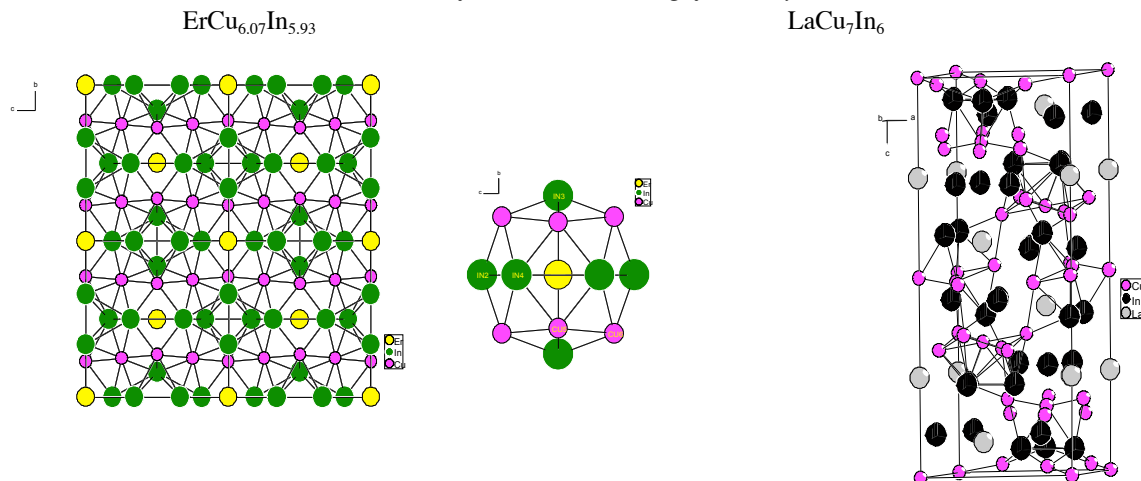
In recent years the use of molten metals as solvents, particularly molten Al and Ga fluxes, has proven invaluable for exploring new intermetallic systems. Our group has investigated the use of molten aluminum and gallium and lately this work was also expanded to include molten In as a flux solvent for the synthesis of intermetallic compounds. Interesting reactivity patterns among Al, Ga and In can be identified.

Among the large body of rare-earth intermetallics, the systems RE/Cu/M (M=In, Ag, Au, Pd etc.) especially with Ce and Yb as the RE, have received a lot of attention, both in theory and experiment. Compounds of this type exhibit a great variety of physical and chemical properties such as mixed-valence transitions or valence fluctuations, e.g. YbCu<sub>4</sub>In<sup>1</sup>, anomalous negative thermal expansion as in CeCu<sub>2</sub>In<sup>2</sup>, crossover from valence transition to Kondo behavior in YbCu<sub>5-x</sub>In<sub>x</sub><sup>3</sup>, and long range magnetic order in YbCu<sub>4</sub>Au and YbCu<sub>4</sub>Pd<sup>4,5</sup> to name a few.

Under this scope we started investigating the RE/Cu/In system with flux reactions. So far we were able to synthesize and characterize by X-Ray diffraction the crystal structure of the new phases RECu<sub>6+x</sub>In<sub>6-x</sub> (RE= Ce, Nd, Sm, Gd, Dy, Ho, Er, Yb) and LaCu<sub>7</sub>In<sub>6</sub>. They all crystallize in the *ThMn<sub>12</sub> structure type*, (orthorhombic *Immm* space group), except for the LaCu<sub>7</sub>In<sub>6</sub> which crystallizes in the rhombohedral space group *R-3c*. Magnetic susceptibility measurements for these compounds have also been performed and will be presented.

1. B. Kindler, D. Finsterbusch, R. Graf, F. Ritter, W. Assmus, B. Lüthi, *Phys. Rev. B* **1994**, 50, 704.
2. A. de Visser, K. Bakker, J. Pierre, *Phys. B* **1993**, 186-188, 577.

- Junhui HE, N. Tsujii, K. Yoshimura, K. Kosuge, T. Goto, *J. Phys. Soc. Jpn* **1997**, *66*, 2481.
- M. J. Besnus, P. Haen, N. Hamdaoui, A. Harr, A. Meyer **1990**, *163*, 571.
- E. Bauer, R. Hauser, E. Gratz, K. Payer, G. Oomi, T. Kagayama *Phys. Rev. B* **1993**, *48*, 873.



### Cation-Cation Interactions in Neptunyl(V) Systems

S. Skanthakumar<sup>1</sup>, L. Soderholm<sup>1,2</sup>, Peter C. Burns<sup>1,2</sup>, M.R. Antonio<sup>1</sup>, and Tori Ziemann<sup>2</sup>

<sup>1</sup>Chemistry Division, Argonne National Laboratory, Argonne IL, 60439

<sup>2</sup>Department of Civil Engineering and Geological Sciences, University of Notre Dame, South Bend, IN 46556

Neptunium is a manmade radioactive element that, because of the long half-life of its major isotope <sup>237</sup>Np, is considered a major concern in the assessment of long term storage options for nuclear waste. Geologically relevant aqueous neptunium chemistry is dominated by the very soluble neptunyl (V) ion,  $\text{NpO}_2^+$ , which is predicted to have a high mobility in natural groundwater. This assessment of solution Np chemistry is based largely on studies of well-defined dilute systems in a laboratory setting. Recent work to assess the crystal chemistry of  $\text{NpO}_2^+$  has indicated both that redox chemistry plays an important role in coordination environment. Neptunyl(V) has a propensity form cation-cation interactions, in which the oxo ligand on one  $\text{NpO}_2^+$  moiety bonds in the equatorial plane of an adjacent  $\text{NpO}_2^+$ . The result is the formation of aggregates in solution that persist in the solid state structures. This connectivity of  $\text{Np}^{5+}$  ions ( $5f^2$  configuration) through bridging oxygens raises the possibility of interesting electronic and magnetic behaviors in the solid state. Neptunyl(VI) does not share this propensity and therefore appears as a single-metal ion complex in solution.

### Reduction of $\text{Mg}_3\text{V}_2\text{O}_8$ to $\text{Mg}_3\text{V}_2\text{O}_6$ : Insight into Catalysis

C. Lanier<sup>1</sup>, L.D. Marks<sup>1</sup>, K.R. Poeppelmeier<sup>2</sup>

<sup>1</sup>Institute for Environmental Catalysis, <sup>1</sup>Department of Materials Science & Engineering

<sup>2</sup>Department of Chemistry, Northwestern University, Evanston, IL, 60208

$\text{Mg}_3\text{V}_2\text{O}_8$  and other phases in the  $\text{MgO-V}_2\text{O}_5$  system have been shown to be catalytically active for the oxidative dehydrogenation (ODH) of propane to propene. While the detailed catalytic mechanism is unknown, reactor studies have provided insight into how the reaction occurs. In addition to these reactor studies using  $\text{Mg}_3\text{V}_2\text{O}_8$  in the standard powder form, we have studied single crystal  $\text{Mg}_3\text{V}_2\text{O}_8$  using transmission electron microscopy (TEM). The large single crystals used in this study were grown in our lab using a floating zone furnace. This furnace allows for the growth of single crystals large enough to prepare samples for study in the transmission electron microscope.

In this poster, we present results from TEM studies on single crystal  $\text{Mg}_3\text{V}_2\text{O}_8$ . Samples were prepared and reduced in a flow of hydrogen at 560°C using a thermogravimetric analyzer (TGA). While it was known in advance that  $\text{Mg}_3\text{V}_2\text{O}_8$  and its reduced phase,  $\text{Mg}_3\text{V}_2\text{O}_6$ , are structurally quite similar, the phase transformation mechanism was unknown. In the work presented here, the relationship between the two phases,  $\text{Mg}_3\text{V}_2\text{O}_8$  and  $\text{Mg}_3\text{V}_2\text{O}_6$ , is discussed. It is believed that with knowledge of how  $\text{Mg}_3\text{V}_2\text{O}_8$  reduces to  $\text{Mg}_3\text{V}_2\text{O}_6$ , we can understand how  $\text{Mg}_3\text{V}_2\text{O}_8$  operates as an ODH catalyst.

## Lone pair distortions involving $ns^2$ cations in ternary metal oxides

Matthew W. Stoltzfus, Pat Woodward, and Bruce Bursten

Department of Chemistry, The Ohio State University

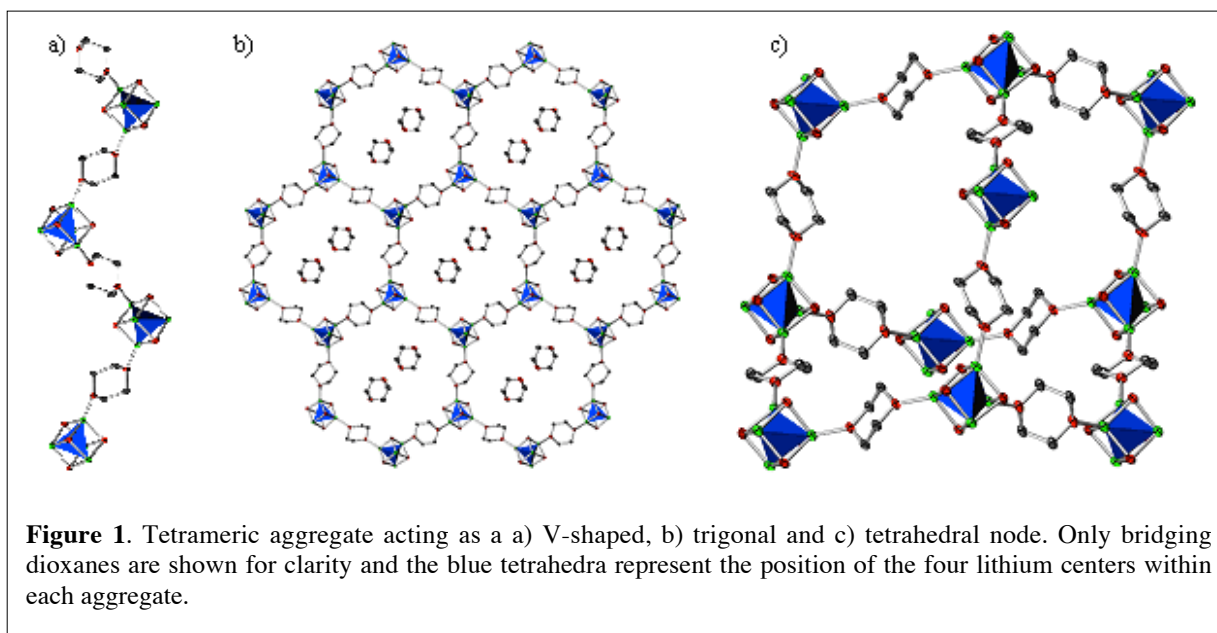
In ternary metal oxides containing a p-block cation with an  $ns^2np^0$  electron configuration, such as  $\text{Bi}^{3+}$ ,  $\text{Sb}^{3+}$ ,  $\text{Pb}^{2+}$ ,  $\text{Sn}^{2+}$ , it is common to observe an asymmetric cation coordination environment due to the presence of a stereoactive electron lone-pair (SELP). The SELP distortion enables mixing between the cation s, cation p and oxygen 2p orbitals. Depending upon the relative energy levels of these three orbitals the presence of an  $ns^2$  ion can be used to manipulate the positions of the valence and conduction band edges in photocatalysts and/or pigments. Furthermore the asymmetric local environment can give rise to noncentrosymmetric structures that are fertile ground for materials exhibiting properties such as ferroelectricity, piezoelectricity, dielectric behavior, and second-order nonlinear optical phenomenon. Density functional theory computations of electronic band structure and total energy have been used to examine a number of  $\text{AMO}_4$  compounds, where A is an  $ns^2$  ion and M is a  $(n-1)d^0$  ion. The results of these studies are used to understand the factors that control the magnitude of the stereoactive electron lone pair distortions, the long range cooperativity of these distortions, and the impact on the positions of the valence and conduction bands with respect to other  $d^0$  transition metal oxides.

## Tetrameric Cage Aggregates of Lithium Organyloxides as Secondary Building Units: Controlling Assembly in Zero One Two and Three Dimensions

Dugald J. MacDougall, J. Jacob Morris, Bruce C. Noll, Kenneth W. Henderson

Department of Chemistry and Biochemistry, University of Notre Dame, Notre Dame

The preparation of highly organized solid state materials remains a challenge to the synthetic chemist. Our approach centers on the use of structurally well defined organolithium aggregates to control network assembly. We recently reported that certain lithio  $\sigma$ -stabilized carbanions form decorated (4,4) networks in the solid state, where the overall architecture can be rationalised in terms of individual molecular dimers acting as square planar nodes. In an extension to this work we are now able to demonstrate that tetrameric lithium organyloxides can be linked through coordination with the linear ditopic linker 1,4-dioxane, creating a series of one, two and three dimensional polymers. The overall topology of the network is controlled by the geometry coded into the tetrameric aggregates, in which a tetrahedral core of four lithium centers act as points of extension through 1,4-dioxane ligation. Either terminal or bridging modes are adopted by the dioxane molecules, thus defining three different nodal shapes: V-shaped with two terminal and one bridging, trigonal with one terminal and three bridging and tetrahedral with 4 bonding (Figure 1). The dimensionality adopted by the network is dependant upon the ability of the system to fill space efficiently. Free dioxane molecules are found within the pores of both the three and two dimensional networks





## Self-Assembly of Two and Three Dimensional Networks by Hexameric Sodium Aryloxides

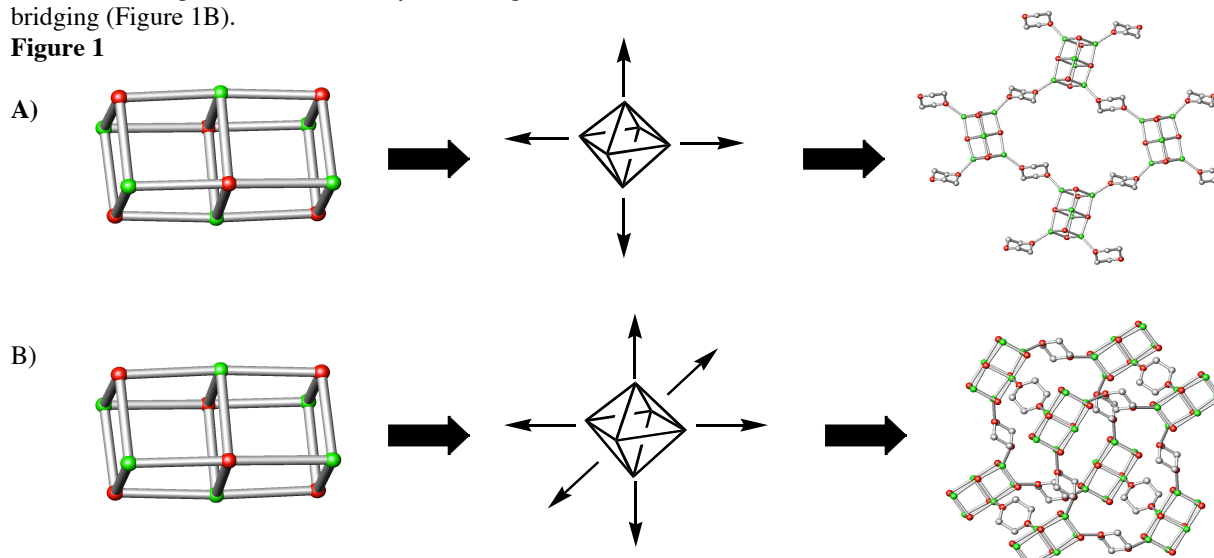
Jeffrey A. Rood, J. Jacob Morris, Dugald J. MacDougall, Bruce C. Noll, Kenneth W. Henderson

*Department of Chemistry and Biochemistry, University of Notre Dame*

The synthesis and characterization of well-defined network assemblies continues to be an area of intense interest due to the potential of these materials in applications as diverse as catalysis, chemical separation, optics, and electronics. Although there have been remarkable advances in our understanding of the principles of self-assembly, the development of rational routes to well-organized solid state materials remains a real challenge to the synthetic chemist. Two main strategies have been adopted in the formation of molecular networks, first through use of hydrogen-bonded organic solids and second using inorganic coordination polymers containing transition elements and ligand spacer molecules. Our interest lies in the use of main group cage complexes as robust secondary building units to control the assembly of network architectures.

We have previously reported that molecular lithium species may be used to direct the synthesis of complex network assemblies, the topologies of which can be rationalized by the fusion of known molecular species through linear Lewis base ligation. Herein we present an extension of this research to the heavier s-block metal sodium. Fusion of hexameric molecular aggregates by sodium aryloxides is achieved by coordination to the ditopic Lewis base 1,4-dioxane. The hexameric aggregates act as distorted octahedral nodes in which the six sodium centers are the points of extension and dictate the direction of network growth. Three types of coordination polymers are isolated. These are dependant on the coordination modes adopted by the dioxane molecules, terminal or bridging. One dimensional chains are formed where two dioxane molecules bridge and four are terminally bonded; (4,4) nets where four bridge and two terminally bond (Figure 1A); and three dimensional cubic networks where all six sites are bridging (Figure 1B).

**Figure 1**



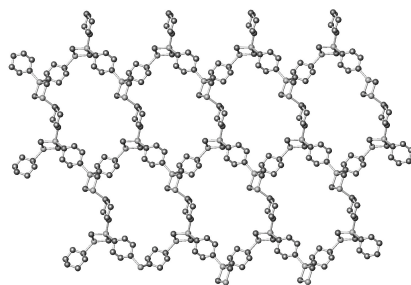
## Control of Lithium Aggregate Assemblies Through Solvent Effects

J. Jacob Morris, Bruce C. Noll, Kenneth W. Henderson

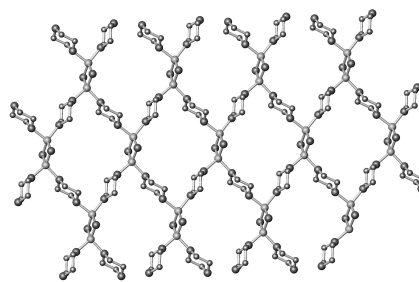
*Department of Chemistry and Biochemistry, University of Notre Dame*

The synthesis and characterization of well-defined network assemblies continues to be an area of intense interest due to the potential of these materials in applications as diverse as catalysis, chemical separation, optics, and electronics. Our approach centers on the use of structurally well-defined organolithium aggregates to control network assembly. We have recently demonstrated that tetrameric lithium organoxydes can be linked through the linear ditopic Lewis base 1,4-dioxane to create a series of one, two and three dimensional polymers. The overall topology of the polymers is controlled by the geometry coded into the tetrameric secondary building units. In particular, the tetrahedral core of the lithium aggregates act as points of extension through 1,4-dioxane ligation. Herein, we present an extension to this work in which the solvent dimethylformamide is used to further control the network assembly through an unexpected templating effect. More specifically, two distinct phases, a (4,4) net or a (6,3) net, crystallizes depending on the amount of dimethylformamide (DMF) present in the precursor solutions. Interestingly, the

resulting networks do not contain any coordinated DMF despite this being a significantly stronger Lewis base than 1,4-dioxane for lithium ligation.



**(6,3) Net**



**(4,4) Net**

### References

1. Henderson, K. W.; Kennedy, A. R.; McKeown, A. E.; Strachan, D. *Dalton Trans.* **2000**, 4348.
2. Henderson, K. W.; Kennedy, A. R.; MacDougall, D. J. *Inorg. Chem.* **2003**, 42(8), 2736.
3. Henderson, K. W.; Kennedy, A. R.; Macdonald, L.; MacDougall, D. J. *Inorg. Chem.* **2003**, 42, 2839.
4. MacDougall, D.J.; Morris, J. Jacob; Noll, B.C.; Henderson, K.W. *Chem. Commun*, **2005**, 456.